

الجمهورية الجزائرية الديمقراطية الشعبية

Democratic and Popular Republic of Algeria

وزارة التعليم العالي و البحث العلمي

Ministry of Higher Education and Scientific Research

University of Mohamed Khider, BISKRA

Faculty of Exact Sciences and Sciences of

Nature and Life

Department: Material sciences

Ref.:



جامعة محمد خيضر بسكرة

كلية العلوم الدقيقة و علوم الطبيعة

و الحياة

قسم : علوم المادة

المرجع :

A thesis submitted to obtain the diploma of:

Doctorate of Science in: Physics

Option: Physics of materials

THEME

THE ROLE OF Ni AND Zn ON DILUTED MAGNETIC SEMICONDUCTOR $Ni_{1-x}Zn_xO$ THIN FILMS

Presented by:

Mr. ZAUCHE Chouaieb

Publicly defended on:

In front of the jury committee composed of:

Dr. Okba BELAHSEN	Prof	Biskra University	President
Dr. Said BENRAMACH	Prof	Biskra University	Supervisor
Dr. Yasmine AOUN	MCA	El Oued University	Assistant Supervisor
Dr. Mohammed El Hadi ATTIA	MCA	El Oued University	Examiner
Dr. Soufiane BENHAMIDA	MCA	Ouargla University	Examiner

Academic year 2019-2020

Acknowledgements

I thank ALLAH the Almighty for giving me the courage, the will and the patience to complete this present work.

First of all, I would like to express my sincere gratitude and all my thanks to my thesis Director **Mr. Said BENRAMACH**, professor at Mohamed Khider University. Biskra, and **Mr. Yasine AOUN**, Lecturer at El Oued University, for their help, guidance and the time they spent witnessing the elaboration of this work. I thank them for their availability, their kindness, their support, their ideas and pieces of advice. May Allah protect them.

I am also grateful to **Mr. Okba BELAHSEN**, professor at Mohamed Khider University. Biskra, for having given me the honor of chairing the jury for the defense of this thesis.

My warm thanks go also to **Mr. Mohammed El Hadi ATTIA**, Lecturer at El Oued University, who kindly agreed to be part of the jury and to examine my work.

My heartfelt thanks also go to **Mr. Soufiane BENHAMIDA**, Lecturer at Ouargla University, who kindly agreed to be part of the jury and to examine my work as well.

I would like to thank **Mr. Aid DHAHBI** from the University of Setif for welcoming me in his laboratory, his conduct of the electrical properties, for all his comments on my work and for his generous help.

Dedication

I dedicate my dissertation work to my dear parents who have meant and continue to mean so much to me. Although they are no longer of this world, their soul still pushes me to be the man they dreamt of.

I also dedicate this dissertation to my wife and all my family members who have never left my side and supported me throughout the process.

It is also dedicated to my close friends. I will always remember what you have done for me.

CONTENTS

Contents

N	Contents	Page
	Acknowledgement	II
	Dedication	III
	Contents	V
	List of figures	VIII
	List of tables	X
	General introduction	2
	 Chapter I: Spray Deposition of Nanostructured NiO Thin Films	
I-1-	Introduction	8
I-2-	Information of Nickel types	9
I-2-1-	NiO Thin Film Deposition from Nickel Chloride Solutions	9
I-2-2-	NiO Thin Film Deposition from Nickel Nitrate Solutions	9
I-2-3-	NiO Thin Film Deposition from Nickel Acetate Solutions	10
I-3-	Physical Properties of NiO Thin Films	10
I-3-1-	Structural Properties of NiO Thin Films	10
I-3-1-A-	Preferred orientation	13
I-3-1-B-	Grain size	14
I-3-1-C-	Lattice parameter	15
I-3-1-D-	Mean strain	16
I-3-2-	Optical Properties of NiO Thin Films	17
I-3-2-A-	The transmittance of NiO thin films	18
I-3-2-B-	Absorbance of NiO thin films	20
I-3-2-C-	Optical bandgap of NiO thin films	20
I-3-2-D-	Refractive index	23
I-3-3-	Electrical Properties of NiO Thin Films	24
I-3-4-	Magnetic Properties of NiO Thin Films	26
I-4-	Nickel oxide application	26
I-5-	Conclusion	27
	References	28
	 Chapter II: Elaboration and characterizations	
II-1-	Introduction:	39
II-2-	Elaboration	39

II-2-1-	Spray Technique	39
II-2-2-	Mechanisme	39
II-2-3-	Advantages of the Spray	40
II-2-4-	Disadvantage of the Spray	40
II-3-	Parameters of the deposition	41
II-4-	Preparation	41
II-4-1-	Preparation of solution	41
II-4-2-	Preparatin of the substrate	43
II-4-3-	Preparation of NiO thin films	44
II-4-4-	Preparation of Zn doped NiO thin films ($\text{Ni}_{1-x}\text{Zn}_x\text{O}$)	45
II-4-5-	Preparation of Ni doped ZnO thin films ($\text{Ni}_{1-x}\text{Zn}_x\text{O}$)	45
II-5-	Characterization of the films	46
II-5-1-	Structural characterization	46
II-5-2-	Optical characterization	49
II-5-3-	Electrical characterization	50
II-6-	Conclusion	51
	References	52

Chapter III: The role of deposition rate on the physical properties of NiO thin films elaborated by spray pyrolysis technique

III-1-	Introduction	54
III-2-	Experimental	55
III-3-	Results and discussion	55
III-4-	Conclusions	60
	References	62

Chapter IV: Synthesis of nanostructured of Zn doped NiO

IV-1-	Introduction	66
IV-2-	Zn doping effect on optical properties of NiO thin films	66
IV-2-1-	Transmittance spectra	66
IV-2-2-	Optical Gap	68
IV-2-3-	The Disorder (Urbach energy)	71
IV-3-	Zn doping effect on Structural properties of NiO thin films	74
IV-4-	Conclusions	81
	References	82

	Chapter V: Synthesis of nanostructured of Ni doped ZnO	
V-1-	Introduction	85
V-2-	Ni doping effect on optical properties of ZnO thin film	86
V-2-1-	Transmittance spectra	86
V-2-2-	Optical Gap	88
V-2-3-	The Disorder (Urbach energy)	91
V-3-	Ni doping effect on Structural properties of ZnO thin films	93
V-4-	Conclusions	98
	References	100
	Generale Conclusion	104
	Abstract	107

Lest of Figures

N	Figure	Page
Chapter I: Spray Deposition of Nanostructured NiO Thin Films		
Figure (I-1)	Unit cell definition using parallelepiped with lengths a, b, c and angles between the sides given by α , β , γ [h1]	16
Figure (I-2)	Band gap in semiconductor	21
Chapter II: Elaboratoin and characterizations		
Figure (II-1)	spray pneumatic technique	40
Figure (II-2)	Glass Substrates	43
Figure (II-3)	Bruker D8 Advanced X-ray Diffractometer	47
Figure (II-4)	Bragg's diffraction	48
Figure (II-5)	(XRD) of semiconductors (a) Polycrystalline (b) Single material (c) Amorphous material	48
Figure (II-6)	Ultraviolet-visible spectrophotometer (LAMBDA 25)	49
Figure (II-7)	Schematic of UV-visible spectrophotometer	50
Figure (II-8)	Schematic of in-line four-point probe configuration	50
Figure (II-9)	Experimental dispositif	51
Chapter III: The role of deposition rate on the physical properties of NiO thin films elaborated by spray pyrolysis technique		
Figure (III-1)	X-ray diffraction spectra of NiO thin films at different deposition rates	56
Figure (III-2)	The variation of crystallite size and diffraction angle as a function of deposition rate in NiO thin films	57
Figure (III-3)	Transmission spectra of ZnO thin films as a function of deposition rate, the inset present the absorbance of the thin films	58
Figure (III-4)	The variation of optical band gap E_g and Urbach energy E_u of NiO thin films with deposition rate	59

Figure (III-5)	Electrical resistivity of NiO thin films at different deposition rate	60
----------------	---	----

Chapter IV: Synthesis of nanostructured of Zn doped NiO

Figure (IV-1)	Optical transmittance spectra of thin films	67
Figure (IV-2)	Optical absorbance spectra of thin films	68
Figure (IV-3)	The variation of $(Ah\nu)^2$ as a function of $h\nu$ for each films	70
Figure (IV-4)	Variations of $\ln(\alpha)$ as a function of $h\nu$ of Zn doped NiO thin films	72
Figure (IV-5)	The variations of optical band gap energy and Urbach energy of Zn doped NiO thin films at various doping levels	73
Figure (IV-6)	X-ray diffraction of $Ni_{1-x}Zn_xO$ thin films as a function of Zn doping level	75
Figure (IV-7)	The variations of the 2θ and lattice parameter a for $Ni_{1-x}Zn_xO$ thin films as a function of Zn doping level	77
Figure (IV-8)	The variations of crystallite sizes of (111) and (200) crystal plans of $Ni_{1-x}Zn_xO$ thin films as a function of Zn doping level	79
Figure (IV-9)	The variations of the main strains of (111) and (200) crystal plans of $Ni_{1-x}Zn_xO$ thin films as a function of Zn doping level	80

Chapter V: Synthesis of nanostructured of Ni doped ZnO

Figure (V-1)	Optical transmittance spectra of Ni doped ZnO thin films	87
Figure (V-2)	Optical absorbance spectra of Ni doped ZnO thin films	88
Figure (V-3)	The variation of $(Ah\nu)^2$ as a function of $h\nu$ for each Ni doped ZnO thin films	90
Figure (V-4)	Variations of $\ln A$ as a function of $h\nu$ of Ni doped ZnO thin films	92
Figure (V-5)	The variations of optical band gap energy and Urbach energy of Zn doped NiO thin films at various doping levels	93
Figure (V-6)	X-ray diffraction of $Ni_{1-x}Zn_xO$ thin films as a function of Ni doping level	94
Figure (V-7)	G and ϵ_{zz} of (0 0 2) diffraction peak as a function of doping level x	97
Figure (V-8)	the variations of crystallite sizes G as a function of doping level x of Ni doped ZnO thin films for (100) (002) (101) and (110) crystal plans	98

Lest of Tables

N	Table	page
Chapter I: Spray Deposition of Nanostructured NiO Thin Films		
Table (I-1)	Summary of the basic physical and chemical properties of NiO material	8
Table (I-2)	Information of Nickel types	10
Table (I-3)	The preferred orientation and thickness of various deposited NiO thin films	12
Table (I-4)	The grain/crystallite size of the various NiO films deposited at the different conditions	14
Table (I-5)	The grain/crystallite size of the various NiO films deposited at the different	17
Table (I-6)	The relation between grain/crystallite size and transmittance NiO films deposited at the different conditions	18
Table (I-7)	Band gap energy and transmittance values of NiO thin films deposited at different conditions	22
Table (I-8)	Refractance index values of NiO thin films deposited at different conditions	24
Table (I-9)	Electrical conductivity values of NiO thin films deposited at different conditions	25
Chapter II: Elaboratoin and characterizations		
Table (II-1)	The physical and chemical properties of Nickel	42
Table (II-2)	The physical and chemical properties of Zinc	43
Table (II-3)	The experimental conditions of preparation NiO thin films	45
Table (II-4)	The experimental conditions of preparation ZnO thin films	45
Chapter IV: Synthesis of nanostructured of Zn doped NiO		
Table (IV-1)	The experimental conditions of prepared of Zn doped NiO thin films	66
Table (IV-2)	Optical gap values of Zn doped NiO thin films	71

Table (IV-3)	Disorder's (Urbach energy) values of Zn doped NiO thin films	73
Table (IV-4)	The structural parameters of NiO thin film as a function of the thickness film to (111) diffraction peak	76
Table (IV-5)	The structural parameters of NiO thin film as a function of the thickness film to (200) diffraction peak	76
Table (IV-6)	The structural parameters of NiO thin film as a function of the thickness film to (111) diffraction peak	78
Table (IV-7)	The structural parameters of NiO thin film as a function of the thickness film to (200) diffraction peak	79

Chapter V: Synthesis of nanostructured of Ni doped ZnO

Table (V-1)	The experimental conditions of prepared of Zn doped NiO thin films	86
Table (V-2)	Optical gap values of Ni doped ZnO	89
Table (V-3)	Disorder's (Urbach energy) values of Ni doped ZnO	91
Table (V-4-a)	The structural parameters of Ni doped ZnO thin film of (100) diffraction peak	94
Table (V-4-b)	The structural parameters of Ni doped ZnO thin film of (002) diffraction peak.	95
Table (V-4-c)	The structural parameters of Ni doped ZnO thin film of (101) diffraction peak.	95
Table (V-4-d)	The structural parameters of Ni doped ZnO thin film of (110) diffraction peak.	95
Table (V-5)	The structural parameters of $Ni_{1-x}Zn_xO$ thin film of (002) diffraction peak	96

GENERALE INTRODUCTION

GENERAL INTRODUCTION

Semiconductor heterostructures have established themselves as the most suitable candidates for optoelectronic devices. Zinc oxide (ZnO) is one of the most promising and largely investigated Transparent Conducting Oxides (TCOs). It is an n-type semiconductor with a bandgap of 3.4 eV. It is commonly used to fabricate UV and blue light devices like lasers, diodes and detectors. The fact that ZnO thin films could be deposited using different methods makes it a perfect candidate for use in transparent electronic devices. Nickel Oxide (NiO) is one of rare p-type semiconducting transparent oxides. NiO is a p type material with a bandgap of 3.8 eV. It is characterized for its interesting thermoelectric, magnetic and electrochromic properties. As the p-n junction is one of the fundamental elements of almost every electronic devices, there is a need to master the process of producing stable, reliable and low-cost transparent diodes. Spray pyrolysis method has distinct potential advantages than other techniques owing to its lower crystallization temperature, low cost, simple deposition procedure, easier compositional control, and large surface area coating capability. In the present work, hetero junction thin films were deposited and characterized for their structural and optical behavior.

In the latest researches, The NiO as a thin film was studied on varieties of substrates with chemical and physical methods; it was used to improve the structural optical and electrical properties. The pulsed laser deposition [1], chemical vapor deposition [2], electrochemical deposition [3], abeam evaporation [4], anodic deposition [5], electroless bath deposition [6] sputtering [7], chemical vapor deposition [8] and spray pyrolysis techniques [9], are used to prepare the NiO thin films, the spray techniques also were favorites with comparing by others methods due to the simple deposition and best cost. The main objective of this research is to study the physical and chemical properties of NiO thin films based on past research. In this work; we have proposed a review of original research to nanostructured NiO prepared by spray techniques.

In the first chapter we gathered information about the basic physical and chemical properties of NiO material and we showed spray deposition methods then we presented physical properties of NiO thin films.

In the second chapter it was studied the NiO and ZnO solutions were sprayed on the heated glass substrates by spray pneumatic method which transforms the liquid to a stream formed with uniform and fine droplets of 25 μm average diameter. The deposition was performed at a substrate temperature of 450 $^{\circ}\text{C}$ with deposition rate was 5.7 mL /min. The structural properties of: NiO, (Zn doped NiO) and (Ni doped ZnO) films were studied by means of X-ray diffraction (XRD Bruker AXS-8D) with $\text{CuK}\alpha$ radiation ($\lambda=0.15406$ nm) in the scanning range of (2θ) was between 20 $^{\circ}$ and 70 $^{\circ}$. The optical transmission of the deposited films was measured in the range of (300 – 900 nm) by using an ultraviolet-visible spectrophotometer (LAMBDA 25) and the electrical resistance R was measured by four point methods

In the third chapter, the spray method was used for technological applications because it is one of the most important techniques to deposition a large-scale production. The prepared the thin films by this method have a good adhesion mechanical, and good electrical conductivity; also it has a high optical transparency and magnetic properties of nanostructures NiO. The main objective of this work is to obtain a semiconductor as NiO thin films with high crystalline structure, good optical and electrical properties. In the present work, nanostructure NiO thin films were investigated, which are elaborated by spray pyrolysis method, the NiO was heated on glass substrate at a deposition temperature of 450 $^{\circ}\text{C}$ with various deposition rates of 20, 40, 60 and 80 ml.

In the last two chapters we discussed the description and the analysis of the measurements and the discussion of the results. It focuses on the structural, optical and electrical properties of thin films Ni with Zn doped $\text{Ni}_{1-x}\text{Zn}_x\text{O}$ with different doping levels (0, 0.02, 0.04, 0.08, 0.12, 0.88, 0.92, 0.96, 0.98 and 1). These films have been deposited on glass substrates by Spraying technique at substrate temperature equal to 450 $^{\circ}\text{C}$.

• Outline of This Thesis

The thesis is structured in five chapters. It begins by an introduction and it is concluded by recommendations for future research.

Chapter I: Spray Deposition of Nanostructured NiO Thin Films.

Chapter II: Elaboratoin and characterizations.

Chapter III: The role of deposition rate on the physical properties of NiO thin films elaborated by spray pyrolysis technique.

Chapter IV: Synthesis of nanostructured of Zn doped NiO.

Chapter V: Synthesis of nanostructured of Ni doped ZnO.

References:

- [1] A. Charef, S. Benramache, Y. Aoun, B. Benhaoua, S. Lakel, M. Marrakchi, Effect of Substrate Temperature on the Growth and Properties of Nanocrystalline NiO Thin Films, *Journal of Nanoelectronics and Optoelectronics*, vol. 14, pp. 1667–1671, 2019.
- [2] A. Diha, S. Benramache, L. Fellah, “The Crystalline Structure, Optical and Conductivity Properties of Fluorine Doped ZnO Nanoparticles,” *Journal of nano- and electronic physics*, vol. 11, p. 03002, 2019.
- [3] S. Benramache, Y. Aoun, S. Lakel, B. Benhaoua, C. Torchi, “The calculate of optical gap energy and urbach energy of Ni_{1-x}CoxO thin films,” *Sādhanā*, vol. 44, p. 26, 2019.
- [4] Y. Aoun, M. Marrakchi, S. Benramache, B. Benhaoua, S. Lakel, A. Cheraf, “Preparation and characterizations of monocryalline Na doped NiO thin films,” *Materials Research*, vol. 21, p. e20170681, 2018.
- [5] Y. Arata, H. Nishinaka, D. Tahara, M. Yoshimoto, ‘Heteroepitaxial growth of single-phase ε-Ga₂O₃ thin films on c-plane sapphire by mist chemical vapor deposition using a NiO buffer layer,’ *CrystEngComm*, vol. 20, pp. 6236-6242, 2018.
- [6] L. Ghimpu, V. Suman, D. Rusnac, ‘Influence of the Growth Temperature on the Properties of the Transparent and Conductive NiO Thin Films Obtained by RF Magnetron Sputtering,’ *International Conference on Nanotechnologies and Biomedical Engineering*, vol. 77, pp. 291–295, 218.
- [7] M.B. Cosar, ‘Plasma assisted low temperature electron beam deposited NiO thin films for electro-optic applications,’ *Journal of Vacuum Science & Technology A*, vol. 36, p. 031501 (2018).

- [8] C. Augustine, M. N. Nnabuchi, R.A. Chikwenze, F.N.C. Anyaegbunam, C. Nwosu, C.O. Dike, C.V. Ezeh, B.J. Robert, E.M. Yohanna, E.N. Taddy, ‘Comparative study of pbs-nio and nio-pbs heterojunction thin films deposited by chemical bath deposition technique,’ *Chalcogenide Letters*, vol. 15, pp. 591-598, 2018.
- [9] S. Akinkuade, B. Mwankemwa, J. Neln W. Meyer, Structural, optical and electrical characteristics of nickel oxide thin films synthesised through chemical processing method,’ *Physica B: Condensed Matter*, vol. 535, pp. 24–28, 2018.

CHAPTER ONE

Spray Deposition of Nanostructured NiO Thin Films

I-1- Introduction

In the latest research, the nickel oxide (NiO) was found in the cubic structure with a lattice parameter ($a = 0.4816 \text{ nm}$) [1]. NiO is forming of nickel metal and oxygen element, it is a p-type of semiconducting nature. NiO was used in a variety of technology such as optoelectronic devices and gas sensing [2,3] due to having a good structure crystallinity, good electrical conductivity and high transparency in the visible region. The optical band gap of NiO thin films varied between 3.6 to 4 eV [4]. However, the NiO thin films can be used in various applications due to the simplicity of synthesis such as solar cells [5], chemical sensors [6], photo detectors [7], electro chromic minors [8], organic light-emitting diodes [9], UV detectors [10], vana pent diodes [11], and defrosting windows [12].

Table (I- 1) shows the physical and chemical properties of NiO material, it is found that the NiO has a high solubility in water with a refractive index of 2.18. The NiO as a thin film was studied on varieties of substrates with chemical and physical methods; it was used to improve the structural optical and electrical properties. The pulsed laser deposition [13], chemical vapor deposition [14], electrochemical deposition [15], abeam evaporation [16], anodic deposition [17], electroless bath deposition [18] sputtering [19], chemical vapor deposition [20] and spray pyrolysis techniques [21], are used to prepare the NiO thin films, the spray techniques also were favorites with comparing by others methods due to the simple deposition and best cost.

Table (I- 1) :Summary of the basic physical and chemical properties of NiO material

Property	Value
Appearance	Green crystalline solid
Molecular mass	74.69 g/mol
Density (N)(cm³)	6.67 g/cm ³
Lattice parameter (a)	0.4186 nm
Stable Phase at 300 K	3.1-4.3 eV
Conductivity σ (Ωcm)⁻¹	1.5×10^{-3}
Melting Point	1995°C
Refractive Index	2.18

Band Gap Energy (Eg)	3.6-4.0 eV
Solubility in water μ (cm²/V.s)	0.1-1
A	4.75 A°
B	11.77 A°
C	8.44A°
B	93° 36'

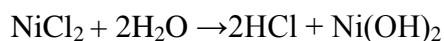
The main objective of this research is to study the physical and chemical properties of NiO thin films based on past research. In this work; we have proposed a review of original research to nanostructured NiO prepared by spray techniques.

I-2- Information of Nickel types

In the deposition of NiO thin films by using the spray techniques with NiO solution, it is prepared by various methods and protocol as shown in the following steps:

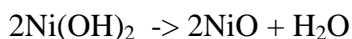
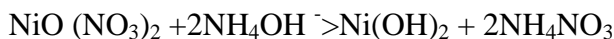
I-2-1- NiO Thin Film Deposition from Nickel Chloride Solutions

The NiO thin films prepared by using chloride nickel can be dissolved in various solvents such as water, ethanol and methanol solution. However in the preparation of NiO solution from water solvent, when dissolving the nickel chloride dehydrate (NiCl₂, 2H₂O) in water (H₂O), before using and deposit NiO thin films into substrates which heating the final solutions at 50 °C than add drops of HCl to the solution for stabilization. Menaka and Umadevi[22] they discussed that process decomposition of nickel chloride to nickel oxide in the presence of water, according to the following equation(see Table 2) [23]:



I-2-2- NiO Thin Film Deposition from Nickel Nitrate Solutions

NiO solution can be prepared by using nitrate Nickel with various solvents such as water, ethanol and methanol. However, in the preparation of NiO solution from water solvent, when introduce of nickel nitrate dehydrate (Ni (NO₃)₂. 2H₂O) in a volume equal to wither solvent (H₂O) (see Table 2) [24]:



I-2-3- NiO Thin Film Deposition from Nickel Acetate Solutions

NiO solution can be prepared by using acetate Nickel with various solvents such as water, ethanol and methanol. However, in the preparation of NiO solution from water solvent, when introduce nickel acetate dehydrate ($\text{Ni}(\text{CH}_3\text{COO})_2 \cdot 4\text{H}_2\text{O}$) in a volume equal to wither solvent (H_2O). ($\text{Ni}(\text{CH}_3\text{COO})_2 \cdot 4\text{H}_2\text{O}$) are monoclinic with space group $P_{21/c}$ the unit cell off dimension(see Table 2) [25]:

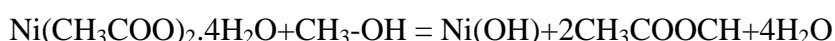


Table (I- 2): information of Nickel types

Molecule	Molecule formula	Molar mass	Aspect	Density	Solubility in water (mg/l)
<i>Nickel Chloride</i>	$\text{Cl}_2\text{H}_{12}\text{NiO}_6$	237.69 g/mol	Green crystalline solid.	1.92 g/cm ³	2540×10^3 (20 °C)
<i>Nickel Acetate</i>	$\text{C}_4\text{H}_6\text{NiO}_4$	$176.78 \text{ g} \cdot \text{mol}^{-1}$	Green crystalline solid.	1.798 g/cm ³	Easily soluble in cold water, hot water
<i>Nickel Nitrate</i>	$\text{Ni}(\text{NO}_3)_2 \cdot 2\text{H}_2\text{O}$	290.08 g/mol	Green crystalline solid.	3.55 g/cm ³	6.42×10^5 at 20°C

I-3- Physical Properties of NiO Thin Films

I-3-1-Structural Properties of NiO Thin Films

The NiO thin films were crystallized with a cubic structure that can be related to obtaining peaks in the XRD diffraction of NiO thin films. The nanostructures NiO thin films were studied by the XRD patterns with two peaks at $2\theta = 37.5$ and 43.3 corresponding to (111) and (200) plans of NiO phase structure. The NiO thin films were

deposited with various conditions such as precursor molarity, substrate temperature, film thickness and doping level.

Ahnet al [26] deposited the NiO thin films on Pt/Ta/glass by (RF) sputtering method at 50 W RF power with 10 m Torr at 600 °C. Found that the NiO thin film has a polycrystalline nature with preferentially (111), it is high than other diffractions which indicating that the preferred orientation with (111) plan. Some authors [27-29] investigated the effect of precursor molarity on the structural property, they discussed that the high crystalline structure of NiO thin films was obtained in the film prepared with 0.1 M.

Kamel et al. [30] studied the influence substrate temperature on the structural properties spray deposition NiO thin films. In this research, the NiO thin films were deposited at different temperatures, where high then of 275°C. They found that the NiO thin films having preferential orientation along (111) direction peak, so that the deposition temperature was affected on the structural property. On the other hand, the effect of substrate temperature was investigated by various authors [31-34]. The structural properties of NiO thin films show that the high crystalline structure was improved with increasing the deposition temperature.

The influences of metal doping on the structural property of NiO thin films were developed by various techniques Na, Fe, Zn, Cu, Co, Ag, Ng, Ti, Li and Mg. Nickel oxide is a compound semiconductor of (II-VI) group of the periodic table and it has a crystalline structure of the rock salt type lattices. Each cubic unit cell has four nickel atoms and four oxygen atoms. Each nickel atom is surrounded by six oxygen atoms and each oxygen atom has six nickel atoms surrounding it. This face-centered cubic (FCC) structure has a lattice parameter of 4.1769Å at 26°C. The nickel distance is 2.9518Å for a cubic cell ($\alpha=60^\circ$ and $a=4.1769\text{Å}$)[35].

NiO thin films also were studied as a function of films thickness by some method, Karaduman et al. [36] prepared the Nanostructured NiO thin films with different film thickness; it is prepared using by SILAR Method to use as gas sensing application. NiO thin films in this work having a high crystalline structure with cubic structure, which was achieved in the film prepared with 330 nm, it is (200) phase. However, the film prepared others film thicknesses have good crystallinity. We have discussed that the film thickness were affected on the structural property, it is achieved with 400 to 500 nm and was found by [37-40].

Table (I- 3): The preferred orientation and thickness of various deposited NiO thin films

S.N.	Condition	Preferred orientation	Thickness of NiO films	Ref.
Li-NiO	420°C	(111)	19 (µm)	[41]
NiO-Ag	400°C Ni : 42.13 % atomic Ag: 11.06 % atomic O: 47.13 % atomic P : 5.10 ⁻⁴ mbar	(200)	13 (nm)	[42]
NiO-B	NiO:97 % B:3% 400°C C = 0.1 M	(111)	15.2 (nm)	[43]
NiO	C = 0.5 M T=500°C	(111)	275 (nm)	[44]
NiO	C = 0.5 M T=500°C Precusar = 10 mL	(111)	2.5 (µm)	[45]
Co_xNi_{1-x}O	C =0.1 M T = 573°K X = 0.15 Nozzl = 28 cm	(111)	78.55 (µm)	[46]
NiO:8Li	C = 1 M T = 600°C	(111)	48 (nm)	[47]
NiO:8Li	C = 1 M T = 400-300°C	(111)	200 (nm)	[48]
NiO	Ni = 58.80 w % O = 22.26 w % C = 18.93 w % T = 470°C	(111)	250 (nm)	[49]

NiO	T = 300°C C = 0.03 M	(111)	1000 (nm)	[50]
NiO	T = 360°C C = 0.1 M	(111)	90 (nm)	[51]
NiO	T = 460°C C = 0.2 M	(200)	0.44 (μm)	[52]
NiO_{1-x} Zn_x	T = 623°K C = 0.1 M X = 0.05	(111)	240 (nm)	[53]
NiO	T = 350°C C = 0.75 M	(220)	390 (nm)	[54]
NiO	T = 450°C C = 0.01	(200)	80 (nm)	[55]
NiO-Cu	T = 1737°F Cu = 16.17 at%	(111)	100 (nm)	[56]
(NiO)_{1-x} (ZnO)_x	T = 400°C C = 0.05 M X = 0.25	(111)	0.3 (μm)	[57]

I-3-1-A-Preferred orientation

The microstructure of thin films can be evaluated by X-ray diffraction, e.g. using the Bragg-Brentano geometry. I find that in a poor vacuum all the diffraction peaks for a given system are present, i.e. the film is “powder-like”, as reported for instance in the JCPDS files; even amorphous films can be obtained, if the vacuum is “bad” enough. However, in a very good vacuum “preferred growth” is observed; in the extreme case only one family peak is present; for instance, only the (111) and (222) peaks are observed for f.c.c (see Table (I- 3)). Elements, like Al or Au. This is due to the fact that the (111) oriented surface is the lower energy ones. Very good vacuum means that the atoms can migrate on the surface long enough to find their lower energy position before the arrival of another atom I used the term “preferred growth” instead of the “preferred orientation” because the latter is an artifact experienced when preparing a sample by computation of powder, and is caused by the relative arrangement of the various crystallites; by contrast the “preferred growth”

has a pregnant physical meaning, as described above. The vacuum is “good” when thermodynamics dominates over kinetics: the probability of the growth of an already nucleated grain is larger than the probability of the nucleation of a new grain[58].

I-3-1-B- Grain size

Particle size, also called grain size(see Table (I- 4)), refers to the diameter of individual grains of sediment, or the lithified particles in classic. The term may also be applied to other granular materials. This is different from the crystallite size, which refers to the size of a single crystal inside a particle or grain.

A single grain can be composed of several crystals. Granular material can range from very small colloidal particles, through clay, silt, sand, gravel, and cobbles, to boulders[59].

Table (I- 4) The grain/crystallite size of the various NiO films deposited at the different conditions

S.N.	Condition	Grain \ Crystallite size (nm)	Technique	Ref
NiO-Ag	400°C Ni : 42.13 % atomic Ag: 11.06 % atomic O: 47.13 % atomic P : 5.10^{-4} mbar	11.00 (nm)	XRD	[42]
NiO-B	NiO:97 % B:3% 400°C C = 0.1 M	30.00 (nm)	XRD	[43]
NiO	C = 0.5 M T=500°C	1100 (nm)	XRD	[44]
NiO	C = 0.5 M T=500°C Precusar = 10 mL	73.62 (nm)	SEM	[45]
Co_xNi_{1-x}	C =0.1 M	124 (nm)	XRD	[46]

$x\text{O}$	T = 573°K X = 0.15 Nozzl = 28 cm			
NiO:8Li	C = 1 M T = 600°C	17.7 (nm)	SEM	[47]
NiO:8Li	C = 0.1 M T = 400-430°C	20 (nm)	SEM	[48]
NiO	C = 0.2 M T = 470°C	50 (nm)	XRD	[49]
NiO	T = 300°C C = 0.03 M	20 (nm)	SEM	[50]
NiCo₂O₄	T = 300° C = 0.1 M	10 (nm)	XRD	[60]
NiO	T = 360°C C = 0.1 M T _a = 30 min	116 (nm)	XRD	[51]
NiO	T = 460°C C = 0.2 M	350 (nm)	XRD	[52]
NiO_{1-x} Zn_x	T = 623°K C = 0.1 M X = 0.05	18.75 (nm)	XRD	[53]
NiO	T = 350°C C = 0.75 M	12.82 (nm)	AFM	[54]
NiO	T = 450°C C = 0.01	92 (nm)	XRD	[55]

I-3-1-C- Lattic parameter

The lattice constant (see Table (I- 5)), or lattice parameter, refers to the physical dimension of unit cells in a crystal lattice. Lattices in three dimensions generally have three lattice constants, referred to as a , b , and c . However, in the special case of cubic crystal structures, all of the constants are equal and we only refer to a . Similarly, in hexagonal crystal structures, the a and b constants are equal, and we only refer to the a and c constants. A group of lattice constants could be referred to as lattice

parameters. However, the full set of lattice parameters consist of the three lattice constants and the three angles between them.

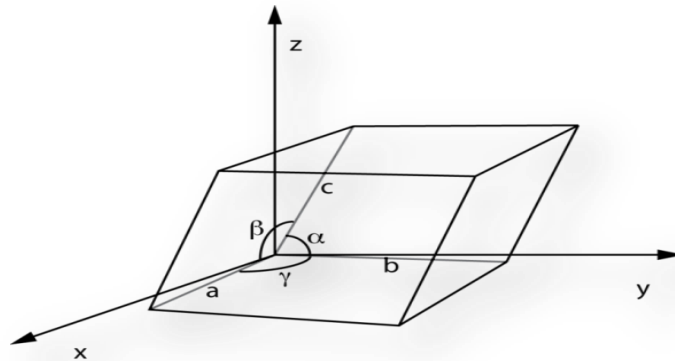


Figure (I- 1): Unit cell definition using parallelepiped with lengths a , b , c and angles between the sides given by α , β , γ [61]

For example, the lattice constant for a diamond is $a = 3.57 \text{ \AA}$ at 300 K. The structure is equilateral although its actual shape cannot be determined from only the lattice constant. Furthermore, in real applications, typically the average lattice constant is given. Near the crystal's surface, the lattice constant is affected by the surface reconstruction that results in a deviation from its mean value. This deviation is especially important in nanocrystals since the surface to nanocrystal core ratio is large [61]. As lattice constants have the dimension of length, their SI unit is the meter. The lattice constants are typically on the order of several angstroms (i.e. tenths of a nanometer). The lattice constants can be determined using techniques such as X-ray diffraction or with an atomic force microscope. The lattice constant of a crystal can be used as a natural length standard of the nanometer range.

In epitaxial growth, the lattice constant is a measure of the structural compatibility between different materials. Lattice constant matching is important for the growth of thin layers of materials on other materials; when the constants differ, strains are introduced into the layer, which prevents the epitaxial growth of thicker layers without defects [61].

I-3-1-D- Mean strain

In general terms, the strain is a macroscopic *measure of deformation*. Truesdell and Toupin, in their famous *Classical Field Theories* review article in *Handbuch der Physik*,

introduce the concept as “The change in length and relative direction occasioned by deformation are called [62], loosely *strain*(see Table(I -5)).

The concept is indeed loose until some additional qualifiers are called upon to render the matter more specific.

Table(I -5) The grain/crystallite size of the various NiO films deposited at the different

S.N.	Condition	Lattice parameter a	ε ($L^{-2}m^{-4}$)	Ref
NiO	C = 0.5 M T=500°C	0.42153 (nm)	--	[63]
NiO	C = 0.2 M T=400°C	0.41903 (nm)	$6.39 \cdot 10^{-3}$	[44]
NiO-Li	C = 0.1 M T=460°C	0.4186 (nm)	--	[64]
Ni _(1-x) Mn _x O	C = 0.2 M T=380°C	0.4173 (nm)	--	[65]

I-3-2-Optical Properties of NiO Thin Films

Nickel oxide is one of the most promising low cost, polarisable materials that exist since it is characterized as having excellent durability, electrochemical stability and high transmittance of 80%-90% at the spectrum range of 400-900 nm [66]. It is known as a good transparent conducting material because it's of wide band gap[67].

The analysis optical observation spectrum is one of the most productive tools for understanding and developing the band structure and energy band gap E_g of crystalline structure. Optical characterization was carried out using a UV-VIS-NIV spectra photometer [68]

In situ transmittance measurement was carried out during the electrochemical measurement at the wavelength ($\lambda = 550$ nm) using an UV-Vis-Nir spectrophotometer ($\lambda = 950$ nm) [69] from variant spectral transmittance of the lingers in the three electrodes cell at normal incident angle against a reference cell that ave a global glass substrate in the devices is measured in the spectral range from 300 to 3000 nm against air as a reference.

The variation in optical density (ΔOD) was calculated by the measured transmittance of the layer or device in the colored (T_c) and bleached (T_d) state by the application of this equation, $\Delta OD = \log_{10}(T_b/T_c)$ [69]

I-3-2-A- The transmittance of NiO thin films

The transmittance of NiO thin films obtained by many researchers confined between 40 to 80%, in the range of visible these values vary from substrate to substrate according to conditions of the experiment, they many experiments obtain the transmittance of NiO thin films equal to 80%.

Pathalet al [70], in their own experiences found when increased the concentrate solution of NiO it leads to decreases of transmittance, latter because of increase atoms of Ni in solution, and when we study, we found that samples, when prepared in high temperature are characterized by good transmittance because of crystallization in the good case [46], in the other direction and from researchers, they spokes about thickness are found the transmittance affected by length of thickness NiO thin films, if the transmittance high so the NiO thin films have superfine thickness these NiO thin films found by many researchers [47], finally there is an effect, the doping by more materials such as Ag, Zn, Li, Co, Cu and Na et al. Eachelement has a special effect:

- Several researchers have found if the value of Zn in the solution of $Zn_xNi_{1-x}O$ is law, so the transmittance have big values [71]
- Many experiments affirm that, if the high value of Mn in the solution $Ni_{1-x}Mn_xO$, so the transmittance is law [72]
- We found several research, the law percentage of Li in the solution of NiO makes big transmittance of NiO thin films [73]

Table (I-6) *The relation between grain/crystallite size and transmittance NiO films deposited at the different conditions*

S.N.	Condition	Grain \ Crystallite size (nm)	Transmittance (%)	Ref
NiO-Ag	400°C Ni : 42.13 % atomic Ag: 11.06 % atomic	11.00 (nm)	39 %	[42]

	O: 47.13 % atomic P : 5.10^{-4} mbar			
NiO-B	NiO:97 % B:3% 400°C C = 0.1 M	30.00 (nm)	12 %	[43]
NiO	C = 0.5 M T=500°C	1100 (nm)	40 %	[44]
NiO	C = 0.5 M T=500°C Precursor = 10 mL	73.62 (nm)	70 %	[45]
Co_xNi_{1-x}O	C =0.1 M T = 573°K X = 0.15 Nozzl = 28 cm	124 (nm)	70 %	[46]
NiO:8Li	C = 1 M T = 600°C	17.7 (nm)	75 %	[47]
NiO:8Li	C = 0.1 M T = 400-430°C	20 (nm)	73 %	[48]
NiO	Ni = 58.80 w % O = 22.26 w % C = 18.93 w % T = 470°C	50 (nm)	68 %	[49]
NiO	T = 300°C C = 0.03 M	20 (nm)	30 %	[50]
NiCo₂O₄	T = 300° C = 0.1 M	10 (nm)	59 %	[60]
NiO	T = 360°C C = 0.1 M T _a = 30 min	116 (nm)	76 %	[51]
NiO	T = 460°C	350 (nm)	75 %	[52]

	C = 0.2 M			
NiO_{1-x}	T = 623°K	18.75 (nm)	75 %	[53]
Zn_x	C = 0.1 M X = 0.05			
NiO	T = 350°C C = 0.75 M	12.82 (nm)	65 %	[54]
NiO	T = 450°C C = 0.01	92 (nm)	71 %	[55]

I-3-2-B- Absorbance of NiO thin films

In the last years, many researchers' spokes to absorbance, they found that the value of absorbance for NiO thin films between 0.1 and 0.8 in the range 380 to 800 nm of the wavelength visible.

Akl and Mahmoud [74], however, the absorbance it's affected by more property such as temperature, she superfast in the law temperature on account of miss-class of atoms, this is last prevented passing the light, they found other researchers [75], that absorbance affected by concentration, so the absorbance law in the highest molarities because of there is no stacking of the grain thin films which facilitate passage of light. And in the other article [76], they found influence to absorbance by thickness, so small values of absorbance resulting from large thickness, finally we saw on other influential it's doping by many materials, such as Ag, Zn, Co, Cu and Na, et al, each element has a special effect :

- The higher the percentage of Zn in Zn_xNi_{1-x}O solution of thin films, so the decreased value of the absorption NiO thin films [77].
- In decrease that value of Mn with NiO, so higher the percentage of absorption [78].
- The solution of NiO:Li if the concentration Li is law, so the absorption of NiO thin films is also weak [79].

I-3-2-C- Optical band gap of NiO thin films

In solid-state physics, a band gap, also called an energy gap or band gap, is an energy range in a solid where no electron states can exist. In graphs of the electronic band structure of solids, the band gap generally refers to the energy difference (in electron volts) between the top of the valence band and the bottom of the conduction

band in insulators and semiconductors. It is the energy required to promote a valence electron bound to an atom to become a conduction electron, which is free to move within the crystal lattice and serve as a charge carrier to conduct electric current. It is closely related to the HOMO/LUMO gap in chemistry. If the valence band is completely full and the conduction band is completely empty, then electrons cannot move in the solid; however, if some electrons transfer from the valence to the conduction band, then the current can flow. Therefore, the band gap is a major factor determining the electrical conductivity of a solid. Substances with large band gaps are generally insulators, those with smaller band gaps are semiconductors, while conductors either have very small band gaps or none, because the valence and conduction bands overlap (see Table(I-7)) [80].

$$(\alpha h\nu)^2 = A (h\nu - E_g)$$

where

- A is a constant
- $h\nu$ is the photon energy
- E_g is the optical band gap energy E_g .

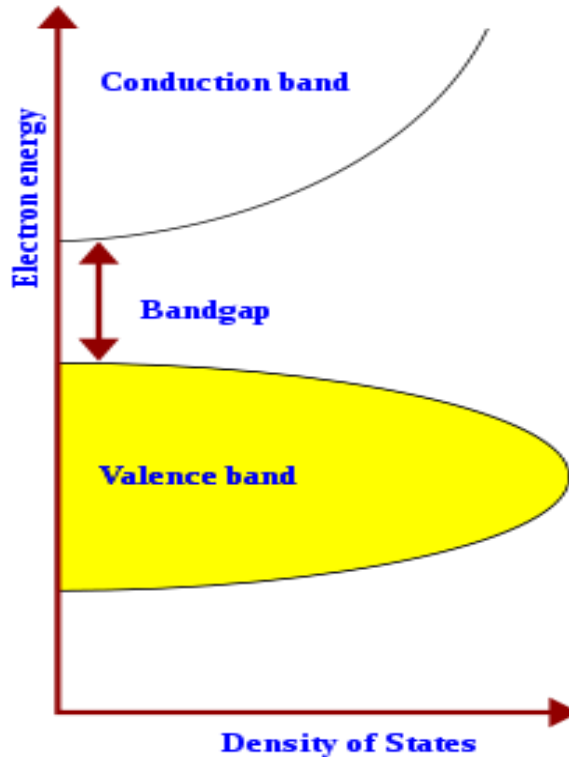


Figure (I- 2): Band gap in semiconductor

Table(I -7): Band gap energy and transmittance values of NiO thin films deposited at different conditions

S.N.	Condition	Band gap energy (eV)	Transmittance (%)	Ref
Li-NiO	T= 420°C C = 0.1 M	Eg=3.51 eV	68 %	[41]
NiO-Ag	400°C Ni : 42.13 % atomic Ag: 11.06 % atomic O: 47.13 % atomic P : 5.10 ⁻⁴ mbar	Eg=3.00 eV	39 %	[42]
NiO-B	NiO:97 % B:3% 400°C C = 0.1 M	Eg=3.58 eV	12 %	[43]
NiO	C = 0.5 M T=500°C	Eg=3.28 eV	40 %	[a4]
NiO	C = 0.5 M T=500°C Precusar = 10 mL	Eg=3.64 eV	70 %	[45]
Co_xNi_{1-x}O	C =0.1 M T = 573°K X = 0.15 Nozzl = 28 cm	Eg = 3.26 eV	70 %	[46]
NiO:8Li	C = 1 M T = 600°C	Eg = 2.28 eV	80 %	[47]
NiO	Ni = 58.80 w % O = 22.26 w % C = 18.93 w % T = 470°C	Eg = 3.11 eV	85 %	[48]
NiO	T = 300°C C = 0.03 M	Eg = 3.56 eV	68 %	[49]

Zn_xNiO_{1-x}	T = 460° C = 0.1 M X = 0.6	Eg = 3.66 eV	30 %	[81]
NiO	T = 360°C C = 0.1 M	Eg = 3.48 eV	86%	[51]
NiO	T = 460°C C = 0.2 M	Eg = 3.41 eV	90 %	[52]
NiO_{1-x}Zn_x	T = 623°K C = 0.1 M X = 0.05	Eg = 3.48 eV	75 %	[53]
NiO	T = 350°C C = 0.75 M	Eg = 3.70 eV	65 %	[54]
NiO	T = 450°C C = 0.01	Eg = 3.82 eV	84 %	[55]
NiO-Cu	T = 1737°F Cu = 16.17 at%	Eg = 3.6 eV	45 %	[56]
(NiO)_{1-x}(ZnO)_x	T = 400°C C = 0.05 M X = 0.25	Eg = 3.67 eV	60 %	[57]

I-3-2-D- Refractive index

The optical reflectance spectra (R) have been used to determine the refractive index (n) (see table I.8) of the film through the relation [82-83].

$$n = \frac{1 + R}{1 - R} \sqrt{\frac{4R}{(1 - R)^2} - K^2}$$

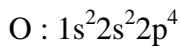
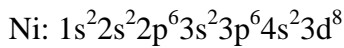
where K is the extinction coefficient, R is the reflection; n is the refractive index [84-85]

Table(I -8): Refractance index values of NiO thin films deposited at different conditions

N.S	condition	n	Ref
Li-NiO	T= 420°C C = 0.1 M	1.72	[41]
NiO	T = 360°C C = 0.1 M	1.98	[51]

I-3-3 - Electrical Properties of NiO Thin Films

The electronic band of the nickel oxygen are expressed as:



NiO is a native p-type semiconducting material [86].

The electrical conductivity of NiO films has a string depended on the microstructure defect existing in NiO crystallites, such as nickel vacancies and interstitial.

Furthermore, the microstructure and composition, as well as the deposition conditions and environment, are the main factor affecting the electrical properties of NiO thin films [87].

They found that the electrical conductivity of NiO is strongly related to the formation of microstructure defect inside the NiO crystallites, such as nickel vacancies and interstitial oxygen, it was related the decreasing in carrier concentration and mobility, which as a p-type semiconductor, in which vacancies occur in caption sites, from each caption vacancy, two electron holes are formed.

- The existing in NiO films are electron holes, which are responsible for the electrical conductivity of the undoped nickel oxide.
- The resistivity is inverse proportional to the product of the carrier concentration with their mobility.
- The decrease in resistivity can be explained by the improved stoichiometry of the film.

Alver et al [88], investigated the synthesis and characterization of born-doped NiO thin films produced by spray pyrolysis. Obtained an electrical resistivity in the range of 0 to 19 Ω .m, they found the resistivity of Boron doped NiO films with doping by annealing

temperature is smaller than without, when they introduced Boron atoms in the ZnO matrix the decrease in resistivity might be mainly due to the substitution of B³⁺ with Ni²⁺ in the lattices, which provides more free electrons for the conduction mechanism. Similar results are obtained with [89].

Table(I -9): Electrical conductivity values of NiO thin films deposited at different conditions

S.N.	Condition	Electrical conductivity ($\Omega\cdot\text{cm}$) ⁻¹	Ref
Li-NiO	420°C	$\sigma = 8$	[41]
NiO-Ag	400°C Ni : 42.13 % atomic Ag: 11.06 % atomic O: 47.13 % atomic P : 5.10 ⁻⁴ mbar	$\sigma = 0.0073$	[42]
NiO-B	NiO:97 % B:3% 400°C C = 0.1 M	$\sigma = 2.8$	[43]
NiO	C = 0.5 M T=500°C	$\sigma = 0.56$ $\sigma = 11.59$	[44]
NiO-Li	NiO = 98 % Li = 2 %	$\sigma = 0.47$	[89]
NiO:8Li	C = 1 M T = 600°C	$\sigma = 0.3$	[47]
NiO:8Li	C = 1 M T = 400-430°C	$\sigma = 10^2$	[48]
NiO	C = 0.2 M T = 470°C	$\sigma = 2.3 \cdot 10^{-5}$	[49]
NiO	T = 360°C	$\sigma = 11.24$	[51]

	C = 0.1 M		
NiO	T = 460°C	$\sigma = 4.34$	[52]
	C = 0.2 M		
NiO_{1-x}Zn_x	T = 623°K	$\sigma = 10^{-9}$	[53]
	C = 0.1 M		
	X = 0.05		
NiO-Cu	T = 1737°F	$\sigma = 0.1$	[56]
	Cu = 16.17 at%		
(NiO)_{1-x}(ZnO)_x	T = 400°C	$\sigma = 10^{-9}$	[57]
	C = 0.05 M		
	X = 0.25		

I-3-4 - Magnetic Properties of NiO Thin Films

The change of crystal structure with temperature actually is associated with the magnetic properties of nickel oxide. The Neel temperature (TN) depends as the temperature at which antiferromagnetism changes to paramagnetism. Nickel oxide is antiferromagnetic at room temperature, and paramagnetic above (TN= 250°C).

Each magnetic unit cell contains four chemical unit cells. Above the Neel temperature, the spin ordering disappears and spin becomes random [90].

I-4- Nickel oxide application

Wide band gap semiconducting nickel oxide (NiO) thin films have attracted considerable attention because of their low material cost, excellent durability, and electrochemical stability in a broad range of application such as:

- An antiferromagnetic material.
- Solar thermal absorber.
- Part of functional sensor layers in chemical sensors.
- The positive electrode in batteries.
- Promising ion storage material in terms of cyclic stability.
- Giant magnetoresistive spin valve structures.
- Resistive memories.
- P-type transparent conducting films.

- Photo electrolysis.
- Fuel cell.
- Electrocatalysis [91].
- Electrochemical device heterogeneous catalysis as well as lithium batteries [92].
- A material for the electro chromic display device [93].

I-5- Conclusion

Nickel oxide (NiO) has attracted a great deal of attention due to its wide direct band gap of (3.6-4.2 eV), which exhibits p-type conductivity. Stoichiometric NiO is an insulator with a resistivity of the order of $10^{13}\Omega\cdot\text{cm}$ at room temperature. NiO is one of the most important oxide materials due to its excellent chemical stability and durability, low toxicity, large span optical density, low cost and good thermal stability and high stability that are similar to ZnO. NiO can be used in various potential applications such as solar cells due to the p-type semiconducting, transparent diodes, transparent transistors, displays and defrosting windows because their transparency can be used for the UV photo detectors and touch screens due to the good responsiveness. NiO can be produced by several techniques such as reactive evaporation, molecular beam epitaxy (MBE), magnetron sputtering technique, pulsed laser deposition (PLD), spray pyrolysis, sol-gel process, chemical vapor deposition, and electrochemical deposition.

References:

- [1] A. Dihaa, S. Benramache, B. Benhaoua, ‘Transparent nanostructured Co doped NiO thin films deposited by sol–gel technique,’ *Optik*, vol. 172, pp.832–839, 2018.
- [2] Y. Adachi, N. Saito, I. Sakaguchi, T.T. Suzuki, ‘Polarity dependent gas sensing properties of ZnO thin films,’ *Thin Solid Films*, vol. 685, pp. 238-244, 2019.
- [3] S Benramache, Y Aoun, A Charef, B Benhaoua, S Lakel, ‘Transition width effect on optical characterizations of ZnO thin films deposited by spray ultrasonic,’ *Inorganic and Nano-Metal Chemistry*, vol. 49, pp.177–181, 2019.
- [4] R. Vinodkumar, J. Varghese, J. Varghese, S.K Saji, N.V. Unnikrishnan, ‘Structural, optical and dielectric properties of gadolinium incorporated laser ablated ZnO thin films,’ *Optik*, vol. 174, pp. 274-281, 2018.
- [5] D. Selvakumar, R. Vasudevan, R. Jayavel, ‘Formation OfPbSe – ZnO Thin Film Based Heterostructure For Solar Cell Applications,’ *Materials Today: Proceedings*, vol. 5, pp. 14468-14472, 2018.
- [6] M.N. Suma, M.V.N. Prasad, V. Gaddam, K. Rajanna, MM Nayak, ‘Development of a Novel Acoustic Sensor using Sputtered ZnO Thin Film,’ *Journal of Pure Appliedand Industrial Physics*, vol. 9, pp. 1-7, 2019.
- [7] H.Y Lee, C.W. Lin, C.T. Lee, Aluminum-nano sphere-stacked MgNiO metal-semiconductor-metal ultraviolet photodetectors, ‘*Journal of Alloys and Compounds*, vol. 773, p. 210-216, 2019.
- [8] D. Dong, W. Wang, A. Barnabé, L. Presmanes, A. Rougier, G. Dong, F. Zhang, H. Yu, Y. He, X. Diao, ‘Enhanced electro chromism in short wavelengths for NiO:(Li, Mg) films in full inorganic device ITO/NiO:(Li, Mg)/Ta2O5/WO3/ITO,’ *ElectrochimicaActa*, vol. 263, pp.277–285, 2018.
- [9] C.T. Tsai, C.T. Wang, Y.Y. Chen, P.C. Kao, S.Y. Chua, ‘Improved hole-injection and external quantum efficiency of organic light-emitting diodes using an ultra-thin K-doped NiO buffer layer,’ *Journal of Alloys and Compounds*, vol. 797, pp. 159-165, 2019.
- [10] L. Li, Z. Liu, L. Wang, B. Zhang, Y. Liu, L., Ji.P. Ao, ‘Self-powered GaN ultraviolet photodetectors with p-NiO electrode grown by thermal oxidation,’ *Materials Science in Semiconductor Processing*, vol. 76, pp. 61-64, 2018.

- [11] S. Joseph, O. N. Balasundaram, Structural, Optical and Electrical Studies on Chemical Spray Deposited Cu Doped NiO Thin Films for p–n Junction Diode Application,” *Journal of Advanced Physics*, vol. 7, pp. 319-324, 2018.
- [12] M. Shkir, V. Ganesh, S. AlFaify, I. S. Yahia, H. Y. Zahran, ‘Tailoring the linear and nonlinear optical properties of NiO thin films through Cr³⁺ doping,” *Journal of Materials Science: Materials in Electronics*, vol. 29, pp. 6446-6457, 2018.
- [13] A. Charef, S. Benramache, Y. Aoun, B. Benhaoua, S. Lakel, M. Marrakchi, Effect of Substrat Temperature on the Growth and Properties of Nanocrystalline NiO Thin Films, *Journal of Nanoelectronics and Optoelectronics*, vol. 14, pp. 1667–1671, 2019.
- [14] A. Diha, S. Benramache, L. Fellah, ‘The Crystalline Structure, Optical and Conductivity Properties of Fluorine Doped ZnO Nanoparticles,” *Journal of nano- and electronic physics*, vol. 11, p.03002, 2019.
- [15] S. Benramache, Y. Aoun, S. Lakel, B. Benhaoua, C. Torchi, ‘The calculate of optical gap energy and urbach energy of Ni_{1-x}CoxO thin films,” *Sādhanā*, vol. 44, p. 26, 2019.
- [16] Y. Aoun, M. Marrakchi, S. Benramache, B. Benhaoua, S. Lakel, A. Cherah, ‘Preparation and characterizations of monocrystalline Na doped NiO thin films,” *Materials Research*, vol. 21, p. e20170681, 2018.
- [17] Y. Arata, H. Nishinaka, D. Tahara, M. Yoshimoto, ‘Heteroepitaxial growth of single-phase ε-Ga₂O₃ thin films on c-plane sapphire by mist chemical vapor deposition using a NiO buffer layer,’ *CrystEng Comm*, vol. 20, pp. 6236-6242, 2018.
- [18] L. Ghimpu, V. Suman, D. Rusnac, ‘Influence of the Growth Temperature on the Properties of the Transparent and Conductive NiO Thin Films Obtained by RF Magnetron Sputtering,” *International Conference on Nanotechnologies and Biomedical Engineering*, vol. 77, pp.291–295, 218.
- [19] M.B. Cosar, ‘Plasma assisted low temperature electron beam deposited NiO thin films for electro-optic applications,” *Journal of Vacuum Science & Technology A*, vol. 36, p. 031501 (2018).
- [20] C. Augustine, M. N. Nnabuchi, R.A. Chikwenze, F.N.C. Anyaegbunam, C. Nwosu, C.O. Dike, C.V. Ezeh, B.J. Robert, E.M. Yohanna, E.N. Taddy, ‘Comparative study of pbs-nio and nio-pbsheterojunction thin films deposited by chemical bath deposition technique,” *Chalcogenide Letters*, vol. 15, pp. 591-598, 2018.

- [21] S. Akinkuade, B. Mwankemwa, J. Neln W. Meyer, Structural, optical and electrical characteristics of nickel oxide thin films synthesised through chemical processing method, "Physica B: Condensed Matter, vol. 535, pp. 24–28, 2018.
- [22] S. Mani Menaka, G. Umadevi, "Concentration Dependent Structural, Morphological, Spectral, Optical and Electrical Properties of Spray Pyrolyzed NiO thin films," Silicon, vol. 10, pp. 2023–2029, 2018.
- [23] P.R.S.I. Abbas, A.Q..Ubaid, "Structural, Optical and photoluminescence Properties of Nanocrystalline NiO Thin Films," Journal of Advances in Physics, vol. 6, pp. 1016-1023, 2014.
- [24] H.A. Juybari, M.M.B.Mohagheghi, M.S. Saremi, Nickel–lithium oxide alloy transparent conducting films deposited by spray pyrolysis technique, Journal of Alloys and Compounds, vol. 509, pp. 2770-2775, 2011.
- [25] C. Mrabet, M. Ben Amor, A. Boukhachem, M. Amlouk, T. Manoubi, "Physical properties of La-doped NiO sprayed thin films for optoelectronic and sensor applications," Ceramics International vol. 42, pp. 5963–5978, 2016.
- [26] Y. Ahn, J. Jang, J.Y. Son, "Resistive switching characteristics and conducting nanobits of polycrystalline NiO thin films," Journal of Electroceramics, vol. 38, pp. 100–103, 2017.
- [27] J. Zhu, J. Jiang, J. Liu, R. Ding, H. Ding, Y. Feng, G. Wei, X. Huang, "Direct synthesis of porous NiO nanowall arrays on conductive substrates for supercapacitor application," Journal of Solid State Chemistry, vol. 184, pp. 578-583, 2011.
- [28] I. A. Dhole, Y. H. Navale, C. S. Pawar, S. T. Navale, V. B. Patil, "Physicochemical and supercapacitive properties of electroplated nickel oxide electrode: effect of solution molarity," Journal of Materials Science: Materials in Electronics, vol. 29, pp. 5675–5687, 2018.
- [29] E.R. Shaaban, M.A. Kaid, M.G.S. Ali, "X-ray analysis and optical properties of nickel oxide thin films," Journal of Alloys and Compounds, vol. 613, pp. 324–329, 2014.
- [30] H.Kamal, E.K. Elmaghraby, S.A. Alic, K. Abdel-Had, "Characterization of nickel oxide films deposited at different substrate temperatures using spray pyrolysis," Journal of Crystal Growth, vol. 262, pp. 424-434, 2004.

- [31] K. Zrikem, G. Song, A.A. Aghzzaf, M. Amjoud, D. Mezzane, A. Rougier, "UV treatment for enhanced electrochromic properties of spin coated NiO thin films," *Superlattices and Microstructures*, vol. 127, pp. 35-42, 2019.
- [32] M. Kaur, B.K. Dadhich, R. Singh, K. Ganapathi, T. Bagwaiya, S. Bhattacharya, A.K. Debnath, K.P. Muthe, S.C. Gadkari, "RF sputtered SnO₂: NiO thin films as sub-ppm H₂S sensor operable at room temperature," *Sensors and Actuators B*, vol. 242, pp. 389–403, 2017.
- [33] K.O. Ukoba, T.C. Jen, "Characterization and Fabrication of Nanostructured TiO₂/NiO Heterojunction Solar Cells," *2019 IEEE 2nd International Conference on Power and Energy Applications (ICPEA)*, Singapore, Singapore, pp. 171-176, 2019.
- [34] M. Tyagi, M. Tomar, V. Gupta, "Enhanced electron transfer properties of NiO thin film for the efficient detection of urea," *Materials Science and Engineering: B*, vol. 240, pp. 147-155, 2019.
- [35] I. Dhanya, B. Sasi, "A Study on the Thermodynamics of Grain Growth in R.F. Magnetron Sputtered NiO Thin Films," *Journal of Coatings*, vol. 2013, p. 981515, 2013.
- [36] I. Karaduman, T.Çorlu, M.A.Yıldırım, A.Ateş, S.Acar, "Hydrogen Gas Sensing Characteristics of Nanostructured NiO Thin Films Synthesized by SILAR Method," *Journal of Electronic Materials*, vol. 46, pp. 4017–4023, 2017.
- [37] E.S. Hassan, A. Abdulmunem, S. Abdulhussain, K. Elttayef, "Doping and thickness variation influence on the structural and sensing properties of NiO film prepared by RF-magnetron sputtering," *Journal of Materials Science: Materials in Electronics*, vol. 27, pp. 1270–1277, 2016.
- [38] Adel M El Sayed, "Opto-structural and surface properties of silkworm-like nickel oxide thin films," *Materials Research Express*, vol. 6, p. 116423, 2019.
- [39] N. Duraisamy, A. Numan, S.O. Fatin, K. Ramesh, S. Ramesh, "Facile sonochemical synthesis of nanostructured NiO with different particle sizes and its electrochemical properties for supercapacitor application," *Journal of Colloid and Interface Science*, vol. 471, pp. 136-140, 2016.
- [40] P.S. Patil, L.D. Kadam, "Preparation and characterization of spray pyrolyzed nickel oxide (NiO) thin films," *Applied surface science*, vol. 199, pp. 211-221, 2002.

- [41] P Puspharajah, S Radhakrishna, A. K Arof, ‘Transparent conducting lithium-doped nickel oxide thin films by spray pyrolysis technique,’ *Journal of Materials Science*, vol. 32, pp 3001–3006, 1997.
- [42] Y.A.K. Reddy, B. Ajitha, P.S. Reddy, M.S.P. Reddy, J.H. Lee, ‘Effect of substrate temperature on structural, optical and electrical properties of sputtered NiO-Ag nanocrystalline thin films,’ *Electronic Materials Letters*, vol. 10, pp. 907–913, 2014.
- [43] U. Alver, H. Yaykaşlı, S. Kerli, A. ‘Tanrıverdi, Synthesis and characterization of boron-doped NiO thin films produced by spray pyrolysis,’ *International Journal of Minerals, Metallurgy, and Materials*, vol. 20, pp 1097–1101, 2013.
- [44] A.A.Yadav, U.J.Chavan, ‘Influence of substrate temperature on electrochemical supercapacitive performance of spray deposited nickel oxide thin films,’ *Journal of Electroanalytical Chemistry*, vol. 782, pp. 36–42, 2016.
- [45] V.Gowthami, M.Meenakshi, P.Perumal, R.Sivakuma, C.Sanjeeviraja, ‘Preparation of rod shaped nickel oxide thin films by a novel and cost effective nebulizer technique,’ *Materials Science in Semiconductor Processing*, vol. 27, pp. 1042-1049, 2014.
- [46] R. Sharma, A.D.Acharya, S. Moghe, S.B. Shrivastava, M. Gangrade, T. Shripathi, V.Ganesan, ‘Effect of cobalt doping on microstructural and optical properties of nickel oxide thin films,’ *Materials Science in Semiconductor Processing*, vol. 23, pp. 42-49, 2014.
- [47] C.C. Wua, C.F. Yang, ‘Effect of annealing temperature on the characteristics of the modified spray deposited Li-doped NiO films and their applications in transparent heterojunction diode,’ *Solar Energy Materials and Solar Cells*, vol. 132, pp. 492-498, 2015.
- [48] X. Yi, W. Wenzhong, Q. Yitai, Y. Li, C. Zhiwen, ‘Deposition and microstructural characterization of NiO thin films by a spray pyrolysis method,’ *Journal of Crystal Growth*, vol. 167, pp.656–659, 1996.
- [49] A. Hakim, J. Hossain, K.A. Khan, ‘Temperature effect on the electrical properties of undoped NiO thin films,’ *Renewable Energy*, vol. 34, 2625–2629, 2009.
- [50] P. Nazari, S. Gharibzadeh, F. Ansari, B. AbdollahiNejand, M. Eskandari, S. Kohnehpoushi, V. Ahmadi, M. Salavati-Niasari, ‘Facile green deposition of

- nanostructured porous NiO thin film by spray coating,” *Materials Letters*, vol. 190, pp. 40–44, 2017.
- [51] R. Sharma, A.D. Acharya, S.B. Shrivastava, T. Shripathi, V. Ganesan, Preparation and characterization of transparent NiO thin films deposited by spray pyrolysis technique, “*Optik*, vol. 125, pp. 6751-6756, 2014.
- [52] K. Sajilal, A. Moses, E. Raj, “Effect of thickness on physico-chemical properties of p-NiO (bunsenite) thin films prepared by the chemical spray pyrolysis (CSP) technique,” *Optik*, vol. 127, pp. 1442-1449, 2016.
- [53] R.Sharma, A.D. Acharya, S.B. Shrivastava, M.M. Patidar, M. Gangrade, T. Shripathi, V. Ganesan, “Studies on the structure optical and electrical properties of Zn-doped NiO thin films grown by spray pyrolysis,” *Optik*, vol. 127, pp. 4661-4668, 2016.
- [54] T. Chtouki, L. Soumahoro, B. Kulyk, H. Bougharraf, H. Erguig, B. Sahraoui, “Comparison of structural, morphological, linear and nonlinear optical properties of NiO thin films elaborated by Spin-Coating and Spray Pyrolysis,” *Optik*, vol. 128, pp. 8–13, 2017.
- [55] R. Romero, F. Martin, J.R. Ramos-Barrado, D. Leinen, “Synthesis and characterization of nanostructured nickel oxide thin films prepared with chemical spray pyrolysis,” *Thin Solid Films*, vol. 518, pp. 4499–4502, 2010.
- [56] S.C.Chen, T.Y.Kuo, Y.C.Lin, H.C. Lin, “Preparation and properties of p-type transparent conductive Cu-doped NiO films,” *Thin Solid Films*, vol. 519, pp. 4944–4947, 2011.
- [57] L. Herissi, L.Hadjeris, M.S. Aida, J. Bougdira, “Properties of (NiO)_{1-x}(ZnO)_x thin films deposited by spray pyrolysis,” *Thin Solid Films*, vol. 605, pp. 116–120, 2016.
- [58] R.KateSuraj, C. BulakheRamesh J. Deokate, “Effect of Substrate Temperature on Properties of Nickel Oxide (NiO) Thin Films by Spray Pyrolysis,” *Journal of Electronic Materials*, vol. 48, pp. 3220–3228, 2019.
- [59] N.G. Cho, I.S. Hwang, H.G. Kim, J.H. Lee, I.D. Kim, “Gas sensing properties of p-type hollow NiO hemispheres prepared by polymeric colloidal templating method,” *Sensors and Actuators B: Chemical*, vol. 155, pp. 366-371, 2011.
- [60] R.J. Deokate, R.S. Kalubarme, C.J. Park, C.D. Lokhande, “Simple Synthesis of NiCo₂O₄ thin films using Spray Pyrolysis for electrochemical supercapacitor application: A Novel approach,” *ElectrochimicaActa*, vol.224, pp. 378–385, 2017.

- [61] H.W. Shin, J.Y. Son, "A conducting atomic force microscopy study of conducting filament nanobits in the epitaxial NiO thin film prepared precisely controlled by the oxidation time of the single crystalline Ni substrates," *Ultramicroscopy*, vol. 205, pp. 57-61, 2019.
- [62] S.H. Wang, S.R. Jian, G.J. Chen, H.Z. Cheng, J.Y. Juang, "Annealing-Driven Microstructural Evolution and Its Effects on the Surface and Nanomechanical Properties of Cu-Doped NiO Thin Films," *Coatings*, vol. 9, pp. 1-13, 2018.
- [63] S. Kerli, U. Alver, H. Yaykaşlı, "Investigation of the properties of In doped NiO films," *Applied Surface Science*, vol. 318, pp. 164–167, 2014.
- [64] S.M. Menaka, G. Umadevi, M. Manickam, "Effect of copper concentration on the physical properties of copper doped NiO thin films deposited by spray pyrolysis," *Materials Chemistry and Physics*, vol. 191, pp. 181-187, 2017.
- [65] B. Kannan, R. Pandeewari, B.G. Jeyaprakash, "Influence of precursor solution volume on the properties of spray deposited α -MoO₃ thin films," *Ceramics International*, vol. 40, pp. 5817–5823, 2014.
- [66] A. Diha, S. Benramache, B. Benhaoua, "Transparent nanostructured Co doped NiO thin films deposited by sol–gel technique," *Optik*, vol. 172, pp. 832-839, 2018.
- [67] S.A. Mahmoud, S. Alshomer, M.A. Tarawnh, "Structural and optical dispersion characterisation of sprayed nickel oxide thin films," *Journal of Modern Physics*, vol. 2, pp. 1178-1186, 2011.
- [68] S. Benramache, Y. Aoun, S. Lakel, H. Mourghade, R. Gacem, B. Benhaoua, "Effect of Annealing Temperature on Structural, Optical and Electrical Properties of ZnO Thin Films Prepared by Sol-Gel Method," *Journal of Nano- and Electronic Physics*, vol. 10, p.06032, 2018.
- [69] V. Panneerselvam, K.K. Chinnakutti, S.T. Salammal, A.K. Soman, K. Parasuraman, V. Vishwakarma, V. Kanagasabai, "Role of copper/vanadium on the optoelectronic properties of reactive RF magnetron sputtered NiO thin films," *Applied Nanoscience*, vol. 8, pp. 1299–1312, 2018.
- [70] D.K.Pathak, A. Chaudhary, S. Mishra, P. Yogi, S.K.Saxena, P.R.Sagdeo, R. Kumar, "Precursor concentration dependent hydrothermal NiO nanopetals: Tuning morphology for efficient applications," *Superlattices and Microstructures*, vol. 125, pp. 138-143, 2019.

- [71] J. Al Boukhari, L. Zeidan, A. Khalaf, R. Awad, "Synthesis, characterization, optical and magnetic properties of pure and Mn, Fe and Zn doped NiO nanoparticles," *Chemical Physics*, vol. 516, pp. 116-124, 2019.
- [72] N.N. Ge, C.H. Gong, X.C. Yuan, H.Z. Zeng, X.H. Wei, "Effect of Mn doping on electroforming and threshold voltages of bipolar resistive switching in Al/Mn[thin space (1/6-em)]:[thin space (1/6-em)]NiO/ITO," *RSC Advances*, vol. 8, pp. 29499-29504, 2018.
- [73] J.Y. Zhang, W.W. Li, R.L.Z. Hoye, J.L. MacManus-Driscoll, M. Budde, O. Bierwagen, L.Wang, Y. Du, M.J. Wahila, L.F.J. Piper, T.L. Lee, H.J. Edwards, V.R. Dhanakg, K.H.L. Zhang," Electronic and transport properties of Li-doped NiO epitaxial thin films," *Journal of Materials Chemistry C*, vol. 6, pp. 2275-2282, 2018.
- [74] A.A. Akl, S.A. Mahmoud, "Effect of growth temperatures on the surface morphology, optical analysis, dielectric constants, electric susceptibility, Urbach and bandgap energy of sprayed NiO thin films," *Optik*, vol. 172, pp. 783-793, 2018.
- [75] I. Manouchehri, S.A.O. AlShiaa, D. Mehrparparvar, M.I. Hamil, R. Moradian, "Optical properties of zinc doped NiO thin films deposited by RF magnetron sputtering," *Optik*, vol. 127, pp. 9400-9406, 2016.
- [76] P.Baraskar, R.J.Choudhary, P. Kumar Sen, P. Sen, "Dispersive optical nonlinearities and optical path length compensation in NiO/Al doped NiO bilayer thin film," *Optical Materials*, vol. 96, p. 109278, 2019.
- [77] I. S. Yahia, G. F. Salem, JavedIqbal, F. Yakuphanoglu, "Linear and nonlinear optical discussions of nanostructured Zn-doped CdO thin films," *Physica B: Condensed Matter*, vol. 511, pp. 54-60, 2017.
- [78] N Zhou, Y Cheng, B Huang, X Liao, "Effect of nonmagnetic dopants (Ag, Cu or Mg) on ferromagnetic half-metallic properties of NiO," *Physica B: Condensed Matter*, vol. 557, pp. 6-11, 2019.
- [79] J. Yang, B. Wang, Y. Zhang, X. Ding, J. Zhang, "Low-temperature combustion synthesis and UV treatment processed p-type Li:NiOx active semiconductors for high-performance electronics," *Journal of Materials Chemistry C*, vol. 6, pp. 12584-12591, 2018.

-
- [80] S. Benramache, B. Benhaoua, N. Khechai, F. Chabane, "Elaboration and characterisation of ZnO thin films," *Matériaux& Techniques*, vol. 100, pp. 573-580, 2012.
- [81] S. Benramache, M. Aouassa, "Preparation and Characterization of p-Type Semiconducting NiO Thin Films Deposited by Sol-Gel Technique," *Journal of Chemistry and Materials Research*, vol. 5, pp. 119–122, 2016.
- [82] S.M.H Al-Jawad, Abbas F.S.Al-Shareefi, A.K. Jurdan, "Effect of Thickness on Optical and Electrical Properties of ZnO Prepared by CBD," *Iraqi journal of Applied physics*, vol. 7, pp.11-16, 2011.
- [83] A. Alshahrie, I.S. Yahia, A. Alghamdi, P.Z. Al Hassan, "Composition and Optical Dispersion Characterization of Nanoparticles ZnO-NiO Thin Films: Effect of Annealing Temperature," *Optik*, vol. 127, pp. 5105–5109, 2016.
- [84] Y. Wang, J. Ghanbaja, P. Boulet, D. Horwat, J. F. Pierson, "Growth, interfacial microstructure and optical properties of NiO thin films with various types of texture," *ActaMaterialia*, vol. 164, pp. 648-653, 2019.
- [85] M. Predanocy, I. Hotový, M. Čaplovičová, "Structural, optical and electrical properties of sputtered NiO thin films for gas detection," *Applied Surface Science*, vol. 395, pp. 208-213, 2019.
- [86] L. Zhang, J. He, W. Jiao, "Synthesis and gas sensing performance of NiO decorated SnO₂ vertical-standing nanotubes composite thin films," *Sensors and Actuators B: Chemical*, vol. 281, pp. 326-334, 2019.
- [87] I. Sta, M. Jlassi, M. Hajji, H. Ezzaouia, "Structural, optical and electrical properties of undoped and Li-doped NiO thin films prepared by sol-gel spin coating method," *Thin Solid Films*, vol. 555, pp. 131-137, 2014.
- [88] W.C. Lee, E.C. Choi, J.H. Boo, B. Hong, "A study on characterization of nano-porous NiO thin film to improve electrical and optical properties for application to automotive glass," *Thin Solid Films*, vol. 641, pp. 28-33, 2017.
- [89] A.A. Ahmed, M.R. Hashim, M. Rashid, "Control of the structural, electrical and optical properties of spin coated NiO films by varying precursor molarity," *Thin Solid Films*, vol. 690, p. 137554, 2019.

- [90] K. Sajilal, A. Moses E. Raj,, ‘’ Effect of thickness on structural and magnetic properties of NiO thin films prepared by chemical spray pyrolysis (CSP) technique,’’ *Materials Letters*, vol. 164, pp. 547-550, 2016.
- [91] D.R. Sahu, T.J. Wu, S.C. Wang, J.L. Huang, ‘’Electrochromic behavior of NiO film prepared by e-beam evaporation,’’ *Journal of Science: Advanced Materials and Devices*, vol. 2, pp. 225-232, 2017.
- [92] G. Bodurov, P. Stefchev, T. Ivanova, K. Gesheva, Investigation of electrodeposited NiO films as electrochromic material for counter electrodes in ‘’Smart Windows,’’ *Materials Letters*, vol. 117, pp. 270-272, 2014.
- [93] C. Li, J.H. Hsieh, T.Y. Su, P.L. Wu, ‘’Experimental study on property and electrochromic function of stacked WO₃/Ta₂O₅/NiO films by sputtering,’’ *Thin Solid Films*, vol. 660, pp. 373-379, 2018.

CHAPTER TWO

Elaboratoin and characterizations

II-1- Introduction:

The NiO and ZnO solutions were sprayed on the heated glass substrates by spray pneumatic method which transforms the liquid to a formed stream with uniform and fine droplets of 25 μm average diameter. The deposition was performed at a substrate temperature of 450°C with deposition rate was 5.7 mL /min.

The structural properties of: NiO, (Zn doped NiO) and (Ni doped ZnO) films were studied by means of X-ray diffraction (XRD Bruker AXS-8D) with $\text{CuK}\alpha$ radiation ($\lambda=0.15406$ nm) in the scanning range of (2θ) was between 20° and 70°. The optical transmission of the deposited films was measured in the range of (300 – 1000 nm) by using an ultraviolet-visible spectrophotometer (LAMBDA 25) while the electrical resistance R was measured by four point methods.

II-2- Elaboration

Preparation of thin layers of nickel oxide and zinc oxide with thermal chemical spraying technology

II-2-1- Spray Technique

This the method which is one of the chemical methods is used in our current research. It was developed in the sixties of the last century and because of the urgent need for less expensive technology for the preparation of large-scale devices in the photovoltaic industries. The Thin layer membranes of sulfides and inorganic cyanides are prepared by hydrolysis on a hot base. The first to use this method was **Auger & Hotle** In 1956 as they prepared a black copper membrane on an aluminum base using a selective surface [1].

II-2-2- Mechanism

The chemical thermal spraying is the most common chemical methods for the preparation of thin films. This method is to spray the solution of the substance to be prepared in the form of very thin droplets (a few tens of micrometers per drop) on the bases Hot and at a certain temperature depends on the type of material used. Chemical

reaction occurs between the atoms of the substance and the hot base. This reaction engenders thin membrane.

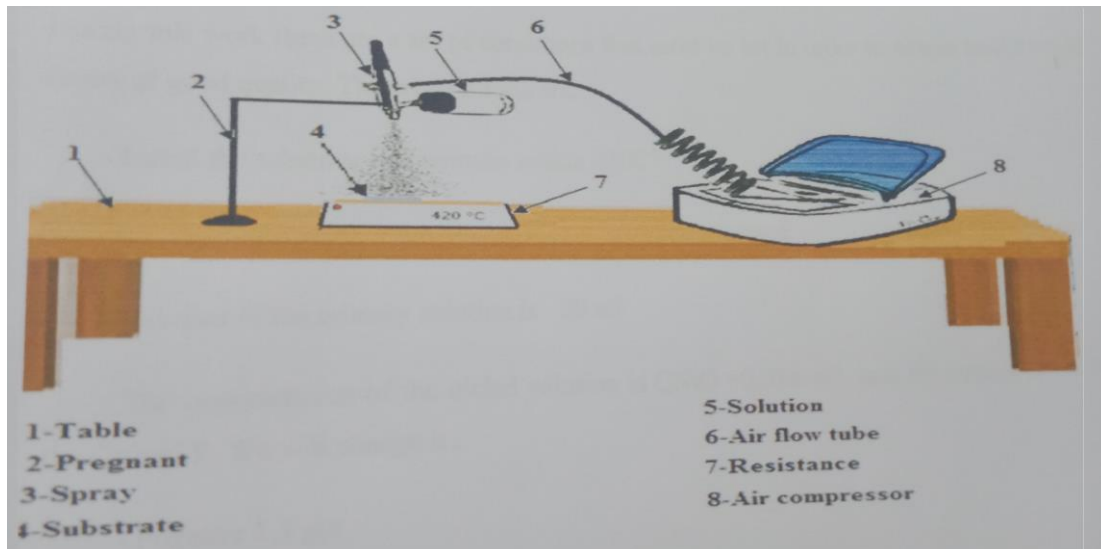


Figure (II-1): spray pneumatic technique.

II-2-3- Advantages of the Spray

- ❖ Economical technology; the fact that the used devices do not need to complex and expensive systems.
- ❖ Membranes can be deposited on a wide area, with thin films prepared with good adhesion and high stability in their physical properties over time.
- ❖ Transient sedimentation is easy to obtain for selected materials in terms of compositional, optical and electrical properties by mixing two or more substances or changing the concentrations of the elements involved in membrane composition or changing the temperature of the base.
- ❖ The preparation of membranes for a wide range of materials with high melting grades is difficult to prepare in other ways.

II-2-4- Disadvantage of the Spray

- ❖ It requires a lot of efforts and time to get homogeneous membranes.
- ❖ Only chemical solutions are used and the powder cannot be deposited directly.

II-3- Parameters of the deposition

During this work there are a set of conditions that must be set in order to obtain nickel oxide and zinc oxide layers of good quality. These conditions are :

- We install the substrate temperature within 450 °C.
- We use nickel acetate ($\text{Ni} (\text{CH}_3.\text{CO}_2)_2 . 4\text{H}_2\text{O}$) as a nickel source .
- We use zinc acetate ($\text{Zn} (\text{CH}_3.\text{CO}_2)_2 . 2\text{H}_2\text{O}$) as a zinc source
- The size of the primary solution is 40 ml
- The concentration of the nickel solution is $C_{\text{NiO}} = 0.05 \text{ mol / l}$.
- The concentration of the zinc solution is $C_{\text{ZnO}} = 0.05 \text{ mol / l}$.
- Pressure 1.0 par
- The distance between the substrate and the sprayer is 42 cm

II-4- Preparation

To prepare thin layers of nickel oxide and zinc oxide, we follow these steps:

II-4-1- Preparation of solution

NiO:

We prepared nickel oxide membranes NiO of nickel acetate solution ($\text{Ni} (\text{CH}_3.\text{CO}_2)_2 . 4\text{H}_2\text{O}$) which is a solid material Green-colored molecular weight $M=248.84 \text{ g/mol}$. The weight of the nickel acetate should be mixed in size $V=40 \text{ ml}$ of distillation water to prepare solution with calculated concentration using the following method.

We have a concentration of NiO solution C:

$$C = n/V \quad (\text{II-1})$$

Where:

C: Concentration of solution (mol/l)

n: material quantity (mol)

V: Volume of the solvent (l)

And on the other hand we have the amount of material n:

$$n = m / M \quad (\text{II-2})$$

Where:

m: Nickel nitrates block (g) , M: Molten mass of nickel nitrates (g/mol)

To compensate the latest relationships to repel that the mass of nickel nitrates are calculated as follows:

$$m=MCV \quad (\text{II-3})$$

The weight of nickel acetate to be dissolved at different concentrations to ensure full solubility. We use a magnetic (disc+) mixer to mix the solution for 20 minutes. This is to ensure that there are no sediments with heating for homogeneity and we add drops HCl to remove undesirable elements. So, we get the required solution.

Table (II-1):The physical and chemical properties of Nickel [2].

Chemical name	Nickel Acetate
Molecular formula	C ₄ H ₆ O ₄ .Ni.4H ₂ O
Molecular weight	248.84 g/mol
Color	Green
Density	1.78 g/cm ³
Melting point	56.7 °C

ZnO:

We prepared zinc oxide membranes ZnO of zinc acetate solution (Zn (CH₃.CO₂)₂ . 2H₂O) which is a solid material White-colored molecular weight M=219.50 g/mol. The weight of the zinc acetate should be mixed in size V=40 ml of distillation water.

Table (II-2):The physical and chemical properties of Zinc [3].

Chemical name	Zinc Acetate
Molecular formula	$C_4H_6O_4 \cdot Zn \cdot 2H_2O$
Molecular weight	219.50 g/mol
Color	White
Density	1.735 g/cm^3
Melting point	237°C

II-4-2-Preparatin of the substrate

❖ Glass Substrates

During this study, NiO and ZnO thin films were deposited on glass substrates (see Figure II.2) which have a length of 2.5cm and a width of 2.5cm. We chose the glass for these reasons:

- The thermal compatibility with NiO (thermal dilation coefficients are $\alpha_{\text{glass}} = 8.5 \times 10^6 \text{ K}^{-1}$, $\alpha_{\text{NiO}} = 3.2 \cdot 10^{-5} \text{ K}^{-1}$ [4]. at room temperature) to minimize the constraints with the interface film/substrate.
- For the transparency of the glass which adapts well for the optical characterization of films in the visible one.
- For economic reasons.
- In order to obtain good adherence and uniformity for the films.

*Figure (II-2):Glass Substrates.*

❖ Substrate Cleaning Process

The adherence and the quality of the depot repose on purity and the state on substrate;thus, the cleaning of the substrate is one of the most important steps to remove any contaminated organic compounds.The cleaning of our substrates surfaces is as follows:

- The substrates are cut using a pen with diamond point.
- Washing with soap solution to clean any dusts or attachments.
- Washing with distilled water to remove soap, and then with acetone for 2 min.
- Rinsing with distilled water again.
- Washing with ethanolfor 2 min at ambient temperature.
- Cleaning in water distilled bath.
- The substrates were then left to dry in air.

II-4-3- Preparation of NiO thin films

After preparing both the substrate and the solution, we begin directly the deposition process using chemical thermal spraying technique where the latter undergoes a series of steps:

- ❖ The substrate is placed above the substrate holder and heated gradually from room temperature to the required temperature 450°C.This is to avoid the effect of the substrate by sudden change of temperature.
- ❖ When heated, sprinkle very fine drops of solution on the hot substrateusing the airbrush. This allows the chemical reaction to be activated between the components of the solution. The solvent evaporates due to high temperature and the nickel oxide layer is formed on the surface of the substrate as a result of the reaction.
- ❖ Do not spray on the substrate at once to avoid frosting since in each time the glass slides back to its original temperature. This prevents the membrane from being broken and allows the prepared membranes to complete the process of interaction and crystalline development to obtain a more homogeneous membrane.
- ❖ The NiO thin films were elaborated at 450 °C in air with various deposition rates of 20, 40, 60 and 80 ml.

II-4-4- Preparation of Zn doped NiO thin films ($\text{Ni}_{1-x} \text{Zn}_x \text{O}$)

We prepared a mixture between solution NiO and solution ZnO according to the change of X as shown in Table (II-3).

The NiO thin films were produced at 450 where we spray 40 ml each time on the substrate.

Table (II-3): The experimental conditions of preparation NiO thin films.

The sample number	X	$\text{Ni}_{1-x} \text{Zn}_x \text{O}$	$V_{\text{nickel acetate}}$ (ml)	$V_{\text{zinc acetate}}$ (ml)	V_T (ml)
1	0	Ni_1O	40	0	40
2	0.02	$\text{Ni}_{0.98} \text{Zn}_{0.02} \text{O}$	39.2	0.8	40
3	0.04	$\text{Ni}_{0.96} \text{Zn}_{0.04} \text{O}$	38.4	1.6	40
4	0.08	$\text{Ni}_{0.92} \text{Zn}_{0.08} \text{O}$	36.8	3.2	40
5	0.12	$\text{Ni}_{0.88} \text{Zn}_{0.12} \text{O}$	35.2	4.8	40

II-4-5- Preparation of Ni doped ZnO thin films ($\text{Ni}_{1-x} \text{Zn}_x \text{O}$)

We prepared a mixture between solution ZnO and solution NiO according to the change of X as shown in Table (II-4).

The ZnO thin films were produced at 450 where we spray 40 ml each time on the substrate.

Table (II-4): The experimental conditions of preparation ZnO thin films.

The sample number	X	$\text{Ni}_{1-x} \text{Zn}_x \text{O}$	$V_{\text{nickel acetate}}$ (ml)	$V_{\text{zinc acetate}}$ (ml)	V_T (ml)
1	1	$\text{Zn}_1 \text{O}$	0	40	40
2	0.98	$\text{Ni}_{0.02} \text{Zn}_{0.98} \text{O}$	0.8	39.2	40
3	0.96	$\text{Ni}_{0.04} \text{Zn}_{0.96} \text{O}$	1.6	38.4	40
4	0.92	$\text{Ni}_{0.08} \text{Zn}_{0.92} \text{O}$	3.2	36.8	40
5	0.88	$\text{Ni}_{0.12} \text{Zn}_{0.88} \text{O}$	4.8	35.2	40

II-5- Characterization of the films

Nano-particles of NiO and ZnO semiconducting electrochromic thin films have been prepared depending on the structural, optical and electrical characteristics which have been studied using different measuring techniques that are listed below:

- X-ray diffraction (DRX)
- Ultraviolet-visible spectroscopy.
- the electrical conductivity was measured by the mean of four points.

II-5-1- Structural characterization

❖ X-ray diffraction

X-ray diffraction (XRD) is a material characterization technique that is used to determine the crystalline quality, chemical composition, and atomic structure of a solid material.

X-rays are typically generated by accelerating electrons at a metal target at several KeV which causes the core electrons in the metal target to become knocked out by the energized electrons. When the higher shell electrons fall into the vacancies in the core shell, it causes x-rays to be emitted. A copper source is one of the most common metal targets. These x-rays are called Characteristic x-rays because they have well-defined wavelengths that corresponds to the energy difference between the two shells in the metal target. The characteristic x-rays are sent towards the sample and they cause the atoms and their electrons to scatter the x-rays [5].



Figure (II-3): Bruker D8 Advanced X-ray Diffractometer[6].

Since the wavelengths of the x-rays (1-100Å) are similar in size to the inter-atomic spacing (d_{hkl}) of the material, the waves diffract and scatter, gathering and carrying information about the material's individual atoms and their arrangement. Crystalline samples which possess long-range order in their atomic arrangement represented by crystal structures, are easy to be measured because they scatter strongly in certain directions. The building block of the crystalline sample is the crystal structure and its unit cell. According to Bragg's law, these unit cells will all scatter.

$$n\lambda = 2d_{hkl} \sin\theta \quad (\text{II-4})$$

Equation (II-4) Bragg's law describes at which angles and wavelengths an incident x-ray wave will cause constructive interference of the scattered waves.

Where:

- n is an integer.
- λ is the wavelength of the incident wave.
- d_{hkl} is the spacing between the planes in the atomic lattice.
- θ is the angle between the scattered wave and the atomic plane [5].

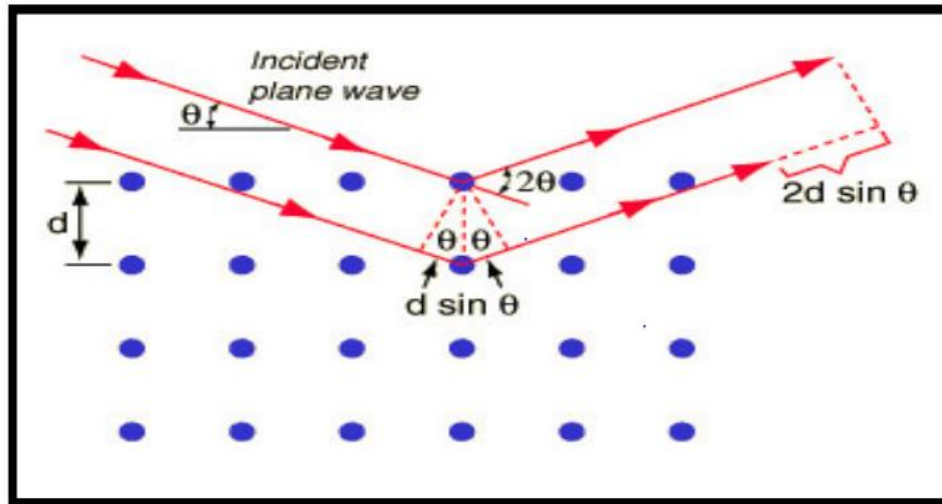


Figure (II-4): Bragg's diffraction [7].

According to the (XRD):

- In the case of polycrystalline films, the (XRD) shows various peaks at different angles of diffraction and diffraction pattern as shown in figure (II-5 a) .
- The single crystal material exhibits sharp reflections (sharp peaks). As shown in Figure (II-5 b).
- For the amorphous films material, the diffraction does not exhibit any sharp peaks. This can be simply represented in Figure (II-5 c) [7].

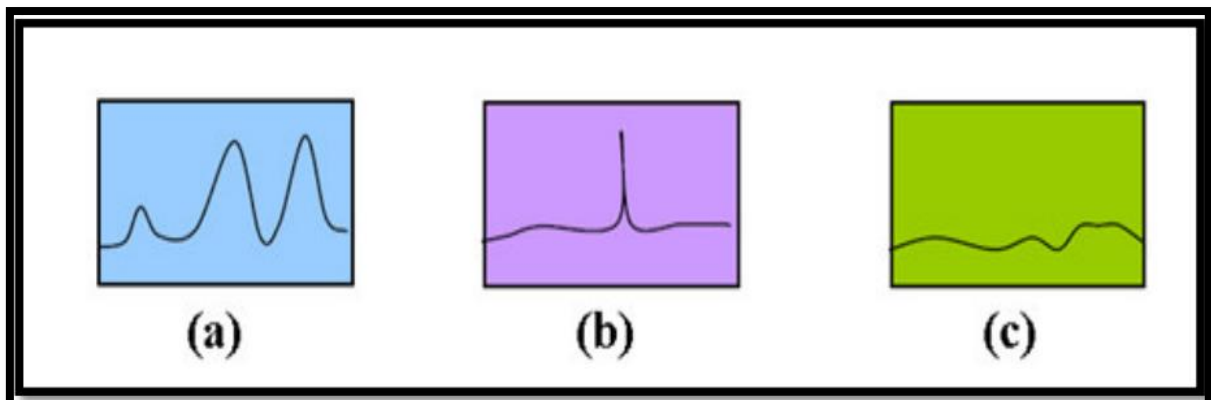


Figure (II-5): (XRD) of semiconductors.

(a) Polycrystalline (b) Single material (c) Amorphous material [8].

II-5-2- Optical characterization

❖ Ultraviolet–visible spectroscopy

Ultraviolet–visible spectroscopy or ultraviolet-visible spectrophotometry (UV-Vis or UV/Vis): refers to the absorption spectroscopy or reflectance spectroscopy in the ultraviolet –visible spectral region. This means it uses light in the visible and adjacent (near-UV and near – infrared [NIR]) ranges. The absorption or reflectance in the visible range directly affects the perceived color of the chemicals involved. In this region of the electromagnetic spectrum, molecules undergo electronic transitions. This technique is complementary fluorescence spectroscopy, that fluorescence deals with transitions from the excited state to the ground state, while absorption measures transitions from the ground state to the excited state.



Figure (II-6):Ultraviolet-visible spectrophotometer (LAMBDA 25)

❖ Principle of ultraviolet-visible absorption

Molecules containing π -electrons or non-bonding electrons (n-electrons) can absorb the energy in the form of ultraviolet or visible light to excite these electrons to higher anti bonding molecular orbital. The more easily excited the electrons(i.e. lower energy gap between the HOMO and the LUMO), the longer the wavelength of light it can absorb [9].

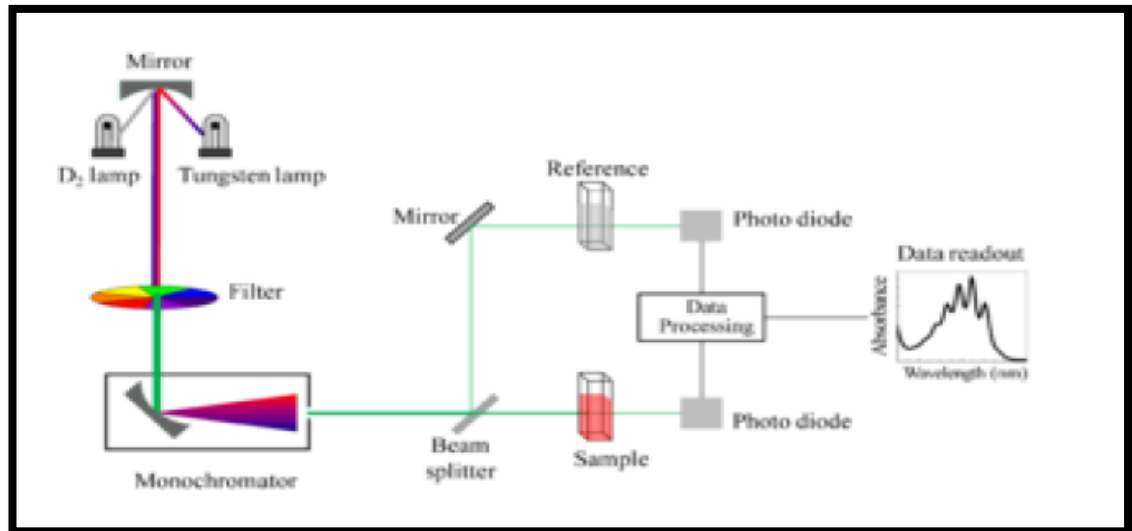


Figure (II-7): Schematic of UV-visible spectrophotometer[10].

II-5-3- Electrical characterization

❖ Four point probe technique

The four-point probe is a very versatile device. It is used widely for the investigation of electrical phenomena. The effect of the contact resistance could be eliminated with the use of such configuration. The most common in-line configuration has been adopted in this work (see Figure (II-8)).

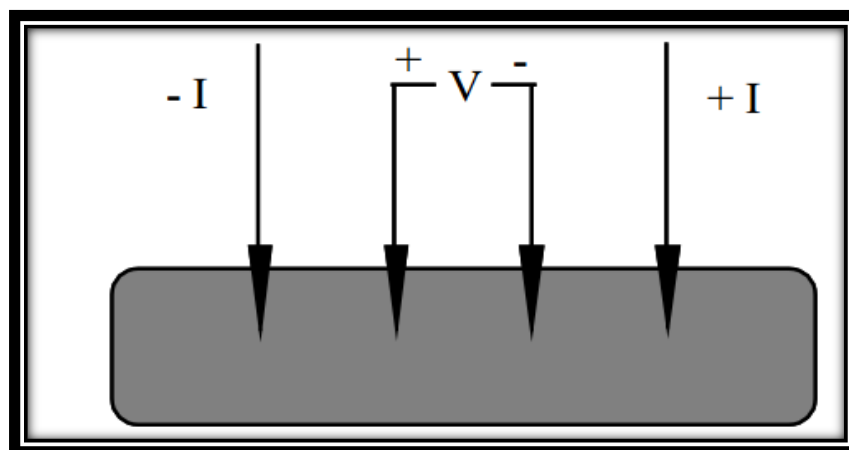


Figure (II-8): Schematic of in-line four-point probe configuration

In the measurement, the four metal tips have been attached to the test sample. A high impedance current source of $I = 0.5 \mu\text{A}$ has been used to supply current through the outer two probes; a voltmeter measured the voltage V across the inner two probes. The probe spacing was 1 mm. Consequently, the sheet resistance of the film is derived from the formula:

$$R_S = \frac{\pi}{\ln 2} * \frac{V}{I} \quad (\text{II-5})$$

where the factor of $(\pi/\ln 2)$ is on account of the effect of the current extending. If the film thickness is known, the resistivity is readily obtained from

$$\rho = R_S * d \quad (\text{II-6})$$

where d is the film thickness. The mean value of three measurements has been taken in order to reduce the measuring error [11].



Figure (II-9): Experimental dispositif.

II-6- Conclusion

In this chapter, we have studied the NiO thin films and ZnO thin films by spray pneumatic method and we have also determined the experimental conditions. Finally we used various characterization methods such as: XRD, The UV-VIS spectroscopy and electrical characterizations (the four points technique)

References

- [1] Y.A. Yan, B. Ajitha, P.S. Reddy, M.S. Pratap Reddy and J.H. Lee, The effect of cardiac resynchronization on morbidity and mortality in heart failure, *Electronic Materials Letters*, vol. 10, pp. 907-913. 2014
- [2] L. Zhang, J. He, W. Jiao, "Synthesis and gas sensing performance of NiO decorated SnO₂ vertical-standing nanotubes composite thin films," *Sensors and Actuators B: Chemical*, vol. 281, pp. 326-334, 2019
- [3] S. Benramache, M. Aouassa, "Preparation and Characterization of p-Type Semiconducting NiO Thin Films Deposited by Sol-Gel Technique," *Journal of Chemistry and Materials Research*, vol. 5, pp. 119–122, 2016.
- [4] Clendenen, R. L., Drickamer, H. G.: *J. Chem. Phys.*, vol. 44 , pp. 4223. 1966
- [5] Adam Olzick , "Deposition, characterization, and fabrication of a Zinc oxide Piezoelectric thin film micro speaker using DC reactive sputtering ", *Master of Science in Engineering*, California Polytechnic State University , June 2012.
- [6] Loren Wellington Rieth, « Sputter deposition of Zn O thin films », *University of Florida*, 2001.
- [7] A. M. Shano AL-Askari «Effect of Aqueous Solution Molarity on Structural and Optical Properties of Nickel- Cobalt Oxide Thin Films Prepared by Chemical Spray Pyrolysis Method » *These Master University of Diyala Iraq* 2012.
- [8] Z. Qiao «Fabrication and Study of ITO Thin Films Prepared by Magnetron Sputtering » *Doctorate Thesis, Universität Duisburg-Essen, China*, 2003.
- [9] Al. Boileau, *These Ph.D.* , *Université de Lorraine, France*. 2013
- [10] L. Li, K.S. Hui, K.N. Hui, H.W. Park, D.H. Hwang, Sh. Cho, S.K. Lee, P.K. Song, Y.R. Cho, H. Lee, Y.G. Son, W. Zhou, Synthesis and characterization of NiO-doped p-type AZO films fabricated by sol-gel method, *Materials Letters* 68, 2012.
- [11] S. Rami «Synthesis, Characterization, and Electrochemical Properties of Polyaniline Thin Films » *Master These University of South Florida* 2015.

CHAPTER THREE

The role of deposition rate on the physical properties of NiO thin films elaborated by spray pyrolysis technique

III-1- Introduction

Nickel oxide (NiO) is a p-type semiconductor of semiconducting material with optical band gap was varied between 3.6 to 4 eV [1]. In the latest research, the NiO is forming of nickel metal and oxygen element, it was found in the cubic structure with lattice parameter ($a = 0.4816$ nm) [2]. NiO is one of the most important oxide materials due to its excellent chemical stability and durability, low toxicity, large span optical density, low cost and good thermal stability [3]. NiO was developed as thin films to be used as a gas sensing due to their good optical transparency and good electrical conductivity [4.5]. The use of NiO thin films in the detection of toxic gases has a role in improving the physico-chemical properties, by researching how to prepare and any possible method. Gavale et al. [6] studied the physical properties of nanocrystalline NiO thin films prepared by spray pyrolysis technique, where investigated the influence of film thickness on the structural, morphological and optical properties of nanocrystalline NiO films, they found that the crystallinity and the morphological properties were increased with increasing the film thickness, also obtained a good transmission in the visible region is found to be 80% with optical band gap found to in the range of 3.48 eV to 3.53 eV.

However, the NiO thin films but were used in various applications due to the simplicity of synthesis can be investigated in solar cells [7], chemical sensors [8], photodetectors [9], electro chromic minors [10], organic light emitting diodes [11], UV detectors [12], vanes parent diodes [13], and defrosting windows [14]. NiO thin films can be prepared by various methods likely molecular beam epitaxy (MBE) [15], electrochemical deposition [16], chemical vapor deposition [17], sol-gel process [18], reactive evaporation [19], pulsed laser deposition (PLD) [20], magnetron sputtering technique [21] and spray pyrolysis [22]. The spray method was used for technological applications because it is one of the most important techniques to deposition a large-scale production. The prepared the thin films by this method have a good adhesion mechanical, and good electrical conductivity; also it has a high optical transparency and magnetic properties of nanostructures NiO.

The main objective of this work is to obtain a semiconductor as NiO thin films with high crystalline structure, good optical and electrical properties. In the present work, nanostructure NiO thin films were investigated, which are elaborated by spray pyrolysis method, the NiO was heated on glass substrate at a deposition temperature of 450 °C with

various deposition rates of 20, 40, 60 and 80 ml. the effect of deposition rate on structural, optical and electrical properties were investigated in the section of results and discussion.

III-2- Experimental

NiO solution was prepared by dissolving 0.05M ($\text{Ni}(\text{CH}_3\text{COO})_2 \cdot 4\text{H}_2\text{O}$) in the solvent containing equal volume absolute ethanol solution (99.995%) purity, the stabilization was carried with stirring the NiO solution for 60 min and addition of drops of HCl solution. The final solution was stirred and heated at 50 °C for 60 min to good transparent solution. The preparation was performed on glass substrates by spray pyrolysis method with heating at 450 °C. The NiO thin films were elaborated at 450 °C in air with various deposition rates of 20, 40, 60 and 80 ml.

The crystalline structure of sprayed final films was carried by X-ray diffraction (XRD, Bruker AXS-8D) with $\text{CuK}\alpha$ radiation ($\lambda = 0.15406$ nm) by varying the scanning range of (2θ) from 20° and 70°. The transmittance and absorbance of the sprayed NiO films was investigated in the wavelength range of 300–900 nm by spectrophotometer (SHUMATZU 1800). Finally, the electrical resistivity was measured by the four point's methods.

III-3- Results and discussion

The X-ray diffraction (XRD) spectrum of the deposit NiO thin films by spray pyrolysis is shown in Figure (III- 1). The NiO thin films were obtained at various deposition rates are 20, 40, 60 and 80 ml. The XRD spectrum of sprayed NiO thin films was matched the structure of NiO thin films is cubic structure with JCPDS (No. 73- 1519) [20]. From this data can observed a only diffraction peak at $2\theta = 37.4^\circ$, which is related to the plan of (111). All the spectra's of NiO thin films having one peak with higher in the sharper indicating that the obtain NiO thin film has a nanocrystalline structure. The good results were found for the film prepared with 60 and 80 ml due to the increase in the FWHM of the peaks. However, the preferred orientation is perpendicular with (111) plane. The crystallite size of all deposited NiO thin films was calculated by the Debye-Scherrer formula [23]:

$$G = \frac{0.9\lambda}{\beta \cos \theta} \quad (1)$$

where G is the crystallite size, λ is the wavelength of X-ray ($\lambda = 1.5406 \text{ \AA}$), β is the FWHM and θ is the half diffraction angle.

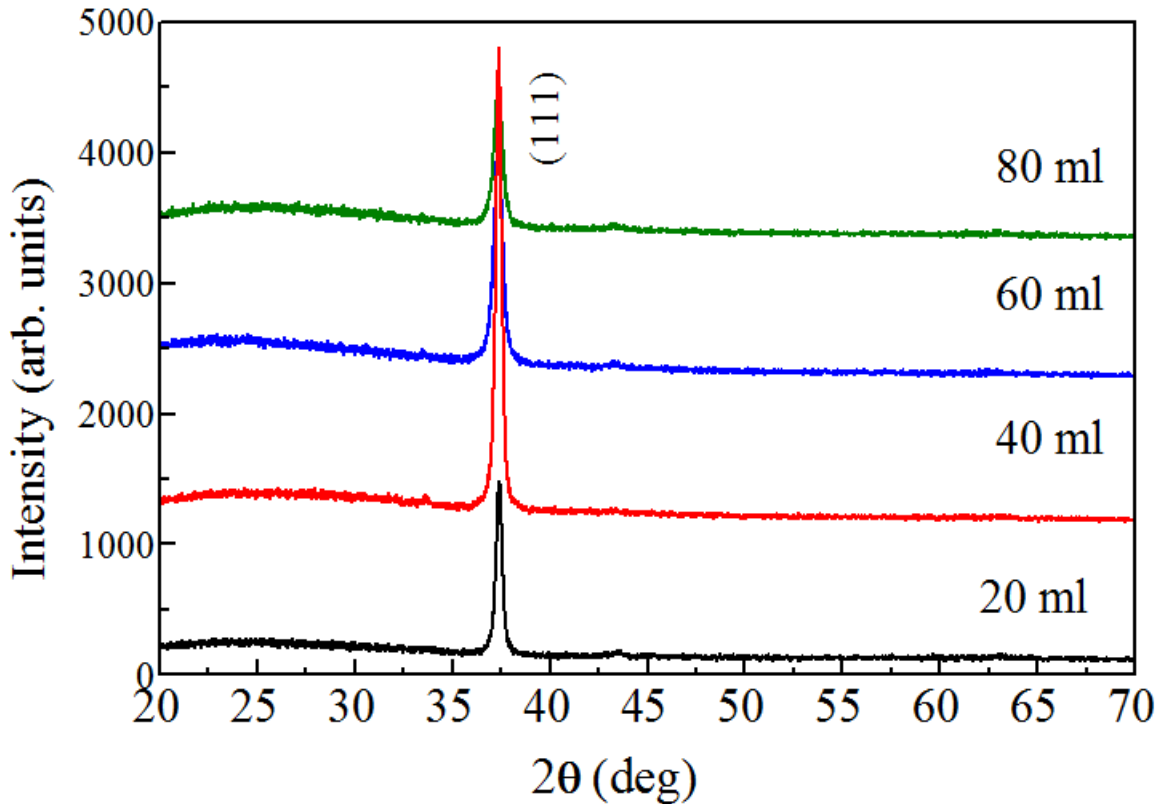


Figure (III- 1) : X-ray diffraction spectra of NiO thin films at different deposition rates.

Reported in the Figure (III- 1) as a function of deposition rate the variation of the crystallite size and the diffraction angle of (111) diffraction peak. The crystallite sizes were stabilized at 20 ml and 40 ml of are taking two values 23.6 and 24.3 nm, respectively. Then decreased to minimum value was found at 60 ml of deposition rate it is 15.8 nm. The decrease in the crystallite size of NiO thon films was indicated to improve of crystalline structure. However, the decrease of diffraction angle with decreasing of crystallite size showed that the existence of sufficiently thicker films in less strained (or more relaxed) state.

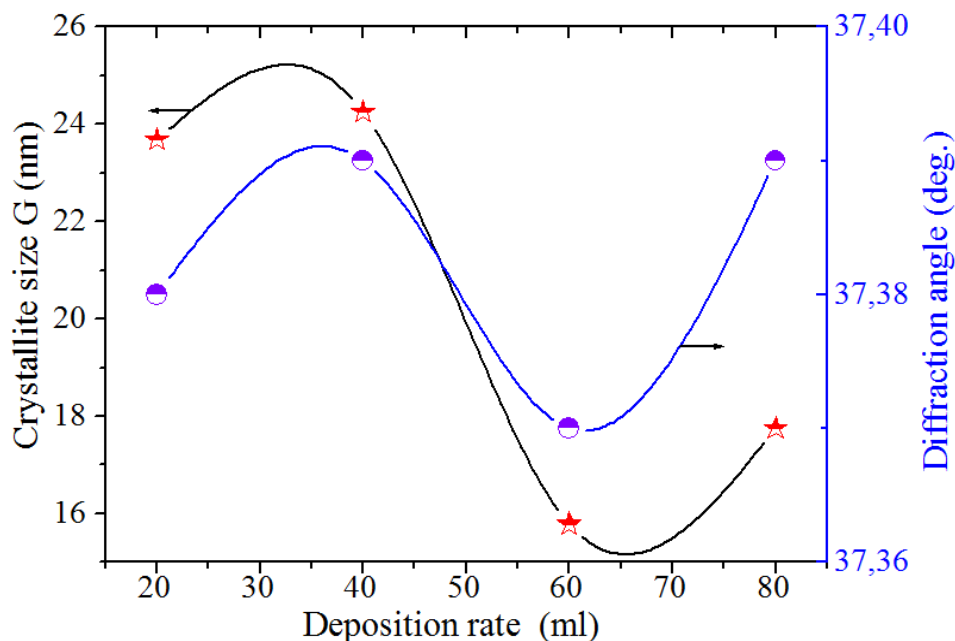


Figure (III- 2) : *The variation of crystallite size and diffraction angle as a function of deposition rate in NiO thin films*

The Optical properties of NiO thin films deposited at various deposition rates were performed by measuring the transmittance and absorbance in the wavelength region 300 to 900 nm, it are shown in Figure (III- 3) . Can see that the height transparency of the NiO thin films in visible region with an average transmission is about 70 %, so that the films exhibit high transparency by comparing with original nature, it is found by various literatures in the range 40 to 60% [24,25]. The region of the absorption edge was observed when the transmission was decreased, which is related transition between the valence band and the conduction band it is located between 320–370 nm. The inset of Figure (III- 3) was present the variation of absorbance data of NiO thin films, the absorption edge shifts was observed clearly at wavelength shorter than 400 nm. The absorption edge shifts of NiO thin films were decreased with increasing the deposition rate. As can be note, the optical property of NiO thin films is affected by deposition rate.

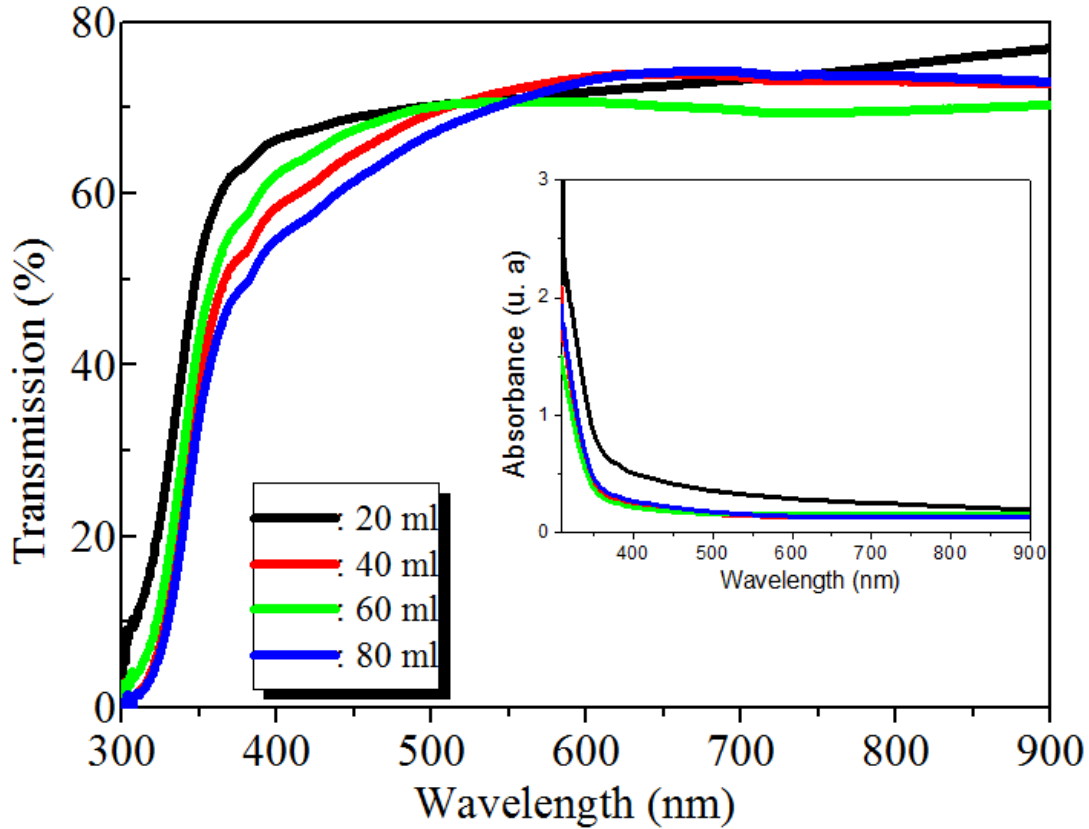


Figure (III-3): Transmission spectra of ZnO thin films as a function of deposition rate, the inset present the absorbance of the thin films..

The role of deposition rate on transmission of NiO thin films was clearly observed on the layer quality. But the absorption edge of NiO film was observed to red shift can be explained by the changes in the optical band gap. So that absorbance and the optical band gap energy E_g of NiO thin films were determined by the following relations [3,26]:

$$A = \alpha d = -\ln T \quad (2)$$

$$(Ah\nu)^2 = C(h\nu - E_g) \quad (3)$$

where A is the absorbance, d is the film thickness; T is the transmission spectra of thin films; α is the absorption coefficient values; C is a constant, $h\nu$ is the photon energy ($h\nu = \frac{1240}{\lambda(nm)} (eV)$) and E_g the band gap energy of the semiconductor. However, the

disorder or Urbach energy (E_u) also was determined by the expression follow [27]:

$$A = A_0 \exp\left(\frac{h\nu}{E_u}\right) \quad (4)$$

where A_0 is a constant $h\nu$ is the photon energy and E_u is the Urbach energy, the Urbach energy was used for characterize the order of the defects.

The variation of optical band gap and Urbach energy was calculated as a function of deposition rate, it is presented in the Figure (III-4). The band gap energy was observed a smaller than 3.5 eV, it is change and decreased with increasing of deposition rate from 3.51 to 3.34 eV of 20 to 80 ml, respectively. The decrease in the optical value of NiO thin films can be explain by effect of quantum confinement due to the diminution in the crystallite size of NiO thin films (see Figure (III-2)). As can be seen in Figure (III-4) that the Urbach energy was increases from 20 to 60 ml, and decrease to minimum value was found at 80 ml is 0.286 eV. This is can be related by the diminution of the crystallite size (see Figure (III-2)).

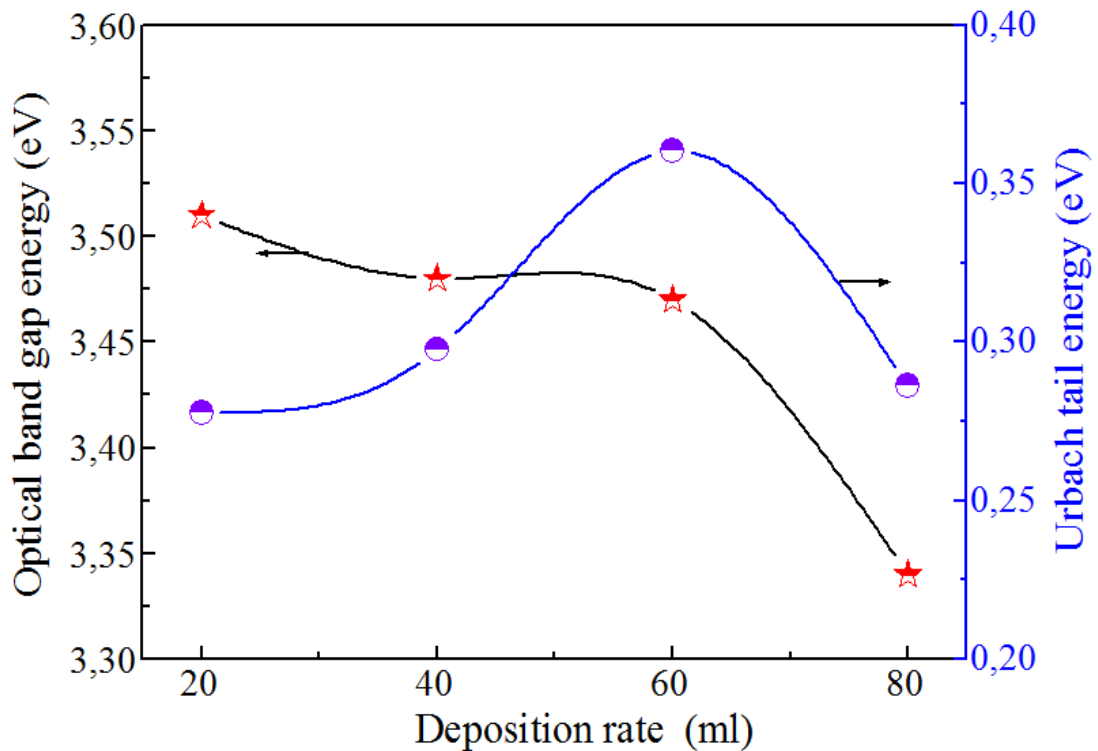


Figure (III-4): The variation of optical band gap E_g and Urbach energy E_u of NiO thin films with deposition rate.

Figure (III-5) shows the variation as a function of deposition rate of the electrical resistivity of NiO thin films. The deposition rate was play an important parameter in prepared the NiO thin films. The variation of electrical resistivity was measured with the

increase in the deposition rate (increase in the film thickness). These variations are rapid decreases to minimum value at 80 ml is 0.152 $\Omega\cdot\text{cm}$. The decrease in the resistivity of NiO films can be explained by the diminution of defects, which was related by the decreasing in the Urbach energy (see Figure (III-4)).

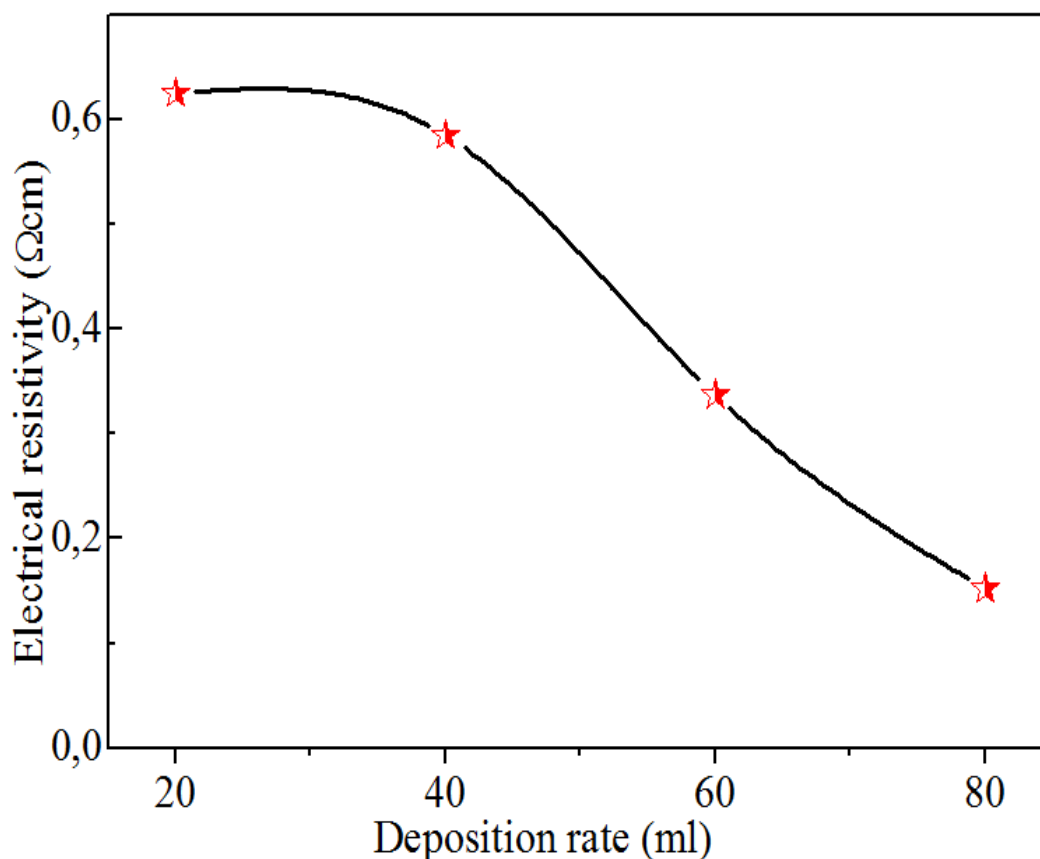


Figure (III-5): Electrical resistivity of NiO thin films at different deposition rate.

III-4- Conclusions

In summary, the NiO thin films were prepared by spray pyrolysis method on glass substrate at 450 °C with various deposition rates (film thickness). The structural, optical and electrical properties of nanostructures NiO thin films were investigated by study the influence of deposition rate on. NiO thin films were observed a nanocrystalline a cubic structure with a strong (111) preferred orientation, it is only phase was observed in all deposited films. The minimum value of crystallite size (15.8 nm) was measured of deposited film with 60 ml. The average transmittance is about 70 % was observed in all NiO thin films. The NiO thin films have a verity in the band gap energy from 3.34 to 3.51

eV because the effect of deposition, the minimum value was found at 80 ml, this condition have a lowest Urbach energy. The NiO thin film elaborated with 80 ml has a minimum electrical resistivity was 0.152 ($\Omega\cdot\text{cm}$). The NiO thin films sprayed with 60 and 80 ml have good structural, optical and electrical properties.

References

- [1] I. Manouchehri, D. Mehrparvar, R. Moradian, K. Gholami, T. Osati, ‘‘Investigation of structural and optical properties of copper doped NiO thin films deposited by RF magnetron reactive sputtering,’’ *Optik*, vol. 127, pp. 8124–8129, 2016.
- [2] M. Krunks, J. Soon, T. Unt, A. Mere, V. Mikli, ‘‘Deposition of p-type NiO films by chemical spray pyrolysis,’’ *Vacuum*, vol. 107, pp. 242-246, 2014.
- [3] A. Diha, S. Benramache, B. Benhaoua, ‘‘Transparent nanostructured Co doped NiO thin films deposited by sol–gel technique,’’ *Optik*, vol. 172, pp. 832-839, 2018.
- [4] S. Benramache, B. Benhaoua, ‘‘Influence of substrate temperature and Cobalt concentration on structural and optical properties of ZnO thin films prepared by Ultrasonic spray technique,’’ *Superlattices and Microstructures*, vol. 52, pp. 807–815, 2012.
- [5] S. Benramache, B. Benhaoua, ‘‘Influence of annealing temperature on structural and optical properties of ZnO: In thin films prepared by ultrasonic spray technique,’’ *Superlattices and Microstructures*, vol. 52, pp. 1062–1070, 2012.
- [6] H.S. Gavale, M.S. Wagh, R.B. Ahirrao, S.R. Gosavi, Study of Physical Properties of Nanocrystalline NiO Thin Films Prepared by Spray Pyrolysis Technique,’’ *Journal of Nanoscience and Technology*, vol. 5, pp. 610–612, 2019.
- [7] S. Benramache, B. Benhaoua, F. Chabane, N. Kachai,. ‘‘Elaboration and characterisation of ZnO thin films,’’ *Matériaux & Techniques*, vol. 100, pp. 573–580, 2012.
- [8] M. Jlassi, I. Sta, M. Hajji, H. Ezzaouia, ‘‘Synthesis and characterization of nickel oxide thin films deposited on glass substrates using spray pyrolysis,’’ *Applied Surface Science*, vol. 308, pp. 199–205, 2014.
- [9] J. Denayer, G. Bister, P. Simonis, P. Colson, A. Maho, P. Aubry, B. Vertruyen, C. Henrist, V. Lardot, F. Cambier, R. Cloots, ‘‘Surfactant-assisted ultrasonic spray pyrolysis of nickel oxide and lithium-doped nickel oxide thin films, toward electrochromic applications,’’ *Applied Surface Science*, vol. 321, pp. 61–69, 2014.
- [10] L. Berkat, L. Cattin, A. Reguig, M. Regragui, J.C. Bernède, ‘‘Comparison of the physico-chemical properties of NiO thin films deposited by chemical bath deposition and by spray pyrolysis,’’ *Materials Chemistry and Physics*, vol. 89, pp. 11–20, 2005.

- [11] Z.T. Khodair, A.A. Kamil, Y.K. Abdalaah, "Effect of annealing on structural and optical properties of Ni_(1-x)Mn_xO nanostructures thin films," *Physica B*, vol.503, pp. 55–63, 2016.
- [12] M.B. Amor, A. Boukhachem, A. Labidi, K.Boubaker, M.Amlouk, "Physical investigations on Cd doped NiO thin films along with ethanol sensing at relatively low temperature," *Journal of Alloys and Compounds*, vol. 693, pp. 490-499, 2017.
- [13] H. Kim, S. Yang, S.H. Ahn, C.S. Lee, "Effect of particle size on various substrates for deposition of NiO film via nanoparticle deposition system," *Thin Solid Films*, vol. 600, pp. 109–118, 2016.
- [14] S. Moghe, A.D. Acharya, R. Panda, S.B. Shrivastava, M. Gangrade, T. Shripathi, V. Ganesan. "Effect of copper doping on the change in the optical absorption behavior in NiO thin films," *Renewable Energy*, vol. 46, pp. 43-48, 2012.
- [15] L. Cattin, B.A. Reguig, A. Khelil, M. Morsli, K. Benchouk, J.C. Bernède, "Properties of NiO thin films deposited by chemical spray pyrolysis using different precursor solutions," *Applied Surface Science*, vol. 254, pp. 5814–5821, 2008.
- [16] B.A. Reguig, A. Khelil, L. Cattin, M. Morsli, J.C. Bernède, "Properties of NiO thin films deposited by intermittent spray pyrolysis process," *Applied Surface Science*, vol. 253, pp. 4330–4334, 2007.
- [17] J.D. Desai, S.K. Min, K.D. Jung, O.S. Joo, "Spray pyrolytic synthesis of large area NiOx thin films from aqueous nickel acetate solutions," *Applied Surface Science*, vol. 253, pp. 1781–1786, 2006.
- [18] C. Chen, P.J. Perdomo, M. Fernandez, A. Barbeito, C. Wang, "Porous NiO/graphene composite thin films as high performance anodes for lithium-ion batteries," *Journal of Energy Storage*, vol. 8, pp. 198–204, 2016.
- [19] N. Shi, S. Yu, S. Chen, L. Ge, H. Chen, L. Guo, "Dense thin YSZ electrolyte films prepared by a vacuum slurry deposition technique for SOFCs," *Ceramics International*, vol. 43, pp. 182–186, 2017.
- [20] P.S. Patil, L.D. Kadam, "Preparation and characterization of spray pyrolyzed nickel oxide (NiO) thin films," *Applied Surface Science*, vol. 199, pp. 211–221, 2002.
- [21] C. Chen, P.J. Perdomo, M. Fernandez, A. Barbeito, "Porous NiO/graphene composite thin films as high performance anodes for lithium-ion batteries," *Journal of Energy Storage*, vol. 8, pp. 198–204, 2016.

- [22] R. Amiruddin, M.C.S. Kumar, "Role of p-NiO electron blocking layers in fabrication of (P-N):ZnO/Al:ZnO UV photodiodes," *Current Applied Physics*, vol. 16, pp. 1052-1061, 2016.
- [23] A. Diha, S. Benramache, L. Fellah, "The Crystalline Structure, Optical and Conductivity Properties of Fluorine Doped ZnO Nanoparticles," *Journal of Nano- and Electronic Physics*, vol. 11, p. 03002, 2019.
- [24] K.O. Ukoba, A.C. Eloka-Eboka, F.L. Inambao, "Review of nanostructured NiO thin film deposition using the spray pyrolysis technique," *Renewable and Sustainable Energy Reviews*, vol. 82, pp. 2900-2915, 2018.
- [25] S. Iftimie, R. Mallet, J. Merigeon, L. Ion, M. Girtan, S. Antohe, "On the structural, morphological and optical properties of ITO, ZnO, ZnO:Al and NiO thin films obtained by thermal oxidation," *Digest Journal of Nanomaterials and Biostructures*, vol. 10, 221 -229, 2015.
- [26] S Benramache, Y Aoun, S Lakel, H Mourghade, R Gacem, B Benhaoua, "Effect of Annealing Temperature on Structural, Optical and Electrical Properties of ZnO Thin Films Prepared by Sol-Gel Method," *Journal of Nano- and Electronic Physics*, vol. 10, p. 06032, 2018.
- [27] W. Daranfed, M.S. Aida, A. Hafdallah, H. Lekiket, "Substrate temperature influence on ZnS thin films prepared by ultrasonic spray," *Thin Solid Films*, vol. 518, pp. 1082–1084, 2009.

CHAPTER FOUR

Synthesis of nanostructured of Zn doped NiO

IV-1- Introduction

This chapter includes the description and analysis of the measurements and the discussion of obtained results of Zn doped NiO thin films. It focuses on the structural, optical and electrical properties of Zn doped NiO thin films with different doping levels (0, 0.02, 0.04 0.08 and 0.12 %), Table IV.1 presents the experimental conditions of prepared of Zn doped NiO thin films, which were deposited on glass substrates by spraying technique at substrate temperature equal to 450°C.

Table IV.1. The experimental conditions of prepared of Zn doped NiO thin films

N	X	Ni _{1-x} Zn _x O	V _{zinc acetate} (ml)	V _{nickel acetate} (ml)	t (min)	C _{nickel acetate} =C _{zinc acetate} (mol/l)	T (°C)
1	0	Ni ₁ O	0	40	7	0.05	450
2	0.02	Ni _{0.98} Zn _{0.02} O	0.8	39.2	7	0.05	450
3	0.04	Ni _{0.96} Zn _{0.04} O	1.6	38.4	7	0.05	450
4	0.08	Ni _{0.92} Zn _{0.08} O	3.2	36.8	7	0.05	450
5	0.12	Ni _{0.88} Zn _{0.12} O	4.8	35.2	7	0.05	450

IV-2-Zn doping effect on optical properties of NiO thin films:

The optical characterization has been done using Perkin Elmer Lambda 25 UV-VIS spectrophotometer. The optical measurement results include relations of the transmittance and absorbance with wavelength for Zn doped NiO thin films with different doping levels (0, 0.02, 0.04 0.08 and 0.12 %). We studied the effect of the concentration on the optical parameters like absorption coefficient, optical energy gap and Urbach energy.

IV-2-1-Transmittance spectra:

Figure (IV.1) shows the relation between transmittance and wave length in the range of (300 - 900 nm) for Zn doped (NiO) thin films with different doping levels. From this figure, we can observe that the transmittance for all samples increases rapidly as the wave

length increases in the range of (300- 360 nm), then increases slowly at higher wavelengths and the optical transmittance of these films increased with increasing level. The spectra show high transmittance about 70% to 80% in the visible region, and the maximum transmittance observed of thin films was about 80% at $x=0.12$. It can be noticed also that the fundamental absorption edge is sharp in the visible region of the spectrum; these results are in agreement with other studies [1].

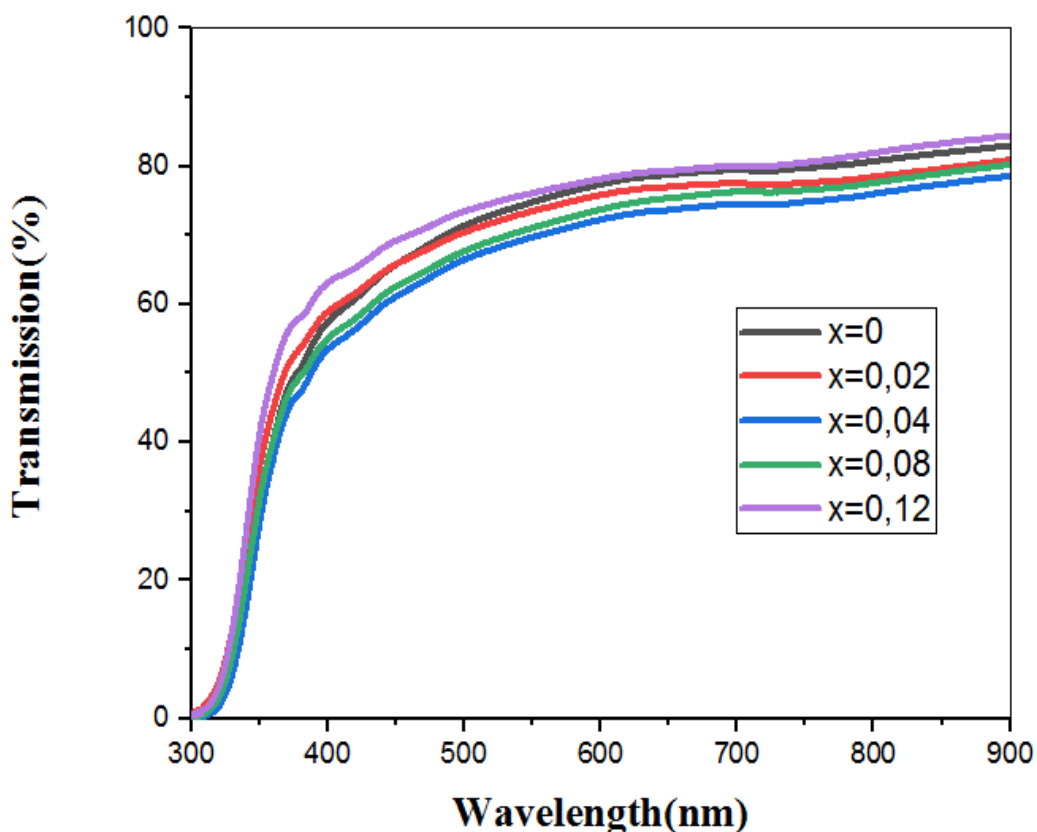


Figure (IV.1): Optical transmittance spectra of thin films

The inset of Figure IV.2 presents the variation of absorbance data of NiO thin films, the absorption edge shifts was observed clearly at wavelength shorter than 400 nm. The absorption edge shifts of NiO thin films were decreased with increasing the Zn deposition rate. As can be note, the optical property of NiO thin films is affected by Zn deposition rate

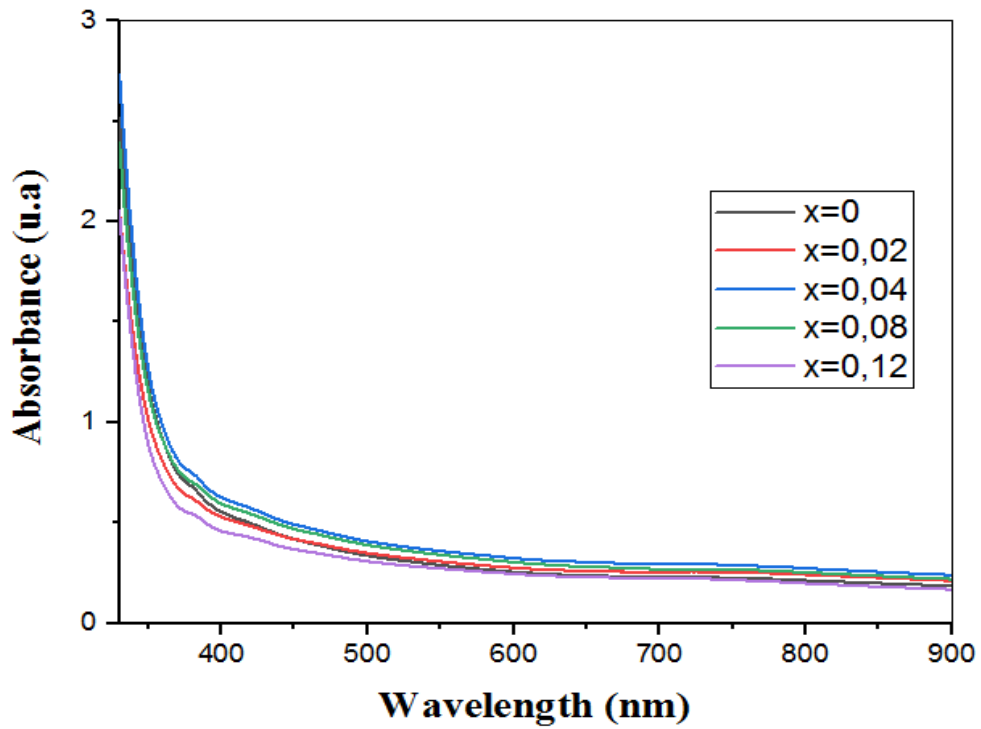


Figure (IV.2): Optical absorbance spectra of thin films

IV-2-2-Optical Gap

The optical band gap E_g was obtained by extrapolating the linear portion of the plot $(Ah\nu)^2$ versus $(h\nu)$ to $A = 0$ [2]. See Figure (IV.3) according to the following equation [3,4]:

$$A = \alpha d = -\ln T \quad (\text{IV.1})$$

$$(Ah\nu)^2 = C (h\nu - E_g) \quad (\text{IV.2})$$

Where A is the absorbance, d is the film thickness; T is the transmission spectra of thin films; α is the absorption coefficient values; C is a constant, $h\nu$ is the photon energy and E_g the band gap energy of the semiconductor.

One can estimate the optical gap (E_g) starting from the extrapolation of the curve which presents the evolution of $(Ah\nu)^2$ as a function of $h\nu$. The intersection

of the linear region on the $h\nu$ axis gives the E_g . As shown in Figure (IV.3), using this method the band gap values of the thin films are located around 3.68eV which is in good agreement with the E_g value of bulk NiO (3.6 - 4 eV) [5].

There is a reverse fit. That is, the higher the vaccination percentage, the lower the E_g value, and this is due to the zinc, which has an energy value within the range of $E_g=3.3$ eV.

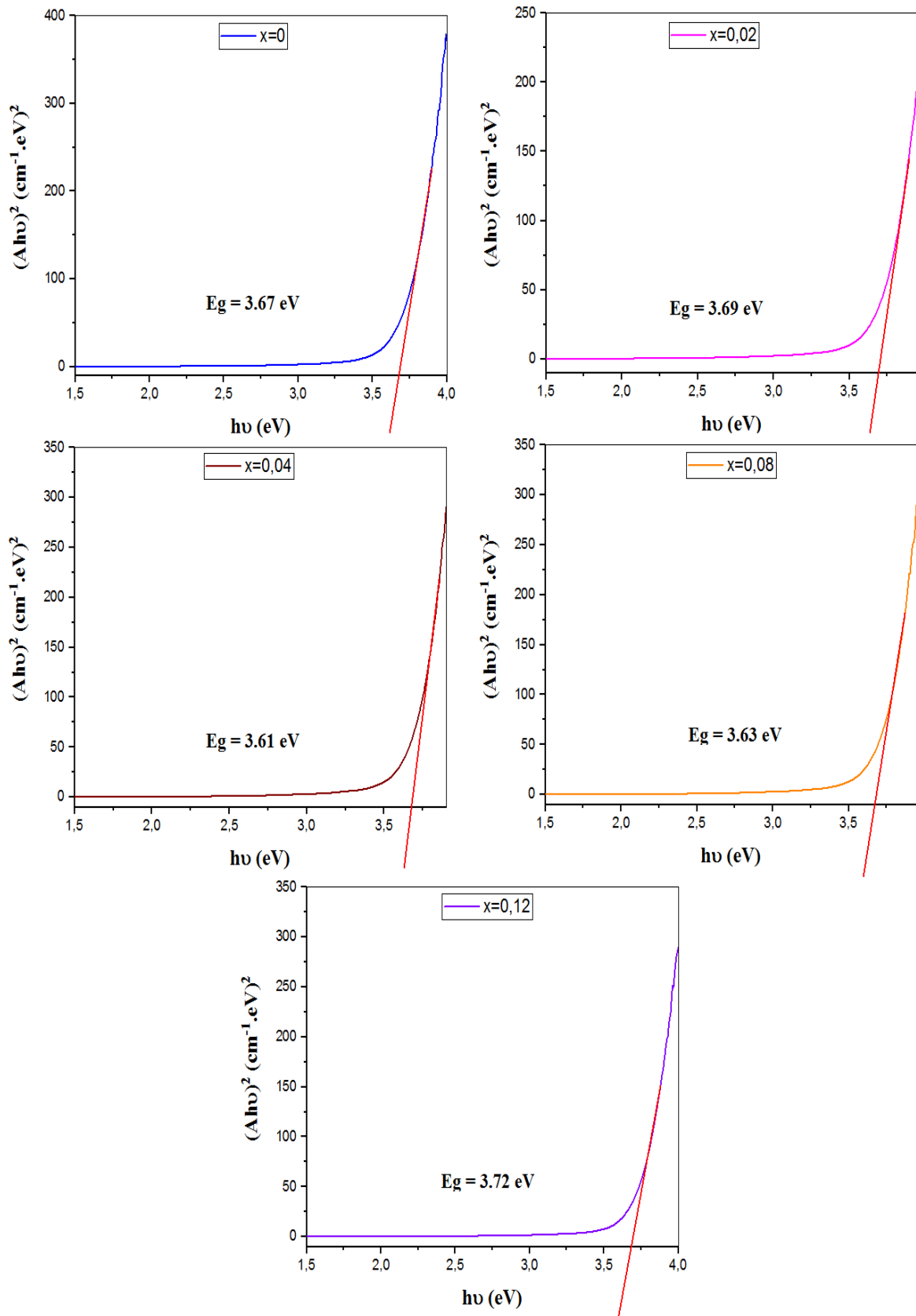


Figure (IV.3): The variation of $(Aho)^2$ as a function of $h\nu$ for each films.

From these curves, we have obtained the various E_g values which are represented in Table (IV.2) and plotted as a function of doping in the Figure (IV.3).

The decrease in the value of the optical band gap of the NiO film to 3.66 eV may be attributed to the improvement in the crystalline quality of the films as well as to the increase in the grain size [6].

Table (IV-2): Optical gap values of Zn doped NiO thin films.

X	E_g (eV)
0	3.67
0.02	3.69
0.04	3.61
0.08	3.63
0.12	3.72

IV-2-3-The Disorder (Urbach energy)

The same thing as the optical gap, the Urbach energy (E_u) is related to the disorder in the film network, as it is expressed follow [7]:

$$A = A_0 \exp\left(\frac{hv}{E_u}\right) \quad (IV.3)$$

Where A_0 constant $h\nu$ is the photon energy and E_u is the Urbach energy, is presented in Table (IV.3). The Figure (IV.4) shows the drawn of $\ln A$ as a function of photon energy $h\nu$ for deduce the Urbach energy. We have obtained these curves for each different doping level.

Through the curves, we notice a decrease in the Urbach energy (E_u) when the increase in the doping level x , to the lowest value of $E_u = 246$ meV

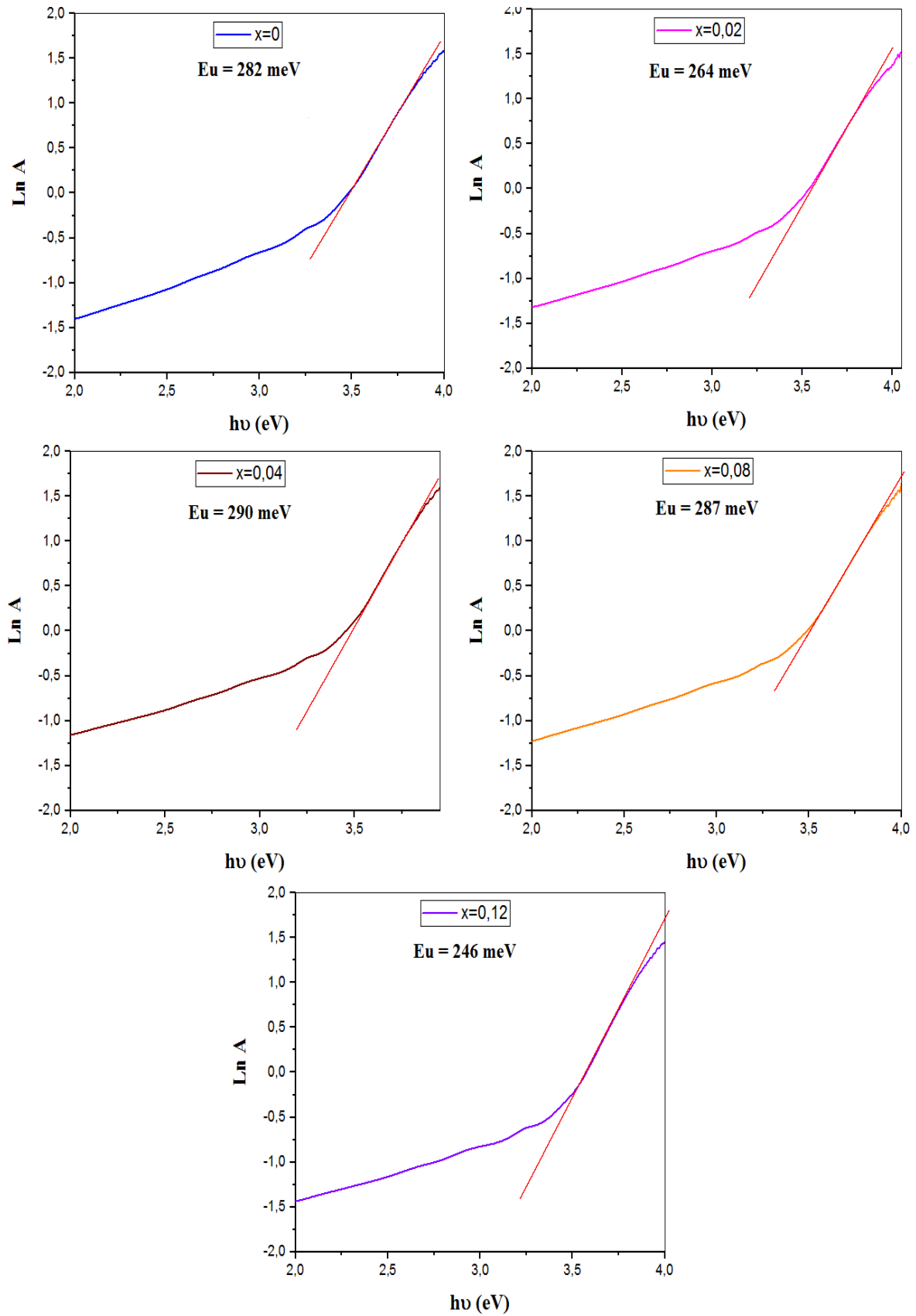
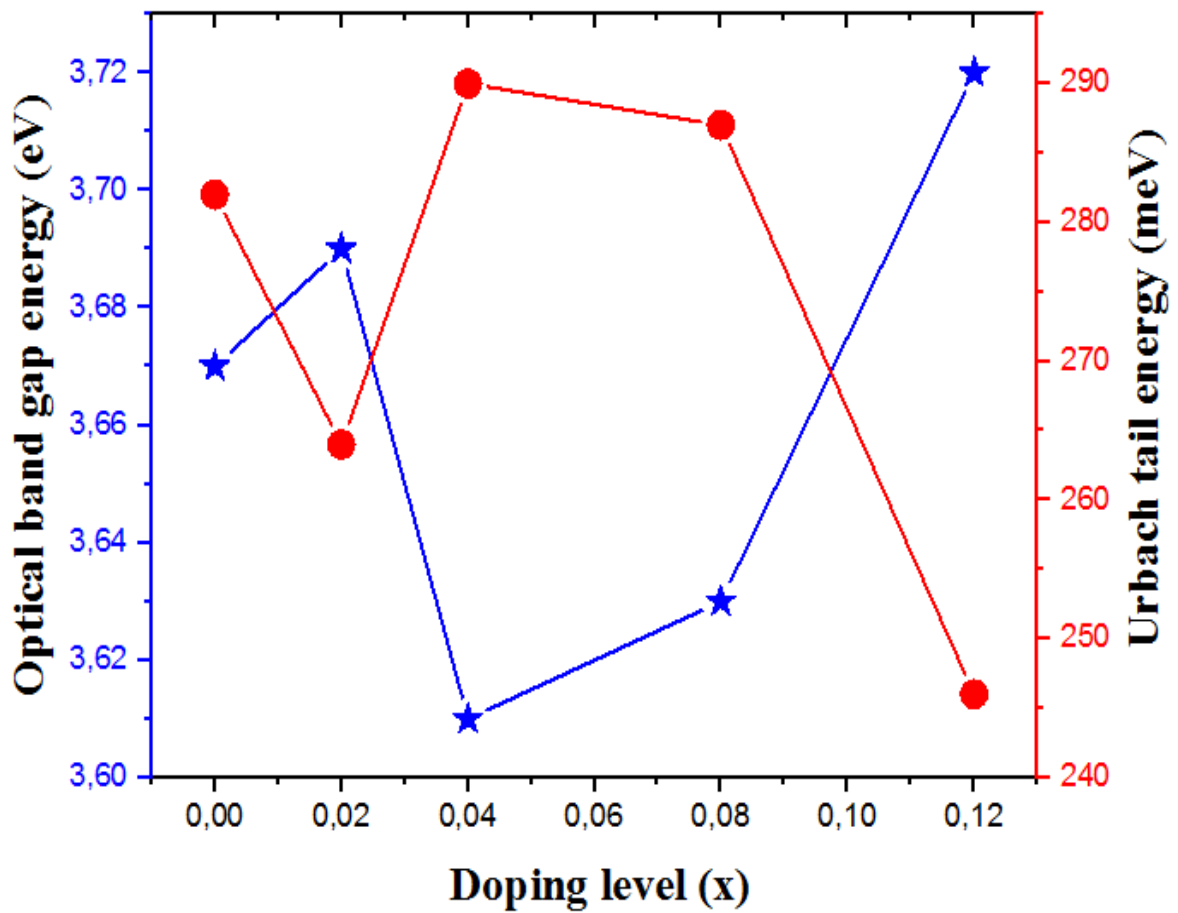


Figure (IV.4): Variations of $\ln(\alpha)$ as a function of $h\nu$ of Zn doped NiO thin films.

Table (IV-3): Disorder's (Urbach energy) values of Zn doped NiO thin films.

X	Eu (meV)
0	282
0.02	264
0.04	290
0.08	287
0.12	246

**Figure(IV.5)** The variations of optical band gap energy and Urbach energy of Zn doped NiO thin films at various doping levels.

We observe that the optical gap (E_g) exhibit a decrease which can be attributed to the growth of crystallite size which is resulted from the rise of doping level.

The Urbach energy decreases with elevating doping level, than exhibit a little increment.

The Urbach energy, corresponding with the tail width of the localized states within the optical band gap, thus it changes inversely with the optical band gap [8].

IV-3-Zn doping effect on Structural properties of NiO thin films:

The structural characterization of the $Ni_{1-x}Zn_xO$ thin films is carried out by X-ray diffraction method is shown in Figure (IV-6). It can be noticed that all the patterns exhibit diffraction peaks around ($2\theta \approx 38$ and 44) referred to (111) and (200) crystal plan, respectively, the peaks position was in accordance with Rahman et al [9]. The positions of obtained peaks with and without presence in the XRD spectra indicating that the $Ni_{1-x}Zn_xO$ thin films are

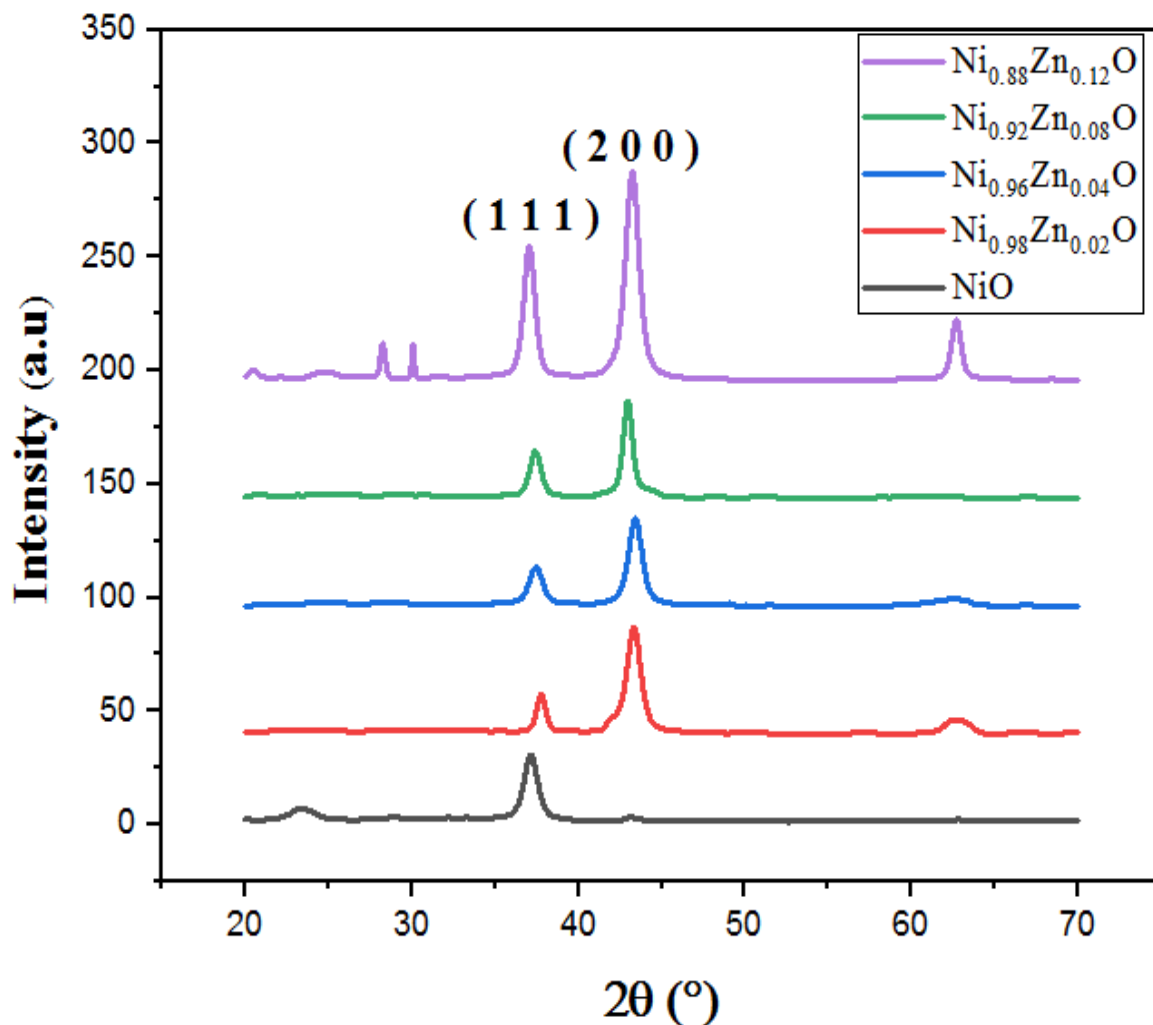


Figure (IV-6) X-ray diffraction of $Ni_{1-x}Zn_xO$ thin films as a function of Zn doping level

polycrystalline in nature with cubic structure, which is in agreement with other reports [10] of the cubic type of NiO (JCPDS) No. 73-1519) [11]. However, the good crystallinity was obtained in the lower doping.

The diffraction peak angles of the NiO thin films to (111) and (200) phases were presented in Table (IV.3) and (IV.4), respectively. The lattice parameter a of a cubic NiO structure was calculated by using XRD data by the following equation [12]:

$$\frac{1}{d_{hkl}^2} = \frac{h^2+k^2+l^2}{a^2} \quad (IV.4)$$

where a is the lattice parameter, h , k and l are the indices of the planes and d_{hkl} is the distance between adjacent planes in these (hkl) were calculated by using Bragg equation :

$$2d_{hkl} \sin \theta = n\lambda \quad (\text{IV.5})$$

Table (IV.4): The structural parameters of NiO thin film as a function of the thickness film to (111) diffraction peak.

x	2 θ (°)	$\beta_{1/2}$ (°)	a(nm)
0	37.3381	0.3936	0,417009
0.02	37.2981	0.6298	0,41744
0.04	37.4183	0.9446	0,416147
0.08	37.3362	0.7872	0,41703
0.12	37.0637	0.6298	0,419987

Table (IV.5): The structural parameters of NiO thin film as a function of the thickness film to (200) diffraction peak.

x	2 θ (°)	$\beta_{1/2}$ (°)	a(nm)
0	42.9067	0.3149	0,421428
0.02	42.9053	0.4723	0,421441
0.04	43.3430	0.7872	0,417386
0.08	42.9439	0.6298	0,42108
0.12	43.3698	0.2362	0,417141

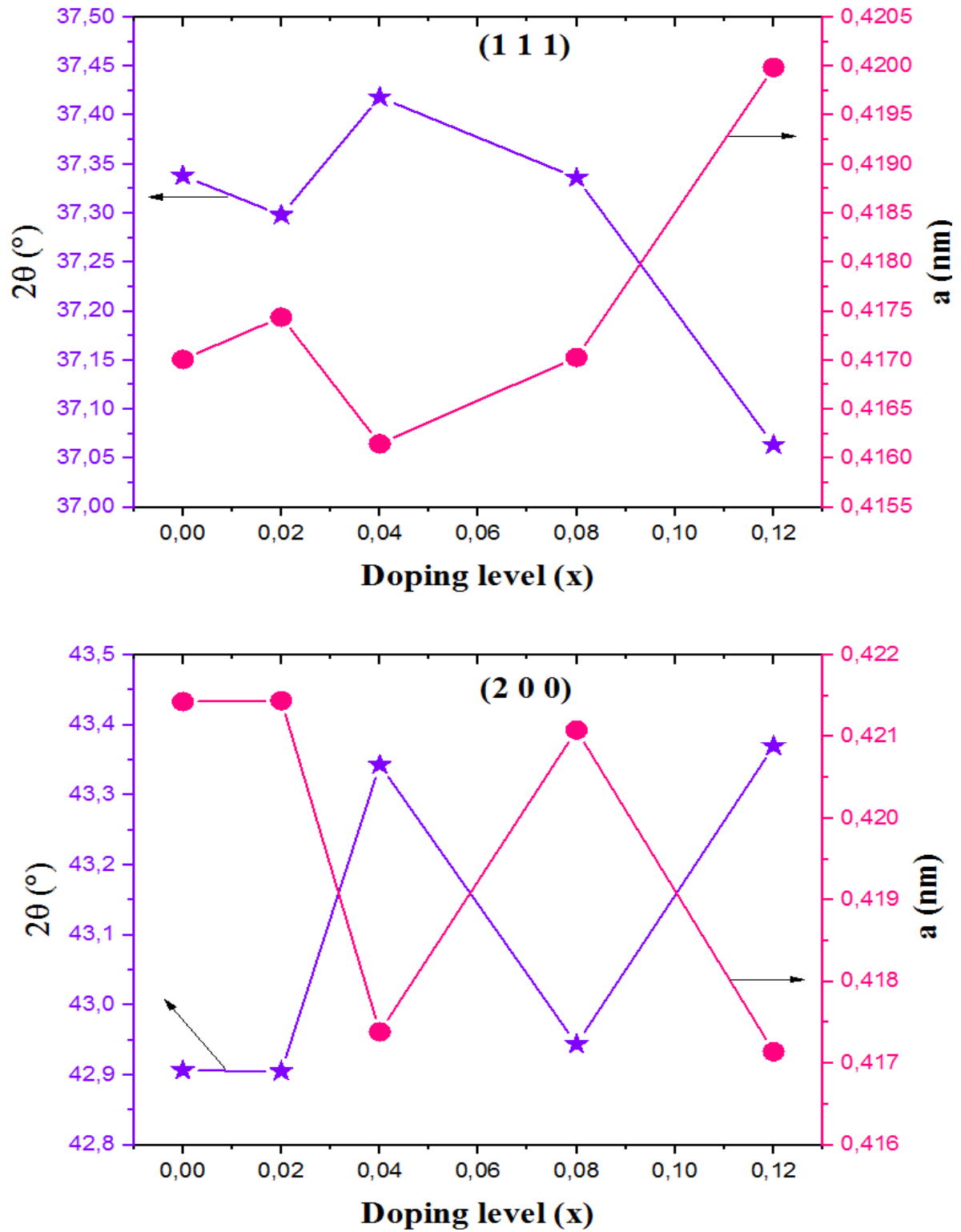


Figure (IV-7) The variations of the 2θ and lattice parameter a for Ni_{1-x}Zn_xO thin films as a function of Zn doping level

The lattice parameters are substrate dependent, which gives rise to a mismatch between the substrate and the deposited thin films. The latter is responsible for the resulting strains and stresses. We estimated the strain ε_{xx} values in each thin film deposition via the formula [13]:

$$\varepsilon_{xx} = \frac{a - a_0}{a_0} * 100 \quad (\text{IV.6})$$

Where ε is the mean strain in NiO thin films, a the lattice constant of NiO thin films and the a_0 lattice constant of bulk (standard $a_0 = 0.4816$ nm). In order to calculate the crystallite size G of (111) and (200) diffraction peaks in NiO films from the XRD patterns, we used Scherer's equation [14]:

$$G = \frac{0.9\lambda}{\beta \cos \theta} \quad (\text{IV.7})$$

where G is the crystallite size, λ is the wavelength of X-ray ($\lambda = 1.5406$ Å), β is the full width at half-maximum (FWHM), and θ is angle of diffraction peak. The values of crystallite sizes and FWHM are illustrated in Table (IV.6) and (IV.7). Note that the experimental accuracy in reading the 2θ angle is 0.02° of arc.

Table (IV.6): The structural parameters of NiO thin film as a function of the thickness film to (111) diffraction peak.

X	$2\theta(^{\circ})$	G(nm)	a(nm)	δ (m ⁻²)
0	37.3381	21.3143	0,417009	$2.2012 * 10^{15}$
0.02	37.2981	13.319	0,41744	$5.63712 * 10^{15}$
0.04	37.4183	8.88342	0,416147	$1.26718 * 10^{16}$
0.08	37.3362	10.6571	0,41703	$8.8049 * 10^{15}$
0.12	37.0637	13.3098	0,419987	$5.64487 * 10^{15}$

Table (IV.7): The structural parameters of NiO thin film as a function of the thickness film to (200) diffraction peak.

x	2 θ (°)	G(nm)	a(nm)	δ (m ⁻²)
0	42.9067	27.1177	0,421428	1.3599 *10 ¹⁵
0.02	42.9053	18.0803	0,421441	3.05906 *10 ¹⁵
0.04	43.3430	10.8641	0,417386	8.47253 *10 ¹⁵
0.08	42.9439	13.5606	0,42108	5.438 *10 ¹⁵
0.12	43.3698	36.2109	0,417141	7.62644 *10 ¹⁴

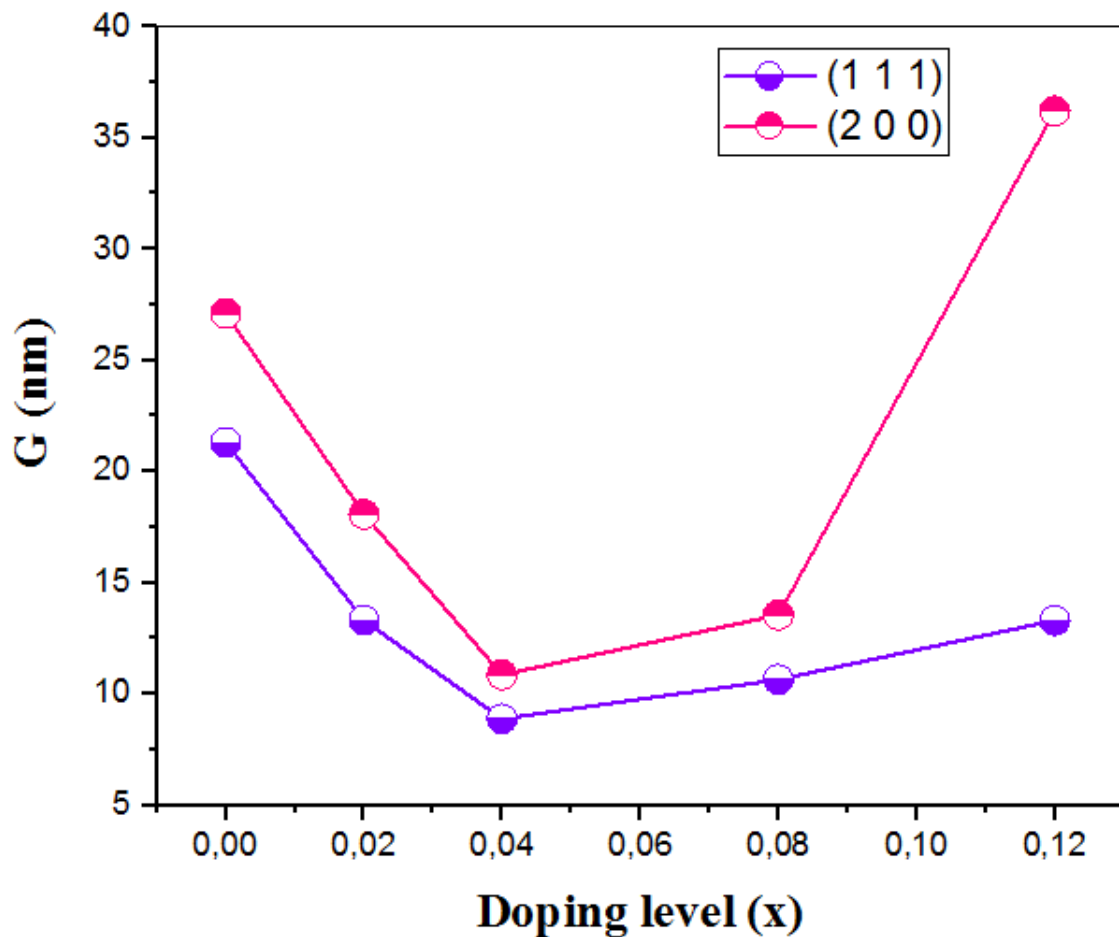


Figure (IV-8) The variations of crystallite sizes of (111) and (200) crystal plans of Ni_{1-x}Zn_xO thin films as a function of Zn doping level

Figure (IV.8) shows the variation of crystallite size as a function of doping level of Zn, it can be observed from Figure (IV.8) that the crystallite sizes of (111) and (200) crystal plans decreased until reaching the value 8.8 and 10.8 nm for $x=0.04$, respectively. And then slowly increased to maximum values, the increasing in the crystallite with the variation of doping level can be indicating to improve of our thin films crystallinity. However, Figure (IV.9) presents the variations of main strain of (111) and (200) crystal plans, the decrease in the main strain can be provide an adequate explanation for the deterioration in the crystallinity of the films.

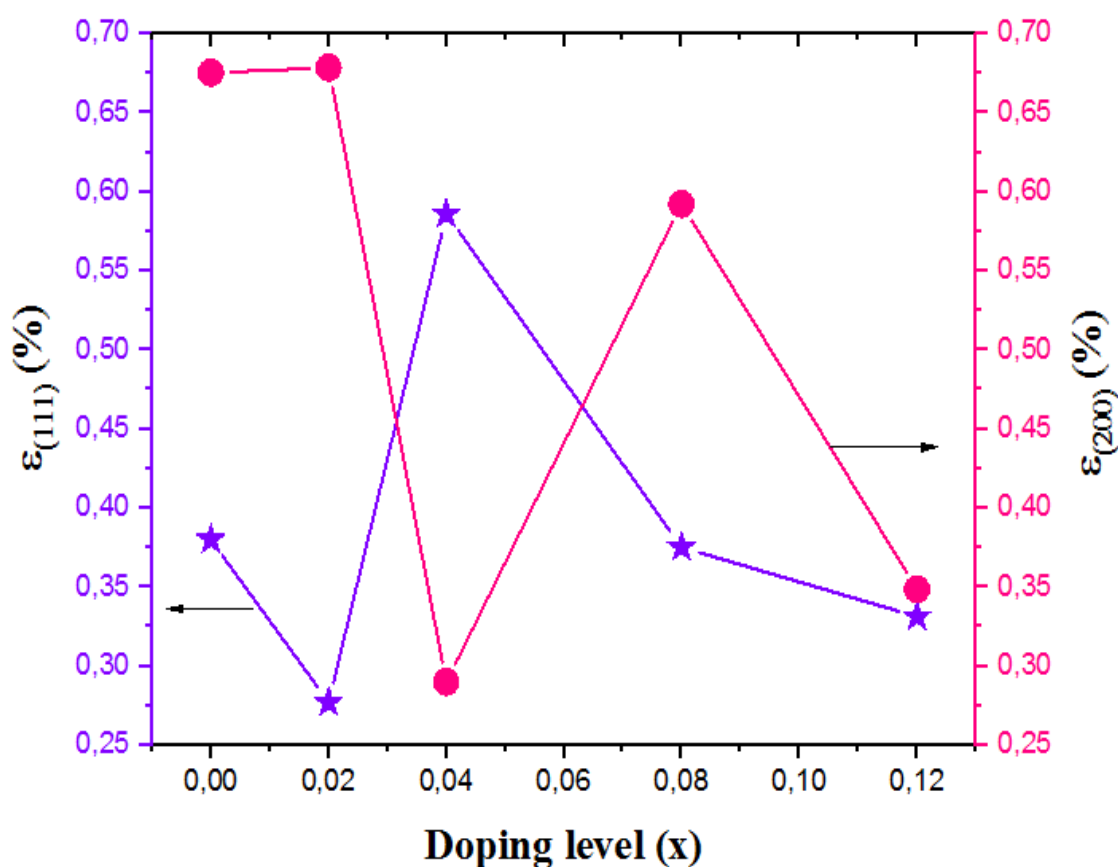


Figure (IV-9) The variations of the main strains of (111) and (200) crystal plans of $Ni_{1-x}Zn_xO$ thin films as a function of Zn doping level

IV.4. Conclusion

In this chapter we examined the properties of saturated zinc $\text{Ni}_{1-x}\text{Zn}_x\text{O}$ thin films with different levels of doping (0, 0.02, 0.04, 0.08 and 0.12%). They were successfully deposited on glass substrate by spray technique using Nickel and Zinc acetates at a substrate temperature of 450 °C.

XRD patterns of the Zn-doped Nickel Oxide thin films indicate that all films are polycrystalline with cubic face centered crystal structure. The main characteristic peaks are assigned to the (111), (200) planes. The undoped NiO thin film has the highest grain size.

The transmittance of Zn-doped Nickel Oxide thin films increases rapidly as the wavelength increases in the range of (300-400) nm, and then increases slowly at higher wavelengths. The band gap decreases as the Zn-concentration increases and the band gap values range between (3.61-3.72 eV). The Urbach energy values range between (246-290 meV).

References

- [1] N. A. Bakr ,A. Salman, A.M.Shano," effect of solution molarity on structural and optical properties of nickel oxide thin films prepared by chemical spray pyrolysis ", International Journal of Current Research, University of Diyala, Iraq , Issue, 11.Vol. 6, pp.9644-9652.2014.
- [2] ShwetaMoghe, A.D. Acharya, Richa Panda, S.B. Shrivastava, Mohan Gangrade, T.Shripathi, V. Ganesan, Renewable Energy, Vol. 6, pp 43-48. 2012
- [3] NasrinTalebian, Maryam Kheiri, Solid State Sciences , Vol. 27,pp.79-83. 2014
- [4] S.R. Nalage, M.A. Chougule, ShashwatiSen, P.B. Joshi, V.B. Patil, Thin Solid Films , Vol. 520 .pp.4835–4840. 2012
- [5] Safwat A. Mahmoud, ShereenAlshomer, Mou’ad A. Tarawnh,” Structural and Optical Dispersion Characterisation of Sprayed Nickel Oxide Thin Films”, Journal of Modern Physics, Vol. 2, pp.1178-1186 , 2011
- [6] Kyung Ho Kim , Chiaki Takahashi, Yoshio Abe, Midori Kawamura, “Effects of Cu doping on nickel oxide thin film prepared by sol–gelsolution process “ , Optik, Vol. 125 ,pp. 2899–2901. 2014
- [7] W. Daranfede, M.S. Aida, A. Hafdallah, H. Lekiket, Thin Solid Films, Vol. 518 ,pp. 1082–1084. 2009
- [8] M. F. Malek, M. H. Mamat, M. Z. Musa, Z. Khusaimi, M. Z. Sahdan, A. B. Suriani, A. Ishak, I. Saurdi, S. A. Rahman, M. Rusop, J. of Alloys and Compounds , Vol. 610 ,pp. 575–588. 2014
- [9] Abdur Rahman M, Radha krishnan R and Gopala krishnan R Structural, Optical, Magnetic and antibacterial properties of Nd doped NiO nanoparticle sprepared by coprecipitation method. Journal of Alloys and Compounds , Vol.742. pp. 421–429. 2018
- [10] Sajilal K and Moses Ezhil Raj A Effect of thickness on physico-chemical properties of p-NiO (bunsenite) thin films prepared by the chemical spray pyrolysis (CSP) technique. Optik , Vol.127, pp. 1442–1449. 2016

- [11] Cao J, Wang Z, Wang R, Liu S, Fei T, Wang L and Zhang T Synthesis of core-shell α -Fe₂O₃@NiO nanofibers with hollow structures and their enhanced HCHO sensing properties. *Journal of Materials Chemistry A* , Vol.3, pp. 5635–5641. 2015
- [12] Kyung Ho Kim, Chiaki Takahashi, Yoshio Abe, Midori Kawamura, *Optik* , Vol.125 , pp. 2899–2901. 2014
- [13] M. Mekhnache, A. Drici, L.S. Hamideche, H. Benzarouk, A. Amara, L. Cattin, J.C. Bernede, M. Guerioune, *Superlattices and Microstructures*, Vol. 49, pp. 510–518. 2011
- [14] A.A. Al-Ghamdi, Waleed E. Mahmoud, S.J. Yagmour, F.M. Al-Marzouki, *Journal of Alloys and Compounds* , Vol. 486 , pp. 9–13. 2009

CHAPTER FIVE

Synthesis of nanostructured of Ni doped ZnO

V-1- Introduction

Metal oxide semiconductors display prominent role in the development of industrial applications due to its wide range of inherent properties such as UV light absorbance, photo-catalyst, magnetic and dielectric properties, high chemical stability, etc[1–2]. Among the metal oxide semi-conductors, ZnO is extensively studied in the past decade owing to their many interesting properties, such as, transparency in the visible and high infrared reflectivity, wide band gap ($E_g = 3.3$ eV), excellent piezo-electric properties and poses n-type conductivity [3]. The porous structure greatly influences the physical characteristics of the material such as elastic moduli, conductivity, permeability, mechanical property, etc. [4]. Since, porous particles have high surface area, large pore volume, tunable pore diameter, and also, preserve chemical stability along with surface functionality which allows the attachment of different functional groups of additives. Moreover, the introduction of trace amounts of dopant induces drastic changes in the physical and chemical properties of ZnO, which offers additional flexibility for designing new functional materials. Previous discovery suggests that the doping of 3d transition-metal impurities into the non-magnetic oxides (ZnO) convert them into a ferromagnetic material above room temperature and they attained the required properties for spintronic applications [5]. Dietl et al. [6] and Sato et al. [7] theoretically predicted the transition metal atom (i.e., Fe, Cu, Cr, Co, Ni, Mn, and V) doped ZnO as so-called Diluted Magnetic Semiconductors (DMS). Among these, nickel (Ni) is an opt dopant due to its properties like stability in alcoholic medium and it can replace the ion without creating a cationic vacancy. Compared to Zn, Ni exhibits a similar ionic radius which permits the occupation of Ni ion in the tetrahedral sites without disturbing the physical properties [8].

Due to the smaller ionic radius of tetrahedrally coordinated Ni^{2+} ensure its larger solubility in ZnO crystal [9]. Furthermore, Ni^{2+} exhibits good chemical stability on incorporating into the Zn^{2+} sites [10]. We used the Spray Technique as a simple and facile method used to improve the electrical, optical, structural properties as well as modify the microstructural parameters (particle size, shape and their anisotropy) which is an economical manner. In this report, five different dopant concentrations ($x = 0.88, 0.92, 0.96, 0.98$ and 1) on $Ni_{1-x}Zn_xO$.

In this work, we deposited Ni doped ZnO thin films on glass substrate using spray pyrolysis technique, and we have studied the Impact of doping level of Ni on the optical

and structural properties of Ni doped Zinc oxide (ZnO) thin films, The main goal for this research is to find optimum information on doping level, Table V.1 presents the experimental conditions of prepared of Ni doped ZnO thin films.

Table IV.1. The experimental conditions of prepared of Zn doped NiO thin films

N	X	Ni _{1-x} Zn _x O	V _{nickel acetate} (ml)	V _{zinc acetate} (ml)	t (min)	C _{nickel acetate} =C _{zinc acetate} (mol/l)	T (°C)
1	1	Zn ₁ O	0	40	7	0.05	450
2	0.98	Ni _{0.02} Zn _{0.98} O	0.8	39.2	7	0.05	450
3	0.96	Ni _{0.04} Zn _{0.96} O	1.6	38.4	7	0.05	450
4	0.92	Ni _{0.08} Zn _{0.92} O	3.2	36.8	7	0.05	450
5	0.88	Ni _{0.12} Zn _{0.88} O	4.8	35.2	7	0.05	450

V-2-Ni doping effect on optical properties of ZnO thin films:

The optical characterization has been done using Perkin Elmer Lambda 25 UV-VIS spectrophotometer. The optical measurement results include relations of the transmittance and absorbance with wavelength for Ni doped (ZnO) thin films with different doping levels (0.88, 0.92, 0.96, 0.98 and 1 %). We studied the effect of the concentration on the optical parameters like absorption coefficient, optical energy gap and Urbach energy.

V-2-1-Transmittance spectra:

Figure (V.1) shows the relation between transmittance and wave length in the range of (300 - 900 nm) for Zn doped (NiO) thin films with different doping levels. From this figure, we can observe that the transmittance for all samples increases rapidly as the wave length increases in the range of (350- 390 nm), then increases slowly at higher wavelengths and the optical transmittance of these films increased with increasing level. The spectra show high transmittance about 80% to 100% in the visible region, and the maximum transmittance observed of thin films was about 95% at x=0.98. It can be noticed also that

the fundamental absorption edge is sharp in the visible region of the spectrum; these results are in agreement with other studies [11].

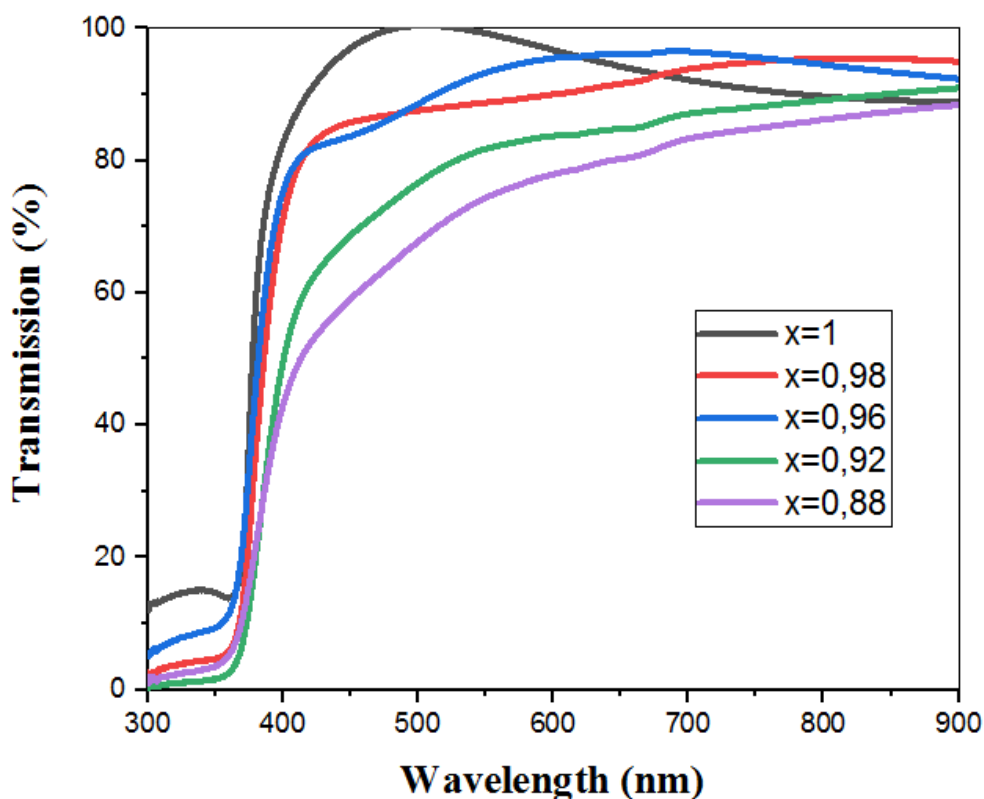


Figure (V.1) Optical transmittance spectra of Ni doped ZnO thin films

The inset of Figure (V.2) presents the variation of absorbance data of ZnO thin films, the absorption edge shifts was observed clearly at wavelength shorter than 400 nm. The absorption edge shifts of ZnO thin films were decreased with increasing the Ni deposition rate. As can be note, the optical property of ZnO thin films is affected by Ni deposition rate. We get the lowest absorption value at $x=0.98$.

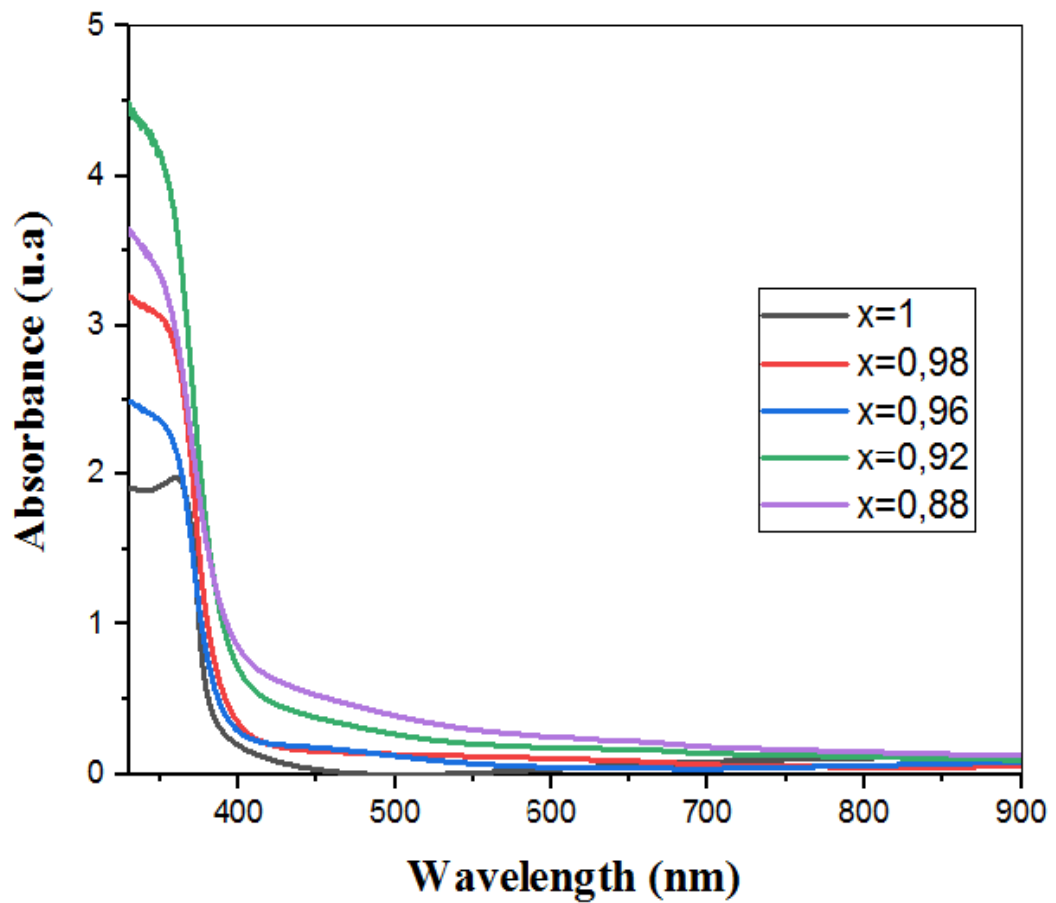


Figure (V.2): Optical absorbance spectra of Ni doped ZnO thin films

V-2-2-Optical Gap

The optical band gap E_g was obtained by extrapolating the linear portion of the plot $(Ah\nu)^2$ versus $(h\nu)$ to $A = 0$ [12]. See Figure (V.3) according to the following equation [13,14]:

$$A = \alpha d = -\ln T \quad (\text{V.1})$$

$$(Ah\nu)^2 = C (h\nu - E_g) \quad (\text{V.2})$$

Where A is the absorbance, d is the film thickness; T is the transmission spectra of thin films; α is the absorption coefficient values; C is a constant, $h\nu$ is the photon energy and E_g the band gap energy of the semiconductor.

One can estimate the optical gap (E_g) starting from the extrapolation of the curve which presents the evolution of $(Ah\nu)^2$ as a function of $h\nu$. The intersection of the linear region on the $h\nu$ axis gives the E_g . As shown in Figure (V.3), using this method the band gap values of the thin films are located around 3.3 eV which is in good agreement with the E_g value of bulk ZnO (3.23 - 3.37 eV) [15].

From these curves, we have obtained the various E_g values which are represented in Table (V.2) and plotted as a function of doping in the Figure (V.3).

The decrease in the value of the optical band gap of the ZnO film to 3.3 eV may be attributed to the improvement in the crystalline quality of the films as well as to the increase in the grain size [16].

Table (V-2): Optical gap values of Ni doped ZnO.

X	E_g (eV)
1	3.35
0.98	3.33
0.96	3.29
0.92	3.28
0.88	3.25

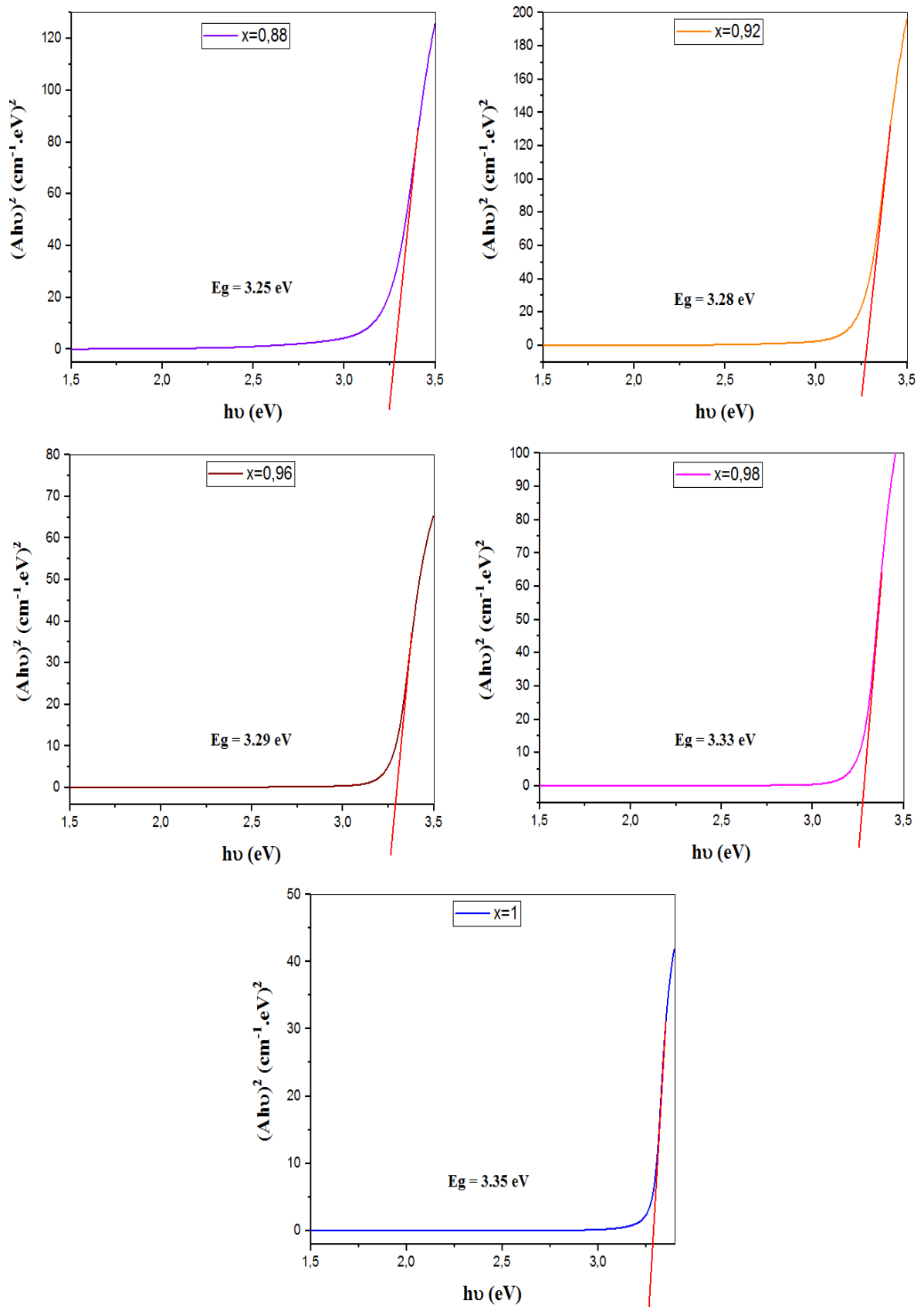


Figure (V.3): The variation of $(Ah\nu)^2$ as a function of $h\nu$ for each Ni doped ZnO thin films.

V-2-3-The Disorder (Urbach energy)

The same thing as the optical gap, the Urbach energy (E_u) is related to the disorder in the film network, as it is expressed follow [17]:

$$A = A_0 \exp\left(\frac{h\nu}{E_u}\right) \quad (\text{V.3})$$

Where A_0 constant $h\nu$ is the photon energy and E_u is the Urbach energy, is presented in Table (V.3). The Figure (V.4) shows the drawn of $\ln A$ as a function of photon energy $h\nu$ for deduce the Urbach energy. We have obtained these curves for each different doping level.

Through the curves, we observe a decrease in the Urbach energy (E_u) upon increasing the value of x which corresponds to a decrease in the ratio of Ni to the lowest value of $E_u=65\text{meV}$. While the percentage of Ni decrease, the value of E is decreasing also, this is consistent with previous studies [18].

Table (V-3): Disorder's (Urbach energy) values of Ni doped ZnO.

X	Eu (meV)
1	65
0.98	132
0.96	135
0.92	171
0.88	230

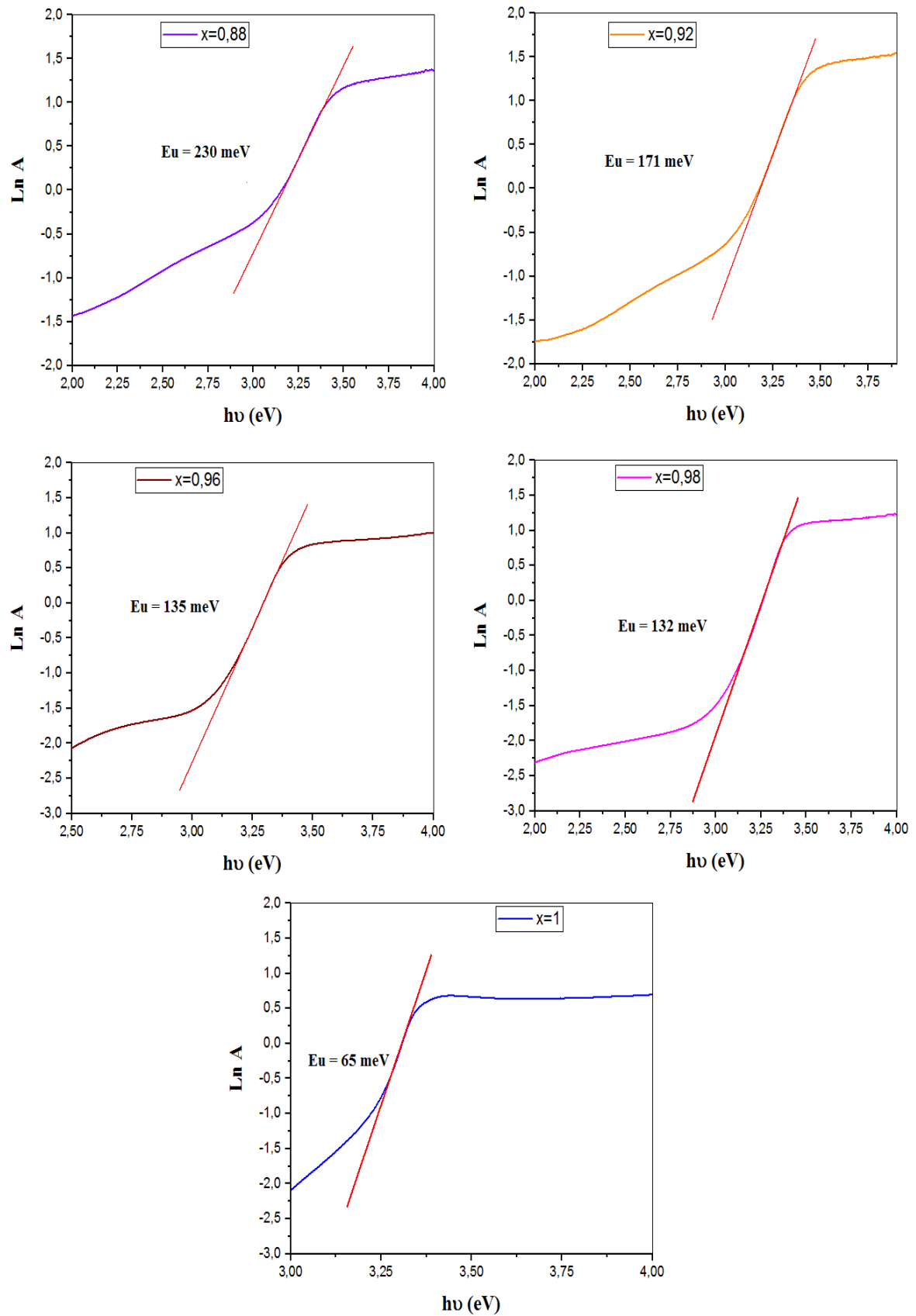
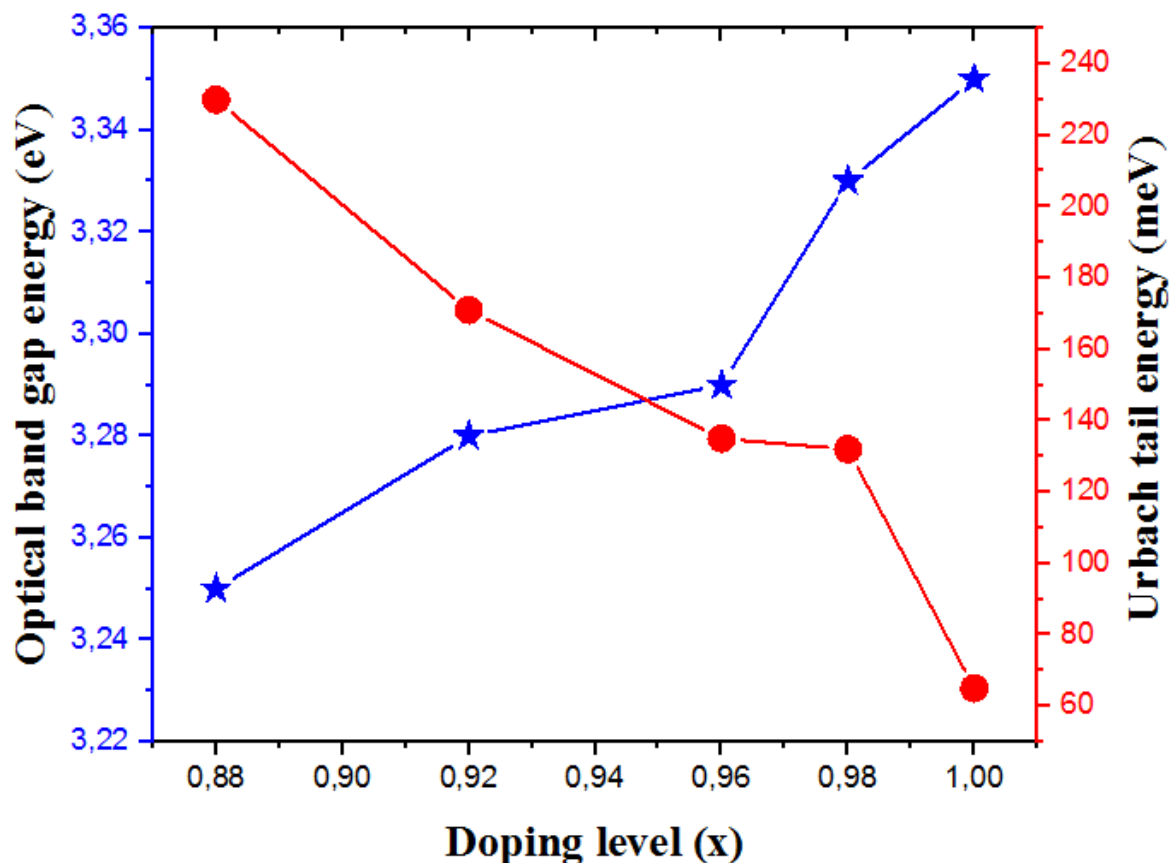


Figure (V.4): Variations of $\ln A$ as a function of $h\nu$ of Ni doped ZnO thin films.



Figure(V.5): The variations of optical band gap energy and Urbach energy of Zn doped NiO thin films at various doping levels.

We observe that the optical gap (E_g) exhibit a decrease which can be attributed to the growth of crystallite size which is resulted from the lower of the amount of Ni. The Urbach energy decreases with the lower of the amount of Ni. The Urbach energy, corresponding with the tail width of the localized states within the optical band gap, thus it changes inversely with the optical band gap [19].

V-3-Ni doping effect on Structural properties of ZnO thin films:

The crystal structure of pure and Ni doped ZnO was analyzed by X-Ray Diffraction (XRD) method. The XRD patterns of the Nickel-doped and pure ZnO thin films obtained were shown in Figure (V.6). Several reflection peaks such as (100), (002), (101) and (110) were found in NZO thin films. For all thin films, XRD results (Ref. JCPDS-Card No.36-

1451) showed that it was hexagonal quartzite structure with have a preferential c-axis orientation [20, 21, 22, 23]. It is understood from Figure (V.6) that the planes are located at their 2θ are showed in the Table(V.4). Figure (V.6) shows that the Ni doping level plays an important role in improving the crystallinity of ZnO thin films.

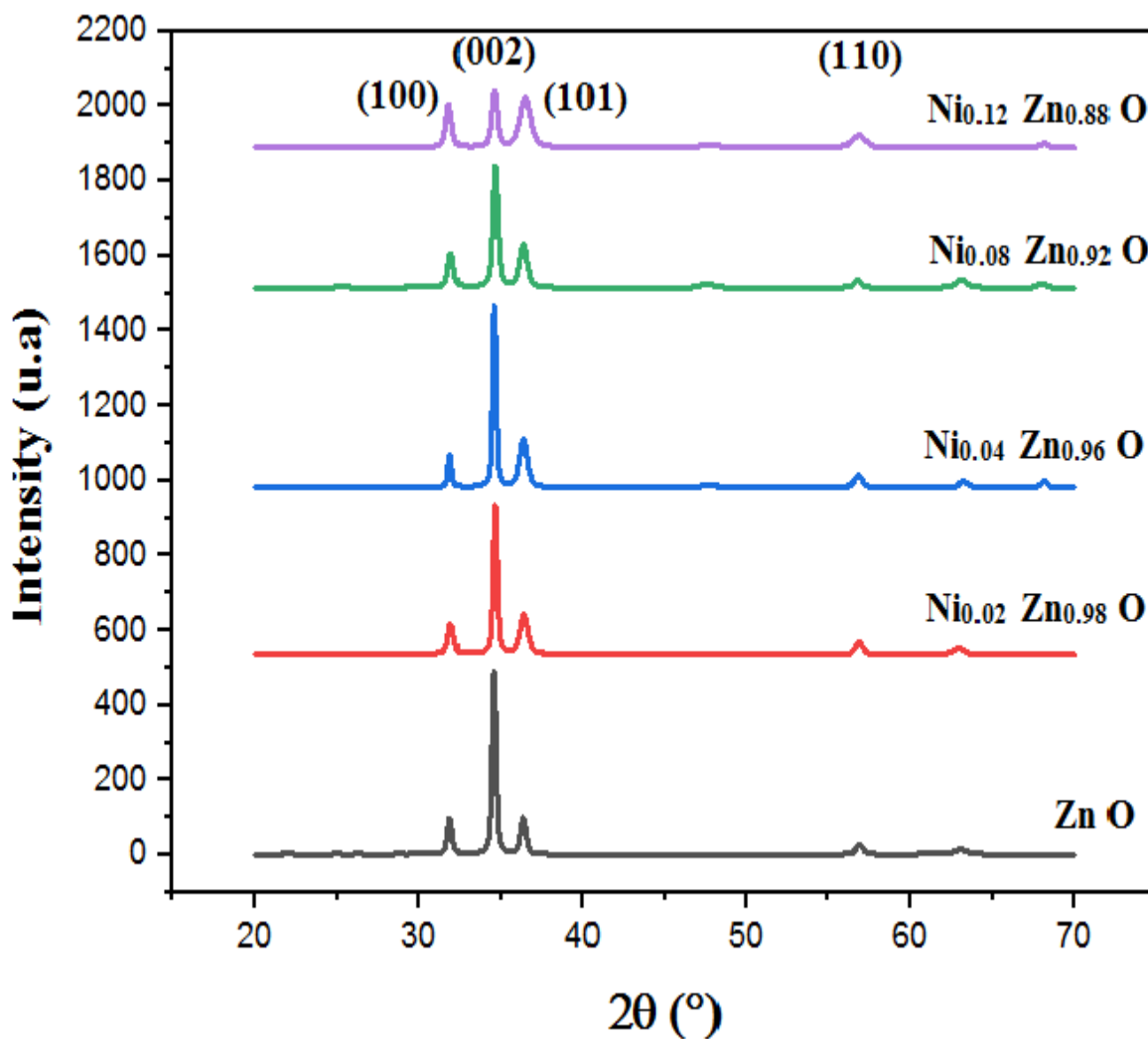


Figure (V-6): X-ray diffraction of $Ni_{1-x}Zn_xO$ thin films as a function of Ni doping level

Table (V- 4-a):The structural parameters of Ni doped ZnO thin film of (100) diffraction peak

x	$2\theta(^{\circ})$	$\beta_{1/2} (^{\circ})$	G(nm)	$\delta (m^{-2})$
1	31,8335	0,0787	105,0173	$9,0673 \cdot 10^{13}$
0.98	31,9218	0,3149	26,25177	$1,45 \cdot 10^{15}$
0.96	31,8793	0,2362	34,99495	$8,17 \cdot 10^{14}$
0.92	31,9175	0,3149	26,25149	$1,45 \cdot 10^{15}$

0.88	31,8084	0,4723	17,49809	$3,27*10^{15}$
-------------	---------	--------	----------	----------------

Table (V- 4-b):The structural parameters of Ni doped ZnO thin film of (002) diffraction peak.

x	2 θ (°)	$\beta_{1/2}$ (°)	G(nm)	δ (m ⁻²)
1	34,5124	0,0787	105,7504	$8,94202*10^{13}$
0.98	34,5978	0,2755	30,21592	$1,1*10^{15}$
0.96	34,5638	0,1378	60,40433	$2,74*10^{14}$
0.92	34,566	0,1378	60,40469	$2,74*10^{14}$
0.88	34,5541	0,3936	21,1471	$2,24*10^{15}$

Table (V- 4-c):The structural parameters of Ni doped ZnO thin film of (101) diffraction peak.

x	2 θ (°)	$\beta_{1/2}$ (°)	G(nm)	δ (m ⁻²)
1	36,2927	0,2362	35,41019	$7,97524*10^{14}$
0.98	36,3865	0,4723	17,71359	$3,19*10^{15}$
0.96	36,343	0,4723	17,71139	$3,19*10^{15}$
0.92	36,3335	0,3936	21,25219	$2,21*10^{15}$
0.88	36,2546	0,6298	13,27878	$5,67*10^{15}$

Table (V- 4-d):The structural parameters of Ni doped ZnO thin film of (110) diffraction peak.

x	2 θ (°)	$\beta_{1/2}$ (°)	G(nm)	δ (m ⁻²)
1	56,8056	0,4723	19,12937	$2,73274*10^{15}$
0.98	56,7736	0,4723	19,12648	$2,73*10^{15}$
0.96	56,7303	0,6298	14,34042	$4,86*10^{15}$
0.92	56,7829	0,551	16,39534	$3,72*10^{15}$
0.88	56,7429	0,6298	14,34127	$4,86*10^{15}$

Crystal defects and stresses are thought to cause significant change in crystal structure. In the XRD spectra, the broadening, narrowing or more intensity of the peaks can be attributed to the crystal structure defects formed by the addition of Ni atoms. The intensity of the diffraction peaks of ZnO decreases greatly with the increase in Ni concentration indicates the reduction in crystallinity by lattice distortion.

Bragg's law is used to determine the inter planar distance (d) and this law is given as follows [24]

$$2d_{hkl} \sin \theta = n\lambda \quad (\text{V.4})$$

n is an integer ($n = 1$) and θ corresponds to the half-diffraction angle. d_{hkl} is the distance between adjacent planes. Tables(V.4) data is in good agreement with standard data (JCPDS No. 36-1451).he average crystallite size (G) was calculated using the Debye-Scherrer equation [25]

$$G = \frac{0.9\lambda}{\beta \cos \theta} \quad (\text{V.5})$$

Where G is the crystallite size, λ is the wavelength of X-ray ($\lambda = 1.5406 \text{ \AA}$). In addition, θ is the Bragg angle, and β is the full width of the half-maximum (FWHM) of the diffraction peak determined for these angles [26]. There is a difference between the two values G for Ni doped ZnO and ZnO pure. In addition, the lattice constant (c) of the thin films was calculated from the XRD data presented in Tables (V.4 and V.5) using the following equation [27].

$$\frac{1}{d_{hkl}^2} = \frac{4}{3} \frac{h^2 + k^2 + hk}{a^2} + \frac{l^2}{c^2} \quad (\text{V.6})$$

Table (V- 5):The structural parameters of $\text{Ni}_{1-x}\text{Zn}_x\text{O}$ thin film of (002) diffraction peak.

X	2 θ (°)	G (nm)	ϵ_{zz} (%)	C (nm)
1	34,5124	105,7504	-0,19269	0,519597
0.98	34,5978	30,21592	-0,43156	0,518353
0.96	34,5638	60,40433	-0,3366	0,518848
0.92	34,566	60,40469	-0,34275	0,518816
0.88	34,5541	21,1471	-0,30948	0,518989

The calculated value of the lattice constant (c) for the pure ZnO thin flm is 0.519597nm and depending on the increased Ni doping rate, these values are 0.518989 nm, 0.518848nm and 0.518816nm for $\text{Ni}_{1-x}\text{Zn}_x\text{O}$ flms. These values calculated for thin films are well agree with standard data (JCPDS No.36-1451, $c_0 = 0.5206 \text{ nm}$). The dopant Ni ions are well allied into ZnO crystal lattice, without altering its overall crystal structure [28].

The strain ϵ values in our films were estimated from the observed shift, in the diffraction peak between their positions in the XRD spectra via the formula [29]:

$$\varepsilon_{zz} = \frac{c-c_0}{c_0} * 100 \quad (V.7)$$

Where ε is the mean strain in ZnO thin films Table (V- 4), c the lattice constant of ZnO thin films and c_0 the lattice constant of bulk (standard $c_0=0,5206$ nm). Figure (V.7) shows the variation of the crystallite size and mean strain of (0 0 2) diffraction peak as a function of doping level x .

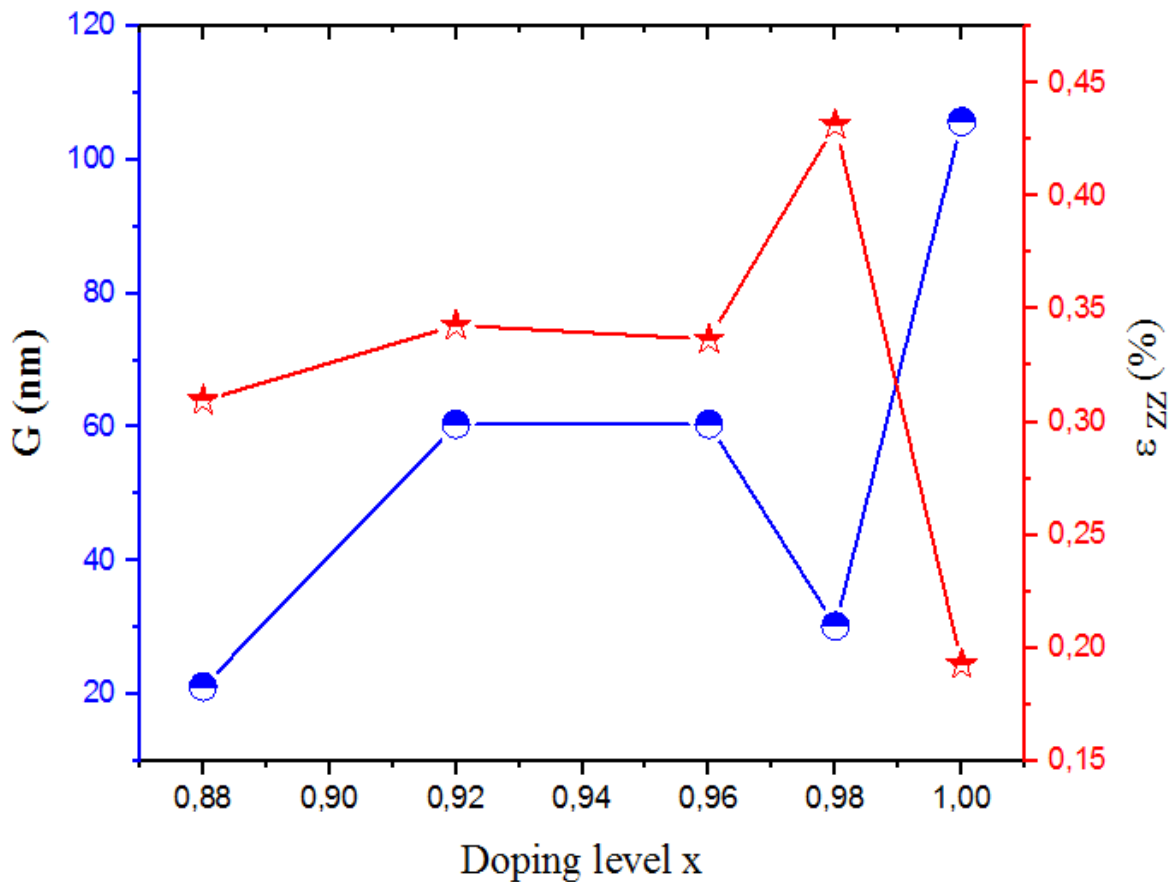
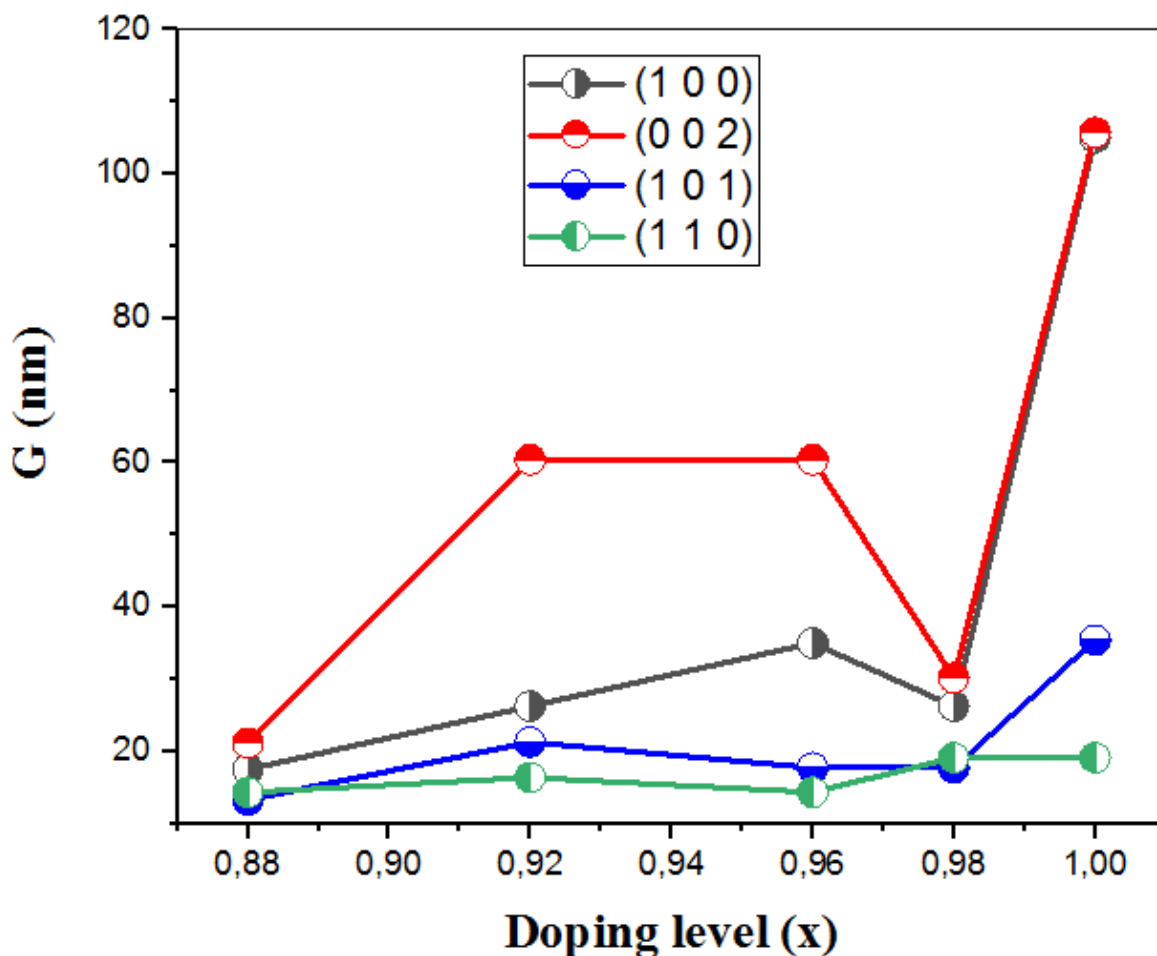


Figure (V.7): G and ε_{zz} of (0 0 2) diffraction peak as a function of doping level x .

It can be seen from Figure (V.7) that the sizes of the crystals increase with increasing the level of doping, then decrease and then increase. Increases in crystal size can be explained by improving film crystallization. Moreover, the decreases of the crystallite size, this confirms the deterioration in the crystallinity of the films. The mean strain decreases from 0.43 to 0.19%. Swapna et al [30]. This result in reduction of mean strain with increase in crystallite size indicates enhancement of crystallinity [31], or by decrease of the defects

in the films. However, the crystallite size of (002) crystal plan is the highest one with comparing by other plans (see Figure V.8)



Figure(V-8): the variations of crystallite sizes G as a function of doping level x of Ni doped ZnO thin films for (100) (002) (101) and (110) crystal plans

V-4- Conclusion:

Nanoporous Ni doped ZnO is prepared in the configuration $\text{Ni}_{1-x}\text{Zn}_x\text{O}$ ($x=0.88, 0.92, 0.96, 0.98$ and 1). Were successfully deposited on glass substrate by Spray technique using Nickel acetates and Zinc acetates. The crystal structure and optical properties of $\text{Ni}_{1-x}\text{Zn}_x\text{O}$ are determined from XRD and Ultraviolet – visible spectroscopy respectively. XRD patterns of the Zn-doped Nickel Oxide thin films indicate that all films are polycrystalline with hexagonal crystal structure. The main characteristic peaks are assigned to the (100)

(002) (101) and (110) planes. At low doping level of Ni, the crystal structure remains identical to ZnO meanwhile some structural imperfection is observed on increasing the doping concentration. Based on the obtained results, $\text{Ni}_{1-x}\text{Zn}_x\text{O}$ is a suitable candidate for Diluted Magnetic Semiconductors for spintronic applications.

References

- [1] N. Doğan, A. Bingölbali, L. Arda, Preparation, structure and magnetic characterization of Ni doped ZnO nano-particles, *J. Magn. Mater.*, vol. 373, pp. 226–230, 2015.
- [2] J. Wang, Y. Ju, Y. Huang, J. Zheng, Z. Zheng, Study of the influence of porous structure on the permeability of rock using Lattice Boltzmann method, *Procedia Eng*, vol. 102, pp. 1835–1841, 2015.
- [3] G. He, J. Cai, G. Ni, ZnO thin films prepared by a modified water-based Pechini method, *Mater. Chem. Phys.*, vol. 110, pp. 110–114, 2008.
- [4] J. Liu, M. Wu, Z. Zhu, Z. Shao, A study on the mechanical properties of the representative volume element in fractal porous media, *Geofluids* 2017.
- [5] U. Philipose, G. Sapkota, Ferromagnetic ZnO nanowires for spintronic applications, *Nanowires -Recent Advances*, InTech, 2012.
- [6] T. Dietl, H. Ohno, F. Matsukura, J. Cibert, E.D. Ferrand, Zener, model description of ferromagnetism in zinc-blende magnetic semiconductors, *Science*, vol. 287, pp. 1019–1022, 2000.
- [7] K. Sato, H. Katayama-Yoshida, Ferromagnetism in a transition metal atom doped ZnO, *Phys.*, vol. 10, pp. 251–255, 2001.
- [8] S. Basri, W.A. Majid, N. Talik, M.M. Sarjidan, Tailoring electronic structure, electrical and magnetic properties of synthesized transition metal (Ni)-doped ZnO thin film, *J. Alloy. Compd.*, vol. 769, pp. 640–648, 2018.
- [9] A. Samanta, M. Goswami, P. Mahapatra, Magnetic and electric properties of Ni doped ZnO nanoparticles exhibit diluted magnetic semiconductor in nature, *J. Alloy. Compd.*, vol. 730, pp. 399–407, 2018.
- [10] J. Tawale, K. Dey, R. Pasricha, K. Sood, A. Srivastava, Synthesis and characterization of ZnO tetrapods for optical and antibacterial applications, *Thin Solid Films*, vol. 519, pp. 1244–1247, 2010.
- [11] T. Minami, *MRS Bull.*, pp. 38–44, 2000.

- [12] Shweta Moghe, A.D. Acharya, Richa Panda, S.B. Shrivastava, Mohan Gangrade, T. Shripathi, V. Ganesan, *Renewable Energy*, vol. 46, pp. 43-48, 2012.
- [13] Nasrin Talebian, Maryam Kheiri, *Solid State Sciences*, vol. 27, pp. 79–83, 2014.
- [14] S.R. Nalage, M.A. Chougule, Shashwati Sen, P.B. Joshi, V.B. Patil, *Thin Solid Films*, vol. 520, pp. 4835–4840, 2012.
- [15] B. Nasr et al., Electrical resistivity of nanocrystalline Al-doped zinc oxide films as a function of Al content and the degree of its segregation at the grain boundaries. *J. Appl. Phys.*, vol. 108, pp. 103–721, 2010.
- [16] S. Mondal, P. Mitra, Preparation of Ni doped ZnO thin films by SILAR and their characterization. *Indian J. Phys.*, vol. 87, pp. 125–131, 2013.
- [17] W. Daranf, M.S. Aida, A. Hafdallah, H. Lekiket, *Thin Solid Films*, vol. 518, pp. 1082–1084, 2009.
- [18] M. Tomakin, Structural and optical properties of ZnO and Al-doped ZnO microrods obtained by spray pyrolysis method using different solvents, *Super lattices Microstruct.*, vol. 51, pp. 372–380, 2012.
- [19] M. F. Malek, M. H. Mamat, M. Z. Musa, Z. Khusaimi, M. Z. Sahdan, A. B. Suriani, A. Ishak, I. Saurdi, S. A. Rahman, M. Rusop, *J. of Alloys and Compounds*, vol. 610, pp. 575–588, 2014.
- [20] L. Peng et al., Growth and characterization of indium doped zinc oxide films sputtered from powder targets. *J. Wuhan Univ. Technol.-Mater. Sci. Ed.*, vol. 32, pp. 866–870, 2017.
- [21] H. Mahdhi et al., Effect of sputtering power on the electrical and optical properties of Ca-doped ZnO thin films sputtered from nanopowders compacted target. *Opt. Mater.*, vol. 45, pp. 97–103, 2015.
- [22] G. Paul et al., Structural, optical and electrical studies on sol–gel deposited Zr doped ZnO films. *Mater. Chem. Phys.*, vol. 79, pp. 71–75, 2003.

- [23] G. Malik et al., Optical and other physical properties of hydrophobic ZnO thin films prepared by dc magnetron sputtering at room temperature. *J. Appl. Phys*, vol. 122, pp. 105–143, 2017.
- [24] R.J. Tilley, *Crystals and Crystal Structures* (Wiley, New York) ,2006
- [25] L.E. Greene et al., General route to vertical ZnO nanowire arrays using textured ZnO seeds. *Nano Lett*, vol. 7, pp. 1231–1236, 2005.
- [26] G. Singla, K. Singh, O. Pandey, Williamson–Hall study on synthesized nanocrystalline tungsten carbide (WC). *Appl. Phys*, vol. 113, pp. 237–242, 2013.
- [27] E. Keskenler, G. Turgut, S. Doğan, Investigation of structural and optical properties of ZnO films co-doped with fluorine and indium. *Superlattices Microstruct*, vol.52, pp. 107–115, 2012.
- [28] R. Saleh, N.F. Djaja, Transition-metal-doped ZnO nanoparticles: synthesis, characterization and photocatalytic activity under UV light, *Spectrochim. Acta Part A Mol. Biomol. Spectrosc*, vol. 130, pp. 581–590, 2014.
- [29] A.J. Hashim, M.S. Jaafar, A.J. Ghazai, N.M. Ahmed, Fabrication and characterization of ZnO thin film using sol–gel method, *Optik*, vol. 124, pp. 491–492, 2013.
- [30] R. Swapna, M. Ashok, G. Muralidharan, M.C. Santhosh Kumar, Microstructural, electrical and optical properties of ZnO:Mo thin films with various thickness by spray pyrolysis, *J. Analyt. Appl. Pyroly*, vol. 102, pp. 68–75, 2013.
- [31] S. Benramache, B. Benhaoua, N. Khechai, F. Chabane, Elaboration and characterization, of ZnO thin films, *Matériaux Tech*, vol. 100, pp. 573–580, 2012.

GENERALE CONCLUSION

GENERAL CONCLUSION

Nickel oxide NiO is a semiconductor material p-type that is a part of this family of TCO; it has applied for gas sensors because of its wide band gap (3.6-4.0 eV). NiO can be used in various potential applications such as solar cells due to the p-type semiconducting, transparent diodes, transparent transistors, displays and defrosting windows because their transparency can be used for the UV photodetectors and touch screens due to the good responsively. NiO is one of the most important oxide materials due to its excellent chemical stability, durability, low toxicity, large span optical density, low cost, good thermal stability and high stability that are similar to ZnO.

The NiO thin films were prepared by spray pyrolysis method on glass substrate at 450 °C with various deposition rates. The structural, optical and electrical properties of nanostructures NiO thin films were investigated by study the influence of deposition rate on glass substrate. NiO thin films were observed a nanocrystalline a cubic structure with a strong (111) preferred orientation, it is only phase was observed in all deposited films. The minimum value of crystallite size (15.8 nm) was measured of deposited film with 60 ml. The average transmittance is about 70 % was observed in all NiO thin films. The NiO thin films have a verity in the band gap energy from 3.34 to 3.51 eV because the effect of deposition, the minimum value was found at 80 ml, this condition have a lowest Urbach energy. The NiO thin film elaborated with 80 ml has a minimum electrical resistivity was 0.152 (Ω .cm). The NiO thin films sprayed with 60 and 80 ml have good structural, optical and electrical properties.

In this study, we have prepared Zn doped NiO thin films, where Zn = 0, 0.02, 0.04, 0.08 and 0.12. XRD patterns of the Zn-doped Nickel Oxide thin films indicate that all films are polycrystalline with cubic face centered crystal structure. The main characteristic peaks are assigned to the (111), (200) planes. The undoped NiO thin film has highest grain size. The transmittance of Zn-doped Nickel Oxide thin films increases rapidly as the wavelength increases in the range of (300-400) nm, and then increases slowly at higher wavelengths. The band gap decreases as the Zn-concentration increases and the band gap values range between 3.61-3.72 eV .The Urbach energy values range between 246-290 meV.

Nanocrystallite Ni doped ZnO is prepared in the configuration $Ni_{1-x}Zn_xO$ (x=0.88, 0.92, 0.96, 0.98 and 1).Were successfully deposited on glass substrate by Spray technique using

Nickel acetates and Zinc acetates. The crystal structure and optical properties of $\text{Ni}_{1-x}\text{Zn}_x\text{O}$ are determined from XRD and Ultraviolet – visible spectroscopy respectively. XRD patterns of the Zn-doped Nickel Oxide thin films indicate that all films are polycrystalline with hexagonal crystal structure. The main characteristic peaks are assigned to the (100) (002) (101) and (110) planes. At low doping level of Ni, the crystal structure remains identical to ZnO meanwhile some structural imperfection is observed on increasing the doping concentration. Based on the obtained results, $\text{Ni}_{1-x}\text{Zn}_x\text{O}$ is a suitable candidate for Diluted Magnetic Semiconductors for spintronic applications.

ABSTRACT

Abstract:

In this work, nickel oxide was elaborated on glass substrate at 450 °C by spray pyrolysis technique. The NiO layers were obtained with 0.05M molarity, which were deposited by various deposition rates 20, 40, 60 and 80 ml. The effects of deposition rate on the structural, electrical and optical properties were examined. NiO thin films were observed a nanocrystalline a cubic structure with a strong (111) preferred orientation, it is only phase was observed in all deposited NiO. The film elaborated with 60 ml have a minimum value of crystallite size was 15.8 nm. All NiO thin films have an average transmittance is about 70 % in the visible region. The NiO thin films have a verity in the band gap energy from 3.34 to 3.51 eV because the effect of deposition, the minimum value was found at 80 ml, this condition have a lowest Urbach energy. The NiO thin films have an electrical resistivity was decreased from 0.625 to 0.152 (Ω .cm) with increasing the deposition rate from 20 to 80ml. The best results of NiO thin films are obtained in the deposition NiO films by 40 and 80 ml. Zn doped NiO is prepared in the configuration $Ni_{1-x}Zn_xO$ ($x = 0, 0.02, 0.04, 0.08$ and 0.12) using Spray technique. XRD investigation confirms the presence of cubic structure of ZnO in all the prepared samples. At low doping level of Zn, the crystal structure remains identical to NiO meanwhile some structural imperfection is observed on increasing the doping concentration. Ni doped ZnO is prepared in the configuration $Ni_{1-x}Zn_xO$ ($x = 0.88, 0.92, 0.96, 0.98$ and 1) using Spray technique. XRD investigation confirms the presence of wurtzite hexagonal structure of ZnO in all the prepared samples. At low doping level of Ni, the crystal structure remains identical to ZnO meanwhile some structural imperfection is observed on increasing the doping concentration. $Ni_{1-x}Zn_xO$ is a suitable candidate for Diluted Magnetic Semiconductors for spintronic applications

Key words:

Nickel oxide; Zinc oxide; Thin films; Transparency; Spray pyrolysis method

المخلص:

في هذا العمل تم إيداع أكسيد النيكل على ركيزة زجاجية عند 450 درجة مئوية بواسطة تقنية الانحلال الحراري بالرش. تم الحصول على طبقات NiO باستخدام تركيز مولي قدره 0.05mol/l، والتي رشت بأحجام مختلفة 20، 40، 60 و 80ml. تم دراسة تأثير معدل الترسيب على الخصائص التركيبية والكهربائية والبصرية. لوحظ أن أغشية NiO الرقيقة عبارة عن هيكل مكعب متناهي الصغر ذو اتجاه مفضل قوي (111)، وقد لوحظ طور فقط في جميع طبقات NiO المترسبة. الطبقة المتحصل عليها من رش 60ml من المحلول أعطت قيمة دنيا لحجم البلورات قدرها 15.8nm. تتمتع جميع أغشية NiO الرقيقة بمتوسط نفاذية تبلغ حوالي 70% في المجال المرئي. الأغشية الرقيقة NiO تتغير فجوة طاقتها من 3.34 إلى 3.51eV حسب تأثير الترسيب، تم العثور على القيمة الدنيا عند 80ml، وهذه الحالة لها أقل طاقة إيرباخ. تم تقليل المقاومة الكهربائية للأغشية الرقيقة NiO من 0.625 إلى 0.152(Ω.cm) مع زيادة معدل الترسيب من 20 إلى 80ml. يتم الحصول على أفضل النتائج لأغشية NiO الرقيقة في ترسيب أفلام NiO عند 40 و 80ml. يتم تحضير NiO المخدر بالزنك النانوي في التكوين $Ni_{1-x}Zn_xO$ حيث $X=0$ ، (0.02, 0.04, 0.08, 0.12) باستخدام تقنية الرش. يؤكد فحص XRD وجود هيكل مكعب من ZnO في جميع العينات المعدة عند مستوى المنشطات المنخفض للزنك، يظل التركيب البلوري مطابقًا للـ NiO وفي الوقت نفسه لوحظ بعض النقص الهيكلي عند زيادة تركيز المنشطات. يتم تحضير ZnO المخدر بالنيكل النانوي في التكوين $Ni_{1-x}Zn_xO$ حيث (1, 0.98, 0.96, 0.92, 0.88) باستخدام تقنية الرش. يؤكد فحص XRD وجود بنية سداسية من ZnO في جميع العينات المعدة عند مستوى المنشطات المنخفض للنيكل، تظل البنية البلورية مطابقة لـ ZnO وفي الوقت نفسه لوحظ بعض النقص الهيكلي عند زيادة تركيز المنشطات. يعتبر $Ni_{1-x}Zn_xO$ مرشح مناسب لأشباه الموصلات المغناطيسية المخففة لتطبيقات spintronic.

الكلمات المفتاحية:

أكسيد النيكل؛ أكسيد الزنك؛ الأغشية الرقيقة؛ الشفافية؛ طريقة الرش الانحلال الحراري.